1962

Rapid approximation of servomechanism frequency response

Sallada, William F.; Wilson, Vaughn E.

Monterey, California: U.S. Naval Postgraduate School

RAPID APPROXIMATION OF SERVOMECHANISM FREQUENCY RESPONSE

WILLIAM F. SALLADA
and
VAUGHN E. WILSON, JR.

RAPID APPROXIMATION OF SERVOMECHANISM FREQUENCY RESPONSE

*****

William F. Sallada

and

Vaughn E. Wilson, Jr.

RAPID APPROXIMATION OF SERVOMECHANISM

FREQUENCY RESPONSE

by

William F. Sallada

Lieutenant Commander, United States Navy

and

Vaughn E. Wilson, Jr.

Lieutenant, United States Navy

Submitted in partial fulfillment of
the requirements for the degree of

MASTER OF SCIENCE
IN
ELECTRICAL ENGINEERING

United States Naval Postgraduate School

Monterey, California

1962

RAPID APPROXIMATION OF SERVOMECHANISM

FREQUENCY RESPONSE

by

William F. Sallada

and

Vaughn E. Wilson, Jr.

This work is accepted as fulfilling
the thesis requirements for the degree of

MASTER OF SCIENCE
IN
ELECTRICAL ENGINEERING

from the

United States Naval Postgraduate School

ABSTRACT

The purpose of this thesis was to develop a technique by which the frequency response of a servomechanism might be rapidly evaluated by graphical methods. The approach consisted of developing several frequency response parameters related to the location of the poles and zeros of the closed loop transfer function of a servomechanism. The systems considered were the pure second order (one pair of complex conjugate poles), second order with one zero (one pair of complex conjugate poles and one real zero), and a pure third order (one pair of complex conjugate poles and one real pole). For the latter two systems, the complex poles and the frequency were redefined as referred values relative to the real pole or zero.

Loci of constant frequency response parameters were mapped onto a complex plane; or loci of constant imaginary referred pole locations were mapped onto an auxiliary complex plane, depending upon the specific system considered. Using the points obtained from the appropriate relationship, the frequency response, M and N contours, could be rapidly and easily sketched. The M and N contours could then be used as a basis for rapid system evaluation in the frequency domain.

The authors wish to thank Professor George J. Thaler for bringing to their attention the thesis by Major Walter B. Patton, USMC, and LT William B. Abbott, III, USN, without which this thesis topic would probably not have been considered /1/.

The authors are deeply indebted to Assistant Professor Robert D. Strum, who acted as their thesis advisor, for the friendly support, encouragement, and advice given so selflessly.

TABLE OF CONTENTS

Table of Contents

LIST OF ILLUSTRATIONS

List of Illustrations

List of Illustrations

List of Illustrations

1. INTRODUCTION

Each year the importance and utilization of servomechanisms and automatic control systems increase. It naturally follows that more papers are submitted pertaining to the design, analysis, synthesis, and compensation of servomechanisms and automatic control systems. Many of these papers and existing texts discuss details and laborious calculations which are certainly a prerequisite to analyze or synthesize the operation of a servomechanism. However, in many cases, a rapid approximation of system operation would be beneficial, and possibly only an approximation would be required upon which an intelligent estimate could be made on the performance of the system under study. There are only a few papers known to the authors in which the use of approximations are presented from which an estimate of system performance can be made, e.g., Floyd's method /2/. One such paper by Patton and Abbott /1/ presents a method for a rapid approximation of servomechanism transient response.

A corollary should exist to the Patton-Abbott development in which a rapid approximation of the frequency response of a servo could be determined. The use of frequency response analysis is still an important criterion in measuring servo performance, although the transient response approach has become very popular and widely used in recent years, almost to the point of neglecting frequency response. There are many ways of determining frequency response from transient response, but lengthy calculations are necessary.

It is the purpose of this paper to present a graphical means for determining a rapid approximation of servomechanism frequency response. This approach eliminates the use of the Bode diagram and Nichols' chart. The M and N contours will be obtained directly from the closed loop transfer function of the servo.

$$F_c(j\omega) \triangleq M\epsilon^{jN} \tag{1.1}$$

This development will parallel the Patton-Abbott approach so that from the same given data (closed loop transfer function, factored form) it is possible to obtain rapidly the transient response from their paper and the frequency response from this paper. This paper will discuss in sufficient detail the development of the frequency response approach so that no reference to the Patton-Abbott paper will be required.

2. GENERAL DEVELOPMENT

Since the time domain or transient response is used so widely in the initial phases of servo study, all developments in this paper originated with the closed loop transfer function expressed in Laplace notation (s-plane) with all initial conditions equal to zero. The transformed equation was then converted into frequency response notation. For this to be a valid conversion, certain basic definitions are in order, plus some additional restrictions and assumptions used in this development. The frequency response of a system was defined in part by considering only steady state conditions. Thus, all transient conditions have vanished. To convert the transfer function from Laplace notation into the frequency response equation, it was only necessary to make a substitution of the variable. This was based on the assumption that the input was a pure sinusoid and that the output was also a pure sinusoid since the steady state condition exists. Furthermore, this forces the restriction that the system must be linear. The complex variable $s = \sigma + j\omega$ then becomes the imaginary frequency variable since the real part equals zero ($\sigma = 0$). Therefore $s = j\omega$; and when this variable substitution was made in the closed loop transfer function, the frequency response equation resulted.

2.1 Basic Definitions and Systems Characteristics

At this point, a tabulation of the various definitions, restrictions, and assumptions would be in order:

a. The system was linear.

b. The system was stable.

c. The system was characterized by unity feedback, i.e., $M = 1$ at $\omega = 0$.

d. The closed loop transfer function was known in its factored form.

Based on the above, some general frequency response characteristics could be stated.

2.2 M-Contour

a. At zero frequency, M is unity.

b. At zero frequency, the slope of the M contour is zero.

c. As the frequency approaches infinity, M approaches zero.

d. As the frequency approaches infinity, the slope of the M contour approaches zero.

e. At the maximum or minimum value of M, the slope of the M contour is zero.

2.3 N-Contour

a. At zero frequency, N is zero.

b. As the frequency approaches infinity, N approaches $\frac{(m-n)}{2}\pi$ degrees.

(m is the number of zeros and n is the number of poles of the closed loop transfer function)

2.4 Parameters

To display graphically the frequency response, parameters were selected to define specific points on the M and N contours. The selected parameters were defined as:

a. M_p: The value of M where the slope of the M contour was zero. (Does not include the value of M at zero frequency when M = 1.0).

b. ω_p: The value of omega ($\omega = 2\pi f$) where the slope of the M contour was zero. (Does not include $\omega = 0$).

c. N_p: The value of N at ω_p.

d. M_{bw}: The bandwidth point, or when M = .707.

e. ω_{bw}: The bandwidth frequency (when M = .707).

f. N_{bw}: The value of N at the bandwidth frequency.

g. M_1: The notation when M = 1.0, except at $\omega = 0$.

h. ω_1: The value of ω when M = 1.0, except at $\omega = 0$.

i. N_1: The value of N at ω_1.

j. ω_n: The undamped natural angular frequency.

k. $M_{\omega n}$: The value of M at the undamped natural angular frequency (ω_n).

l. $N_{\omega n}$: The value of N at the undamped natural angular frequency (ω_n).

The above selected parameters defined the general shape of the M and N contours. However, it was discovered that with only these points, the M and N contours were in some cases too general; the contours had insufficient shape to be of significant value. Better approximation of the M and N contours were provided by the selection of additional M, N, and ω points to "fill-in" the shape of the contours. It was discovered that, mathematically, the choice of ω_p as the basis for these additional points reduced the M and N equations to relatively simple relationships and insured that the additional points were located in the critical regions of the contours. The benefits gained by the additional points more than compensate for the slight additional labor by providing a much more accurate approximation to the M and N contours. The additional parameters selected were:

m. ω_k: An arbitrary frequency proportional to ω_p ($\omega_k \propto k\ \omega_p$), where k was a selected constant as discussed later.

n. M_k: The value of M at ω_k.

o. N_k: The value of N at ω_k.

A sketch of the general M and N contours is shown in Fig. 2-1.

2.5 Classes of Servomechanisms Studied

From Fig. 2-1, it can be seen that it was relatively easy to construct an approximate frequency response if the above defined parameters were known. This paper contains the above parameters presented in graphical form. This paper also contains the technique utilized in the parameter determination such that the frequency response can be rapidly approximated for specific classes of systems. The three systems covered in this paper were:

I. Pure Second Order - The closed loop transfer function consisted of two complex poles only.

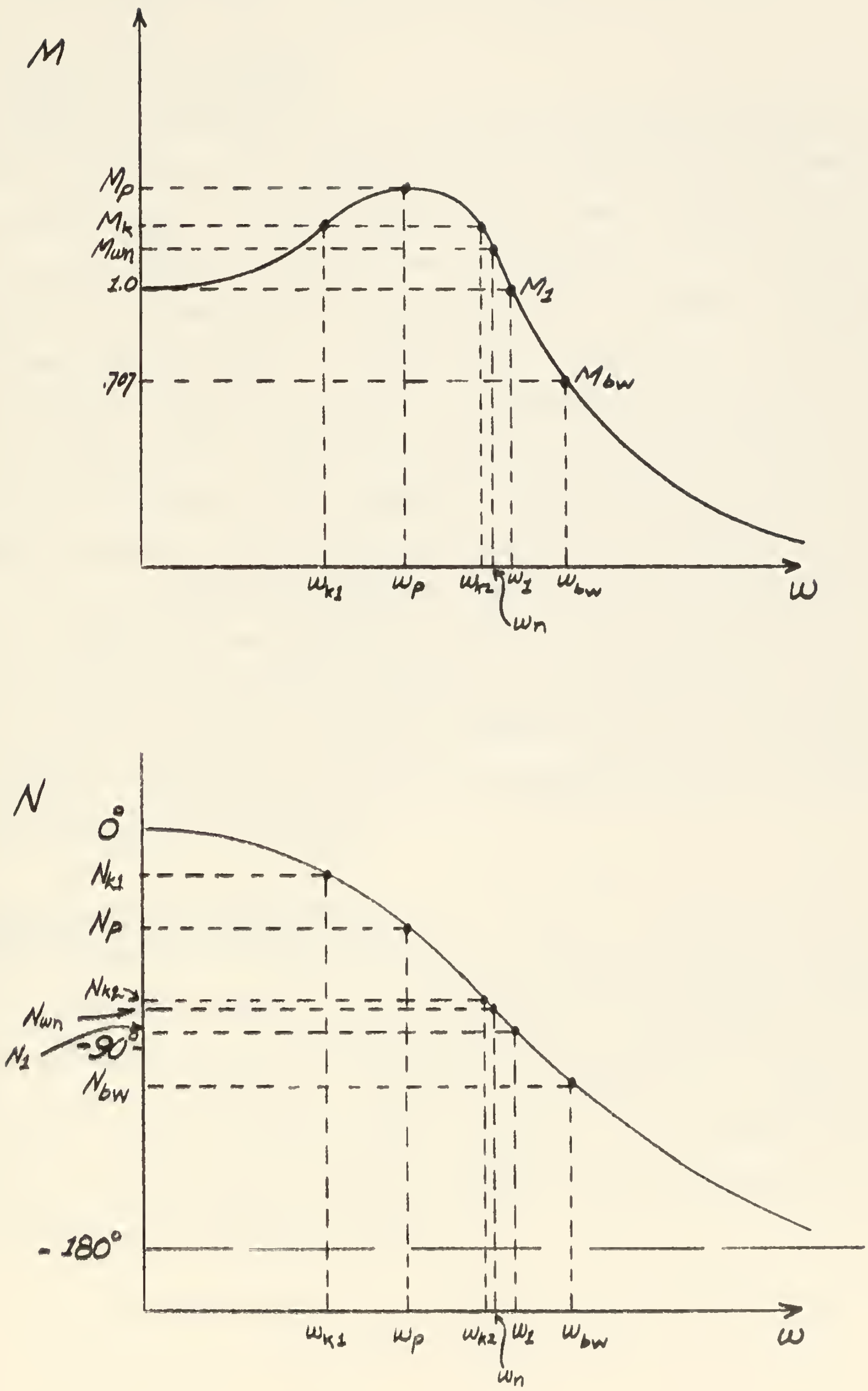

Fig. 2-1 General M and N Contours Showing Parameters Chosen

II. Second Order with One Zero - The closed loop transfer function consisted of one pair of complex poles and one real zero.

III. Pure Third Order - The closed loop transfer function consisted of one pair of complex poles and one real pole.

2 6 Presentation of Parameters

The graphical presentations for the pure second order system were, for the most part, loci of constant values of the various parameters plotted on the s-plane. For the other two systems covered in this paper, it was necessary to express the coordinates of the complex poles as a function of the magnitude of the real pole or zero. In accomplishing this, the angular frequency, ω, also became a function of the real pole or zero location. Thus the magnitude and phase shift for the frequency response was shown to be a function of the complex pole location relative to the real pole or zero. The graphical presentations for the second order plus one zero and for the pure third order systems were plotted in two ways. First, by loci of constant values of the various parameters plotted on a referred complex plane, that is, with ordinate and abscissa being the complex pole location relative to the real pole or zero. Second, by loci of constant referred imaginary part of the complex pole plotted against referred real part of the complex pole as abscissa versus the chosen parameter as ordinate.

2.7 Digital Computer Utilization

The solutions of the equations that will be presented later when a specific system is discussed were obtained from a Control Data Corporation high-speed digital computer Model 1604, located at the U. S. Naval Postgraduate School, Monterey, California (Appendix A). Without the availability of a high speed digital computer, it is doubtful that this paper could have been developed without the utilization of an analog computer plus excessive labor.

3 THE PURE SECOND ORDER SYSTEM

The pure second order system treated in this section was previously defined as a system whose closed loop transfer function consisted of only two complex conjugate poles. This system has been extensively treated in most servo textbooks, usually in terms of the damping ratio and the undamped natural frequency. Here, however, it will be treated by the rectangular location of the closed loop poles. The closed loop transfer function of the pure second order system was stated as /1/:

$$F_c(s) = \frac{C(s)}{R(s)} = \frac{a^2+b^2}{(s+a)^2+b^2} \tag{3.1}$$

The poles of this system were plotted on the s-plane in Fig. 3-1.

Converting Eq. (3.1) to the frequency response form, it became

$$F_c(j\omega) = \frac{a^2+b^2}{(j\omega+a)^2+b^2} \tag{3.2}$$

3.1 M and ω Calculations

Equation (3.2) rearranged became

$$F_c(j\omega) = \frac{a^2+b^2}{a^2+b^2-\omega^2+2aj\omega} \triangleq M e^{jN} \tag{3.3}$$

from which

$$M = \frac{a^2+b^2}{\sqrt{(a^2+b^2-\omega^2)^2+4a^2\omega^2}} \tag{3.4}$$

Note that if the system gain were constant, then "a" and "b" would be fixed and the magnitude would be a function only of system frequency, i.e., M = f(ω)

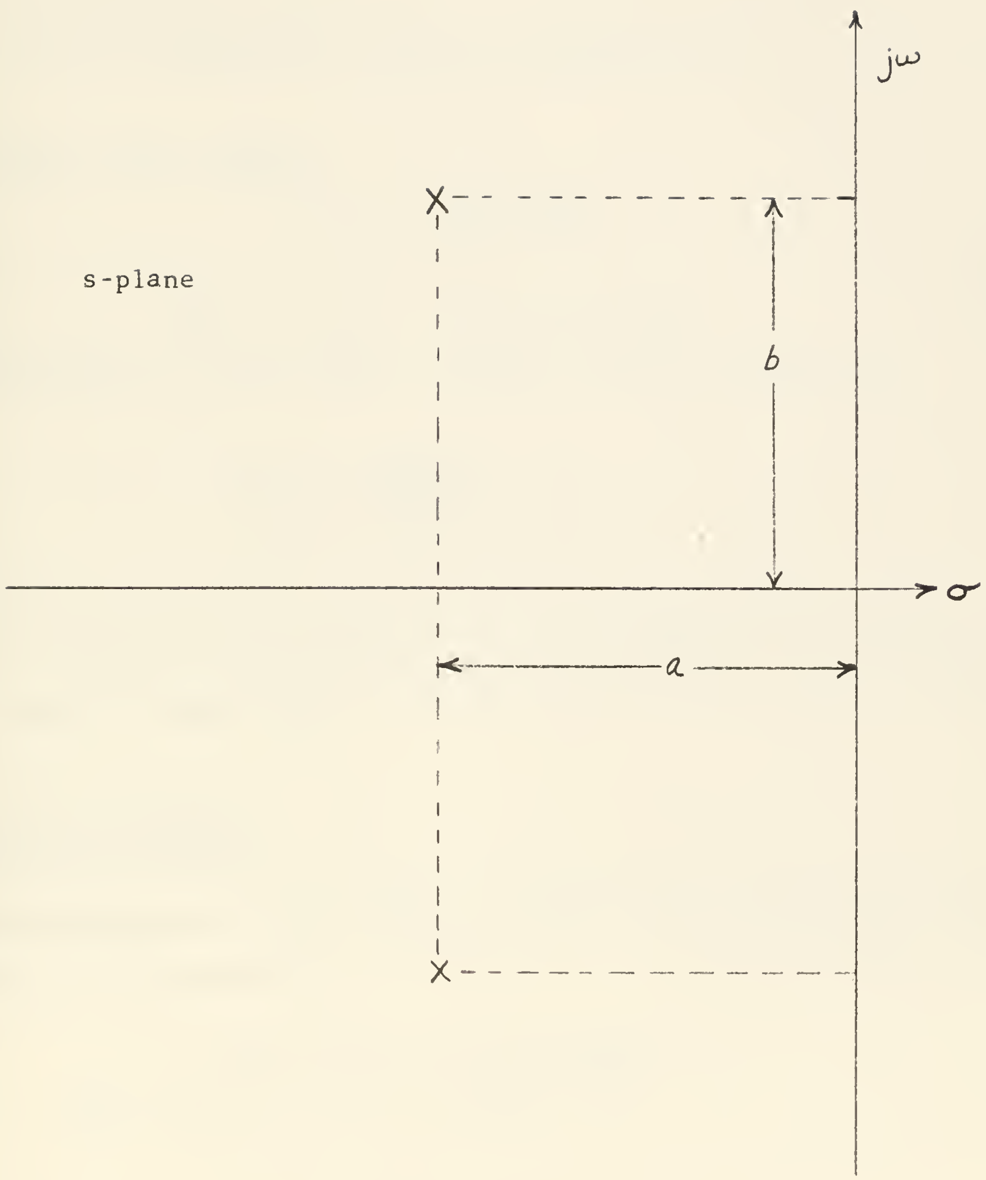

Fig. 3-1 Poles of the Pure Second Order System (s-plane)

3.2 M_p and ω_p Determination

ω_p was obtained by finding the value of ω where the slope of the M versus ω curve was equal to zero. For mathematical convenience, this was done by first squaring Eq. (3.4), then taking the first derivative and setting the numerator equal to zero.

$$-(a^2+b^2)^2\left[2(a^2+b^2-\omega^2)(-2\omega)+8a^2\omega\right]=0 \tag{3.5}$$

Simplifying, this becomes

$$\omega=\omega_p=\sqrt{b^2-a^2} \tag{3.6a}$$

$$\text{and} \quad \omega = 0 \quad \text{(see Section 2.4b)} \tag{3.6b}$$

Substituting Eq. (3.6a) in Eq. (3.4) gave the value of M at ω_p

$$M_p=\frac{a^2+b^2}{2ab} \tag{3.7}$$

Note that from Eq. (3.6), M_p would not occur whenever "a" was less than "b", i.e., when the real part of the pole was greater than the imaginary part. (Figs. 3-2 and 3-3)

3.3 ω_{bw} Determination

The equation for the bandwidth frequency was obtained by substituting the bandwidth magnitude (M = .707) into Eq. (3.4) and solving for the frequency. This resulted in

$$\omega_{bw}=\sqrt{(b^2-a^2)+1.414\sqrt{a^4+b^4}} \tag{3.8}$$

(Fig. 3-4)

3.4 $M_{\omega n}$ and ω_n Determination

The undamped natural frequency was defined as

$$\omega_n \triangleq \sqrt{a^2 + b^2} \tag{3.9}$$

This equation expressed ω_n directly in terms of "a" and "b". (Fig. 3-5) The substitution of ω_n into Eq. (3.4) yielded

$$M_{\omega_n} = \frac{\sqrt{a^2+b^2}}{2a} \tag{3.10}$$

Equation (3.10)expressed $M_{\omega n}$ in terms of the closed loop poles of the system. (Fig. 3-6)

3.5 ω_1 Determination

As defined previously, ω_1 was the frequency, other than zero, at which M was unity. Letting M = 1.0 in Eq. (3.4) and solving for ω_1 yielded

$$\omega_1 = \sqrt{2(b^2 - a^2)} \tag{3.11}$$

Simplifying this expression by recalling $\omega_p = \sqrt{b^2 - a^2}$

resulted in

$$\omega_1 = \sqrt{2}\,\omega_p \tag{3.12}$$

(Fig. 3-7)

3.6 M_k and ω_k Determination

As stated in Section 2, intermediate values of M and N, in addition to those determined above, would result in a smoother plot approximating the M and N contours. The values of k chosen for this class of servo were .5 and 1.5. These particular values were selected as being those

points which would be most beneficial in smoothing the plot of the M and N contours, and because the M_k equation was the same for k = .5 as for k = 1.5. In Section 2,

$$\omega_k \propto k\omega_p$$

or

$$\omega_{k_1} = \sqrt{k_1}\,\omega_p = \sqrt{.5}\,\omega_p$$

and

$$\omega_{k_2} = \sqrt{k_2}\,\omega_p = \sqrt{1.5}\,\omega_p$$

(Fig 3-7)

The value of ω_{k_1} and ω_{k_2} were substituted into Eq. (3.4) and yielded

$$M_k = \frac{2}{\sqrt{1 + \dfrac{12a^2b^2}{(a^2+b^2)^2}}} \qquad (3.13)$$

Where $M_k = M_{k_1} = M_{k_2}$, recalling $\omega_p = \sqrt{b^2 - a^2}$. Loci of constant values of M_k were plotted in relation to "a" and "b". (Fig. 3-8)

3.7 N Calculations

From Eq. (3.3)

$$F_c(j\omega) = \frac{a^2 + b^2}{a^2 + b^2 - \omega^2 + 2aj\omega} \triangleq M\epsilon^{jN}$$

from which,

$$N = -\arctan\left[\frac{2a\omega}{a^2+b^2-\omega^2}\right] \qquad (3.14)$$

Equation (3.14) was then the basic N equation for the pure second order system.

3.8 N_p Determination

ω_p was previously calculated by Eq. (3.6). The substitution of Eq. (3.6) into Eq. (3.14) resulted in the solution of N_p related directly to "a" and "b", the closed loop poles of the system.

$$N_p = -\arctan\left[\frac{\sqrt{b^2 - a^2}}{a}\right] \tag{3.15}$$

Loci of constant values of N_p were then determined for all possible "a" and "b" values. (Fig. 3-9)

It is pertinent to note that the equations presented were in most cases not solved as stated. Algebraic manipulations were performed to make the equation compatible to digital calculations by writing the equations in terms of "b" as a function of "a" and the particular parameter.

3.9 $N_{\omega n}$ Determination

$N_{\omega n}$ was determined in a manner similar to N_p. The value of ω_n in terms of "a" and "b" was stated in Eq. (3.10). This relationship of ω_n was substituted in Eq. (3.14) and resulted in

$$N_{\omega_n} = -\arctan\left[\frac{2a\sqrt{a^2+b^2}}{a^2+b^2-\left(\sqrt{a^2+b^2}\right)^2}\right] \tag{3.16}$$

which simplified to

$$N_{\omega_n} = -\arctan\left[\frac{2a\sqrt{a^2+b^2}}{0}\right]$$

or

$$N_{\omega n} = -90^{\circ}$$

Thus, $N_{\omega n}$ for a pure second order system was a constant and equal to -90°.

3.10 N_{bw} Determination

The equation for N_{bw} in terms of "a" and "b" was obtained by substituting Eq. (3.8) into Eq. (3.14). This resulted in

$$N_{bw} = -\arctan\left[\frac{2a\sqrt{b^2 - a^2 + 1.414\sqrt{a^4 + b^4}}}{2a^2 - 1.414\sqrt{a^4 + b^4}}\right] \tag{3.17}$$

(Fig. 3-10)

3.11 N_1 Determination

Equation (3.12) determined the values of ω when M = 1.0 for non-zero frequencies. When the expression of ω_1, determined from Eq. (3.12), was substituted into Eq. (3.14),

$$N_1 = -\arctan\left[\frac{2a\sqrt{2(b^2 - a^2)}}{3a^2 - b^2}\right] \tag{3.18}$$

Solutions to Eq. (3.18) were plotted as constant N_1 loci for all values of "a" and "b". (Fig. 3-11)

3.12 N_k Determination

As stated above, the k values selected were .5 and 1.5 where $\omega_k \triangleq \sqrt{k}\,\omega_p$. In a manner similar to the determination of N_1 above,

$$N_k = -\arctan\left[\frac{2a\sqrt{k(b^2 - a^2)}}{a^2(1+k) + b^2(1-k)}\right] \tag{3.19}$$

from which N_k values were determined explicitly in terms of "a" and "b" for both values of k. (Figs. 3-12 and 3-13)

3.13 Use of the Curves

At this point, all the selected parameters necessary to sketch the M and N contours have been determined from the location of the closed loop poles. With the values of the closed loop poles known and the

curves plotted as described above, a rapid graphical approximation of the frequency response of the pure second order system can be constructed. For convenience, the following recommended procedure is presented for the use of the pure second order curves:

a. Enter Fig. 3-2 with the complex pole coordinates $-a + jb$, and obtain M_p. Enter Fig. 3-3 with $-a + jb$, and obtain ω_p. (Note that ω_p is the ordinate in Fig. 3-3.)

b. Similarly obtain ω_{bw} ($M = .707$) from Fig. 3-4, ω_n and $M_{\omega n}$ from Figs. 3-5 and 3-6 respectively.

c. Obtain ω_1 ($M = 1.0$) from Fig. 3-7, entering with the ω_p determined above.

d. Obtain M_k for both $k_1 = .5$ and $k_2 = 1.5$ from Fig. 3-8, entering with "a" and "b". Determine ω_{k_1}, $(\omega_{k_1} = \sqrt{.5}\,\omega_p)$,

and ω_{k_2}, $(\omega_{k_2} = \sqrt{1.5}\,\omega_p)$,

from Fig. 3-7, entering with the value of ω_p obtained from step (a) above.

The M contour for the specified closed loop poles may then be sketched, having easily obtained the M and corresponding ω for six known points and realizing that $M = 0$ and has a slope of zero at $\omega = 0$, and also that the slope is zero at ω_p and at $\omega = \infty$.

The N contour points are obtained in the same manner by using Figs. 3-9 through 3-12 to obtain the values of N corresponding to the same frequencies found for the M contour above. The one exception is $N_{\omega n}$, which is always equal to -90^o for this system. Using these N, ω values and knowing that $N = 0^o$ and has zero slope for $\omega = 0$, and also that $N = -180^o$ for $\omega = \infty$ for a pure second order system, the N contour can now be accurately sketched.

Note that this paper does not present curves which will give any values at frequencies higher than ω_{bw}, since it is unlikely that there would ever be any interest in the region beyond the bandwidth frequency.

3 14 Example

Given: $-a \pm jb = -1 \pm j2$

Solution:

SPECIFIC DATA

TABLE OF PARAMETER VALUES

x	ω_x	ω_x Fig. No.	M_x	M_x Fig. No.	N_x	N_x Fig. No.
p	1.71	3-2	1.25	3-3	-60°	3-9
bw	2.95	3-4	.707	N.A.	-123°	3-10
ω_n	2.25	3-5	1.12	3-6	-90°	N.A.
1	2.42	3-7	1.0	N.A.	-101°	3-11
k_1	1.22	3-7	1.175	3-8	-35°	3-12
k_2	2.10	3-7	1.175	3-8	-82°	3-13

GENERAL DATA (for all pure second order systems)

ω	M	$dM/d\omega$	N	$dN/d\omega$
0	1.0	0	0°	0
ω_p	M_p	0	——	——
∞	0	0	-180°	0

Fig 3-14 (page 17) compares the frequency response obtained from this rapid approximation method to the actual M and N contours obtained from a digital computer program of the general M and N equations.

Note: Although a scale is shown on these pure second order curves for convenience, the loci are really independent of scale as they depend only on the ratio of "a" to "b" Hence, any convenient scale for σ, $j\omega$, and ω_x may be substituted for the scales shown as long as all scales are in agreement.

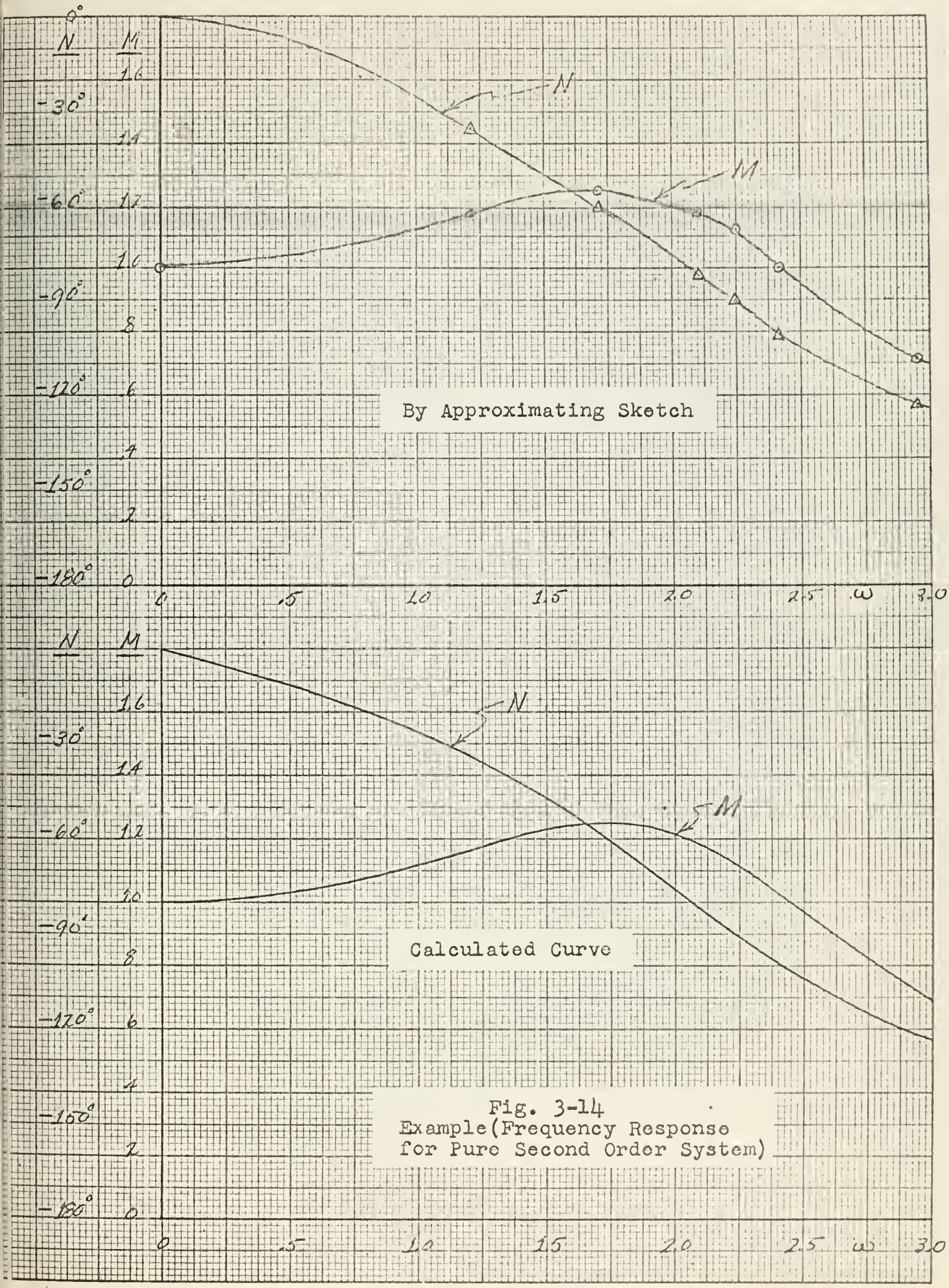

Fig. 3-14
Example(Frequency Response
for Pure Second Order System)

Fig. 3-2
ω_p for Pure Second Order System

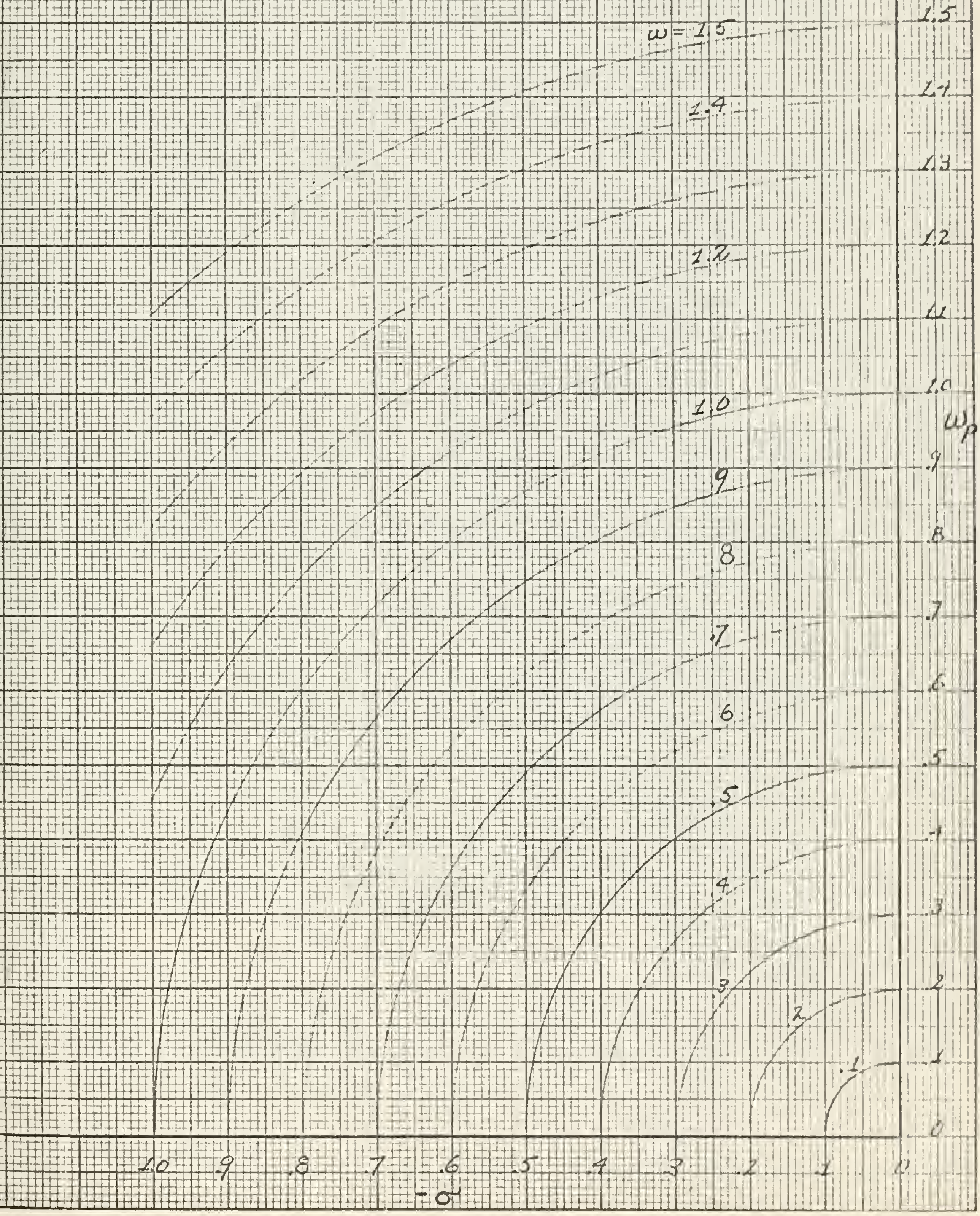

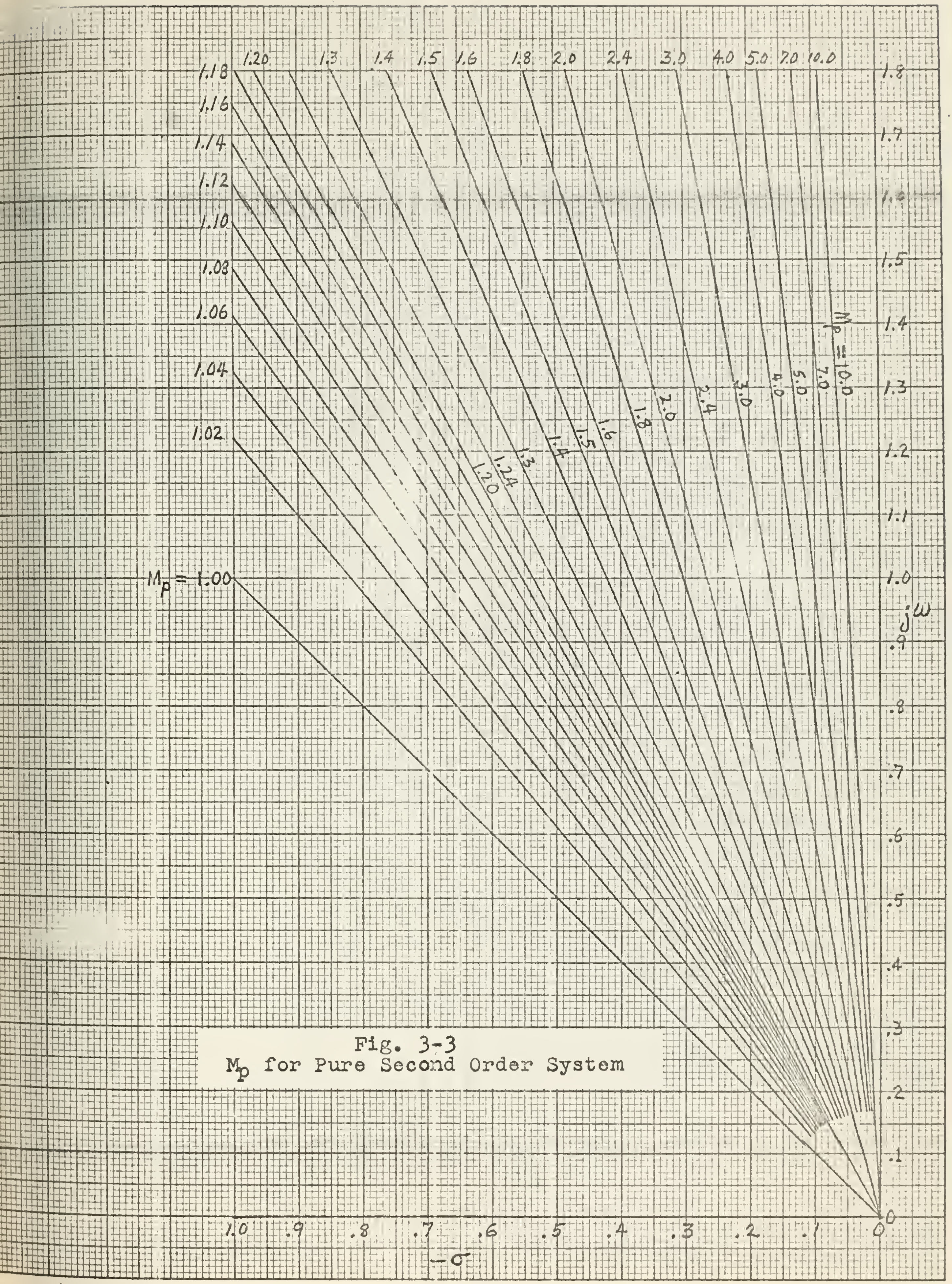

Fig. 3-3
M_p for Pure Second Order System

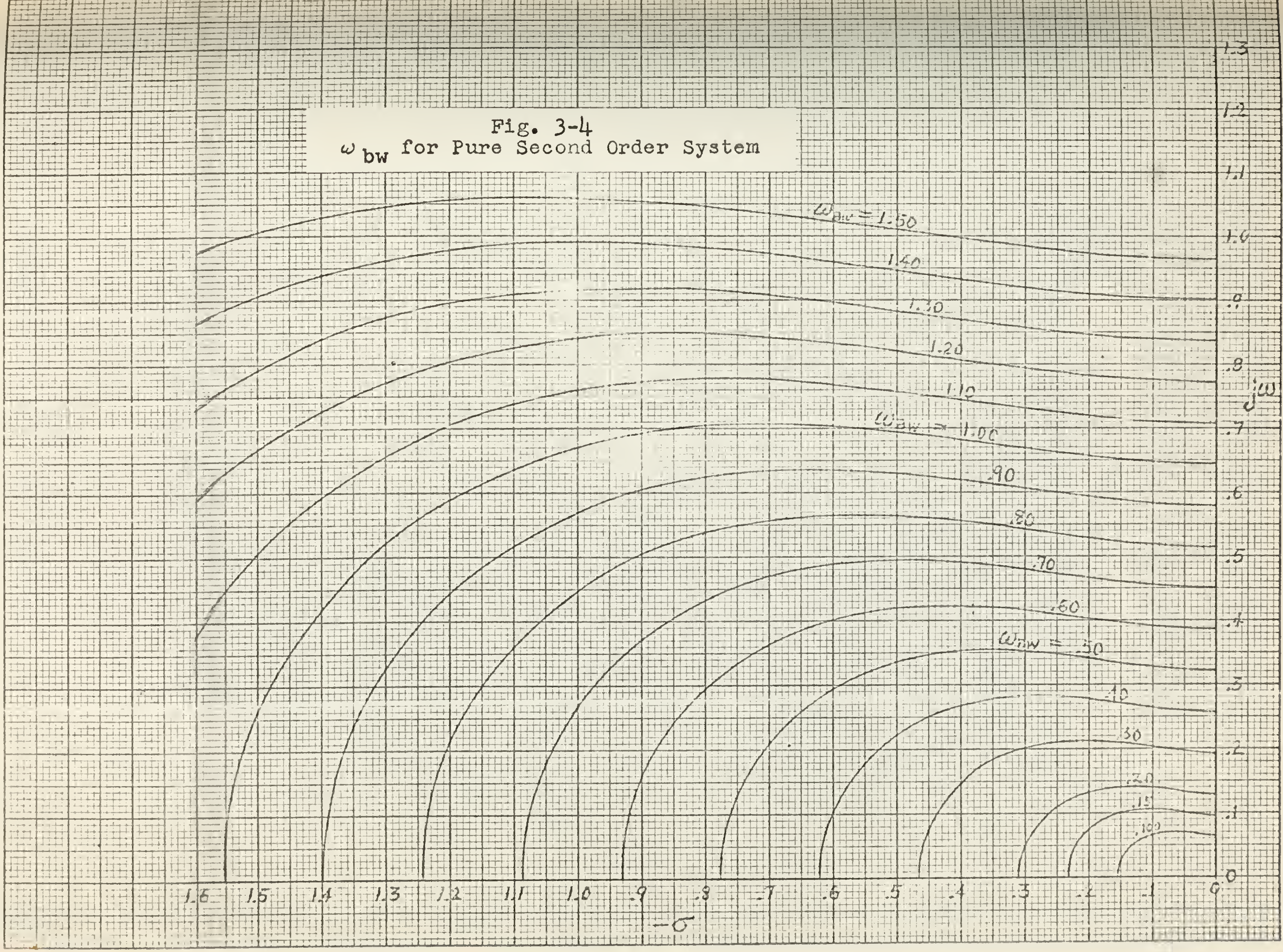

Fig. 3-4
ω_{bw} for Pure Second Order System

Fig. 3-5
ω_n for Pure Second Order System

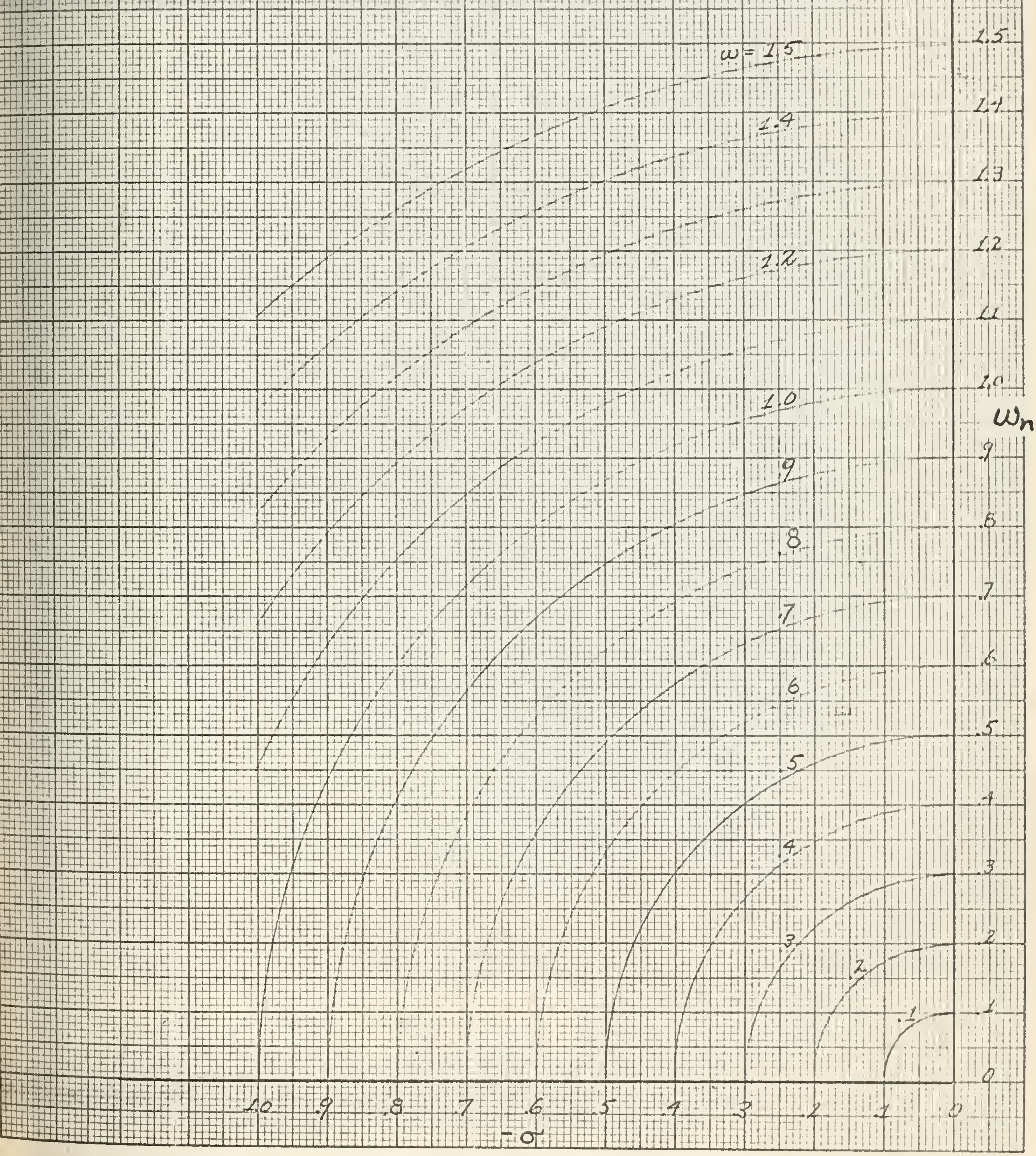

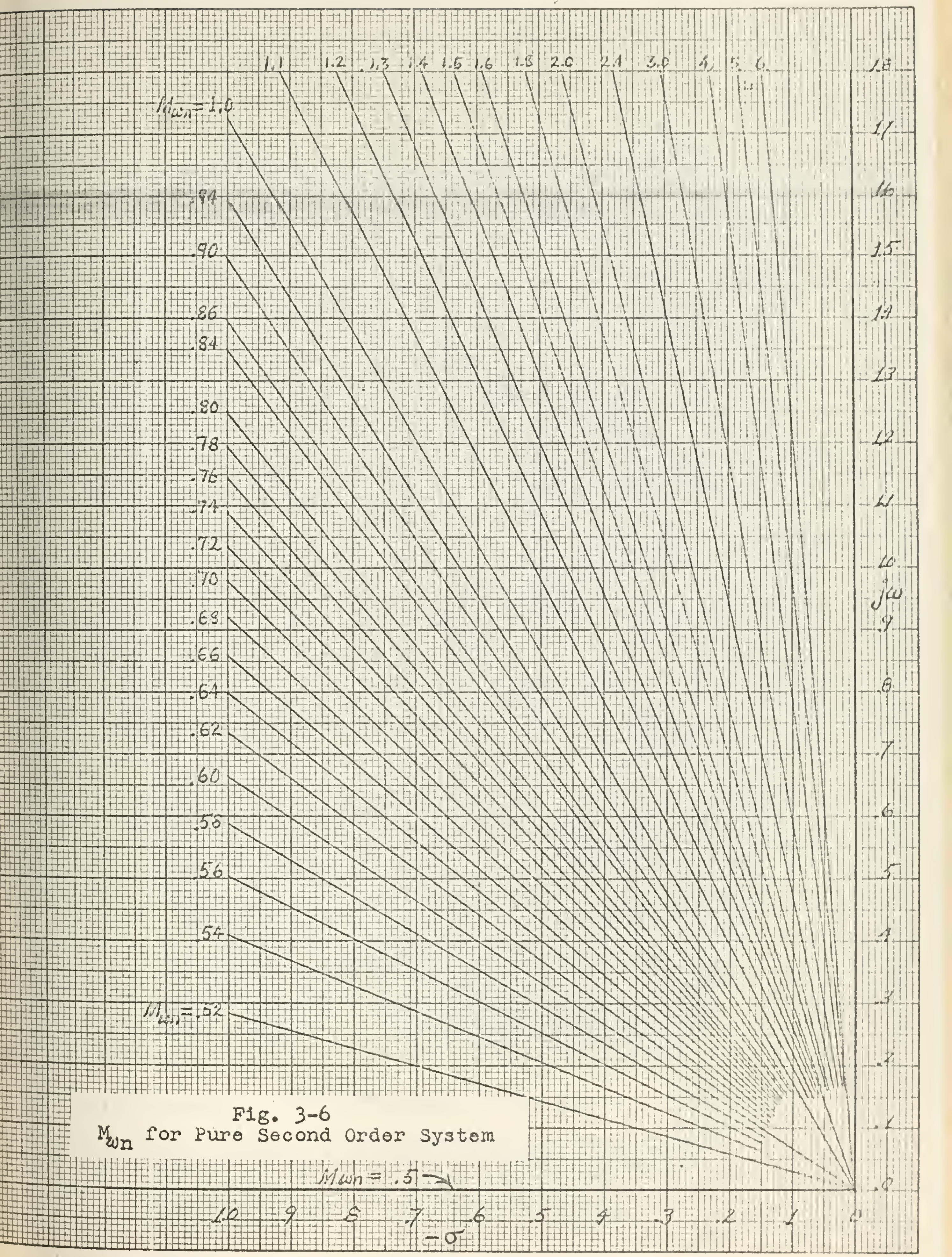

Fig. 3-6
$M_{\omega n}$ for Pure Second Order System

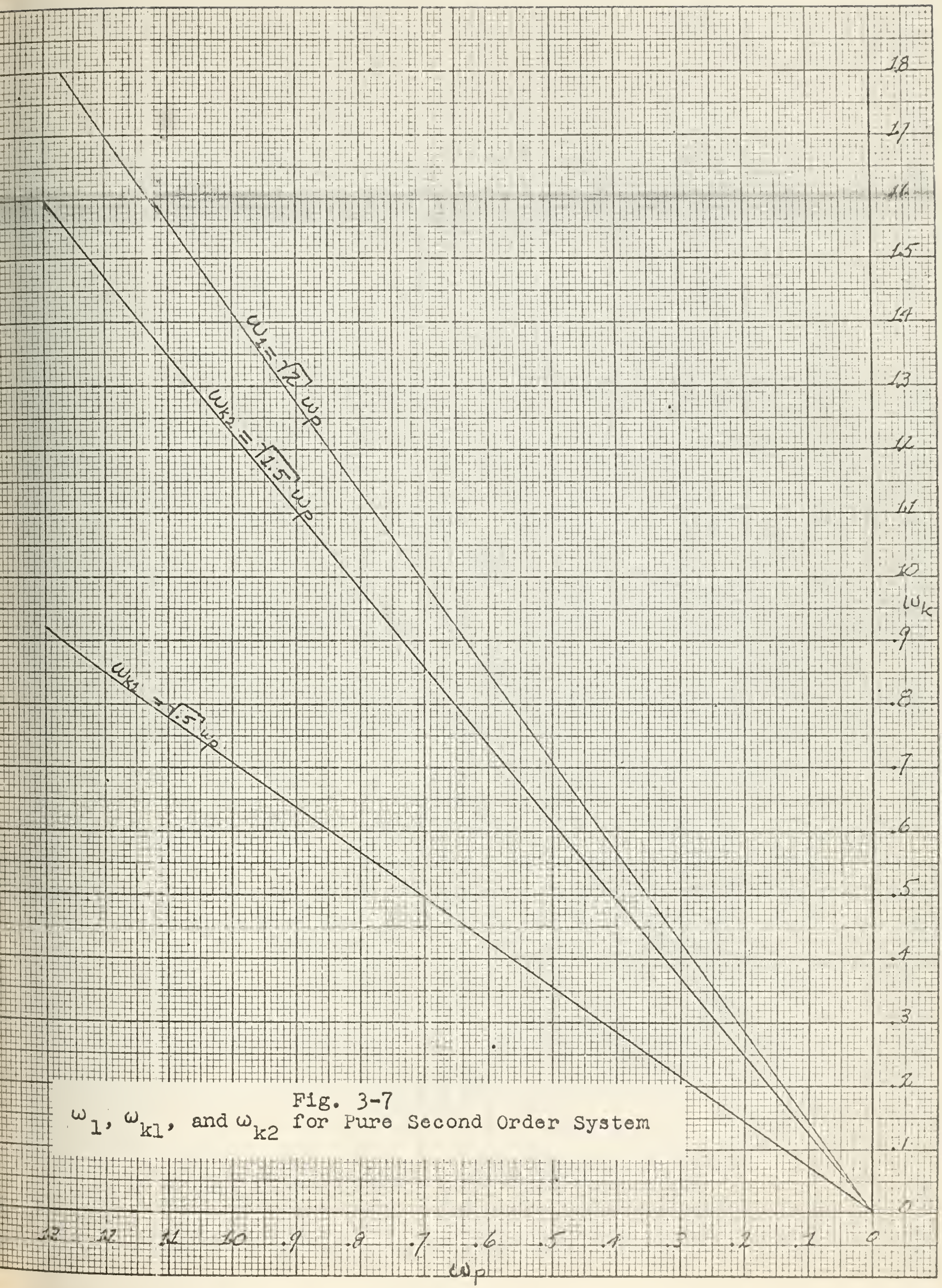

Fig. 3-7
ω_1, ω_{k1}, and ω_{k2} for Pure Second Order System

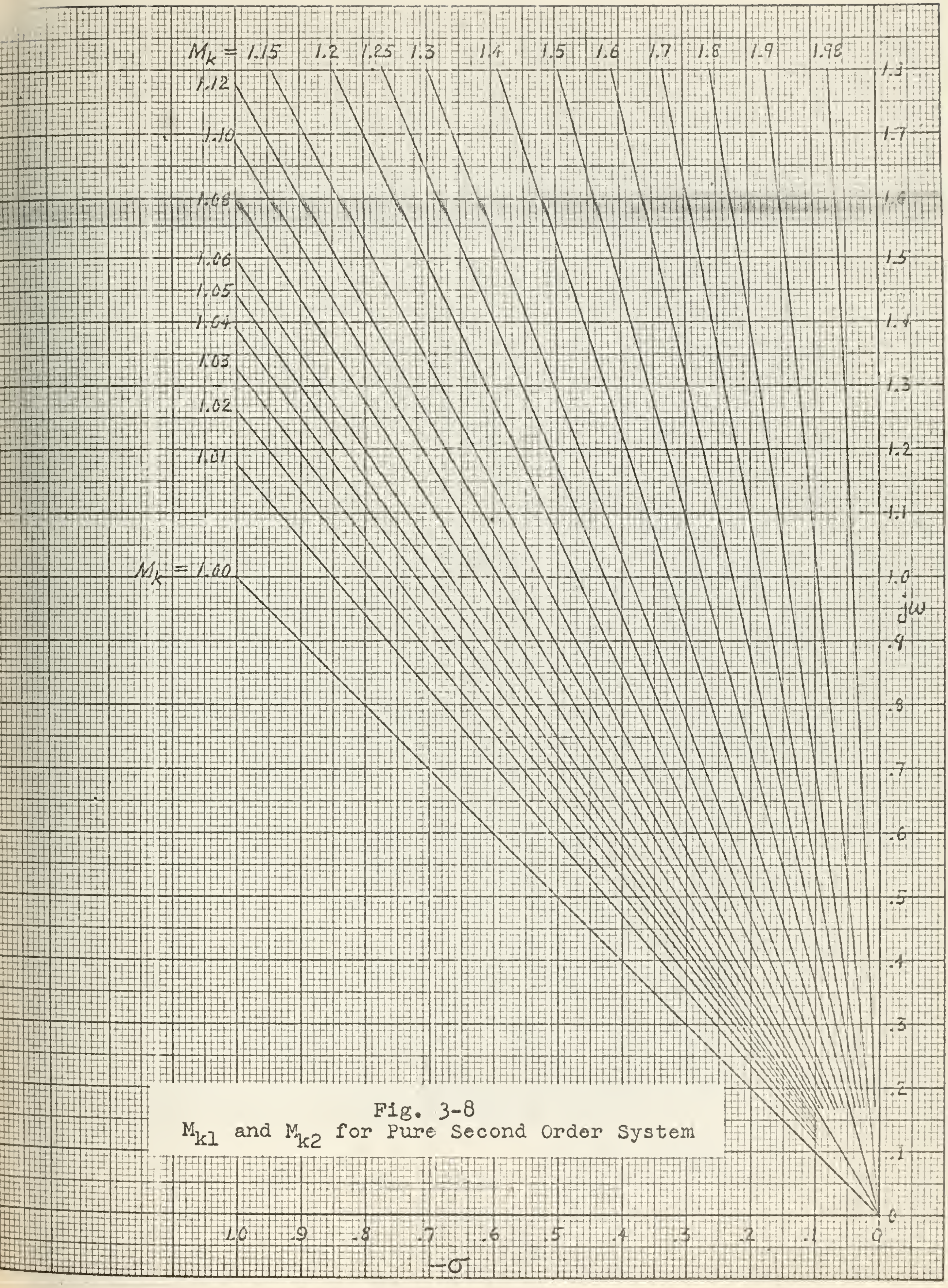

Fig. 3-8
M_{k1} and M_{k2} for Pure Second Order System

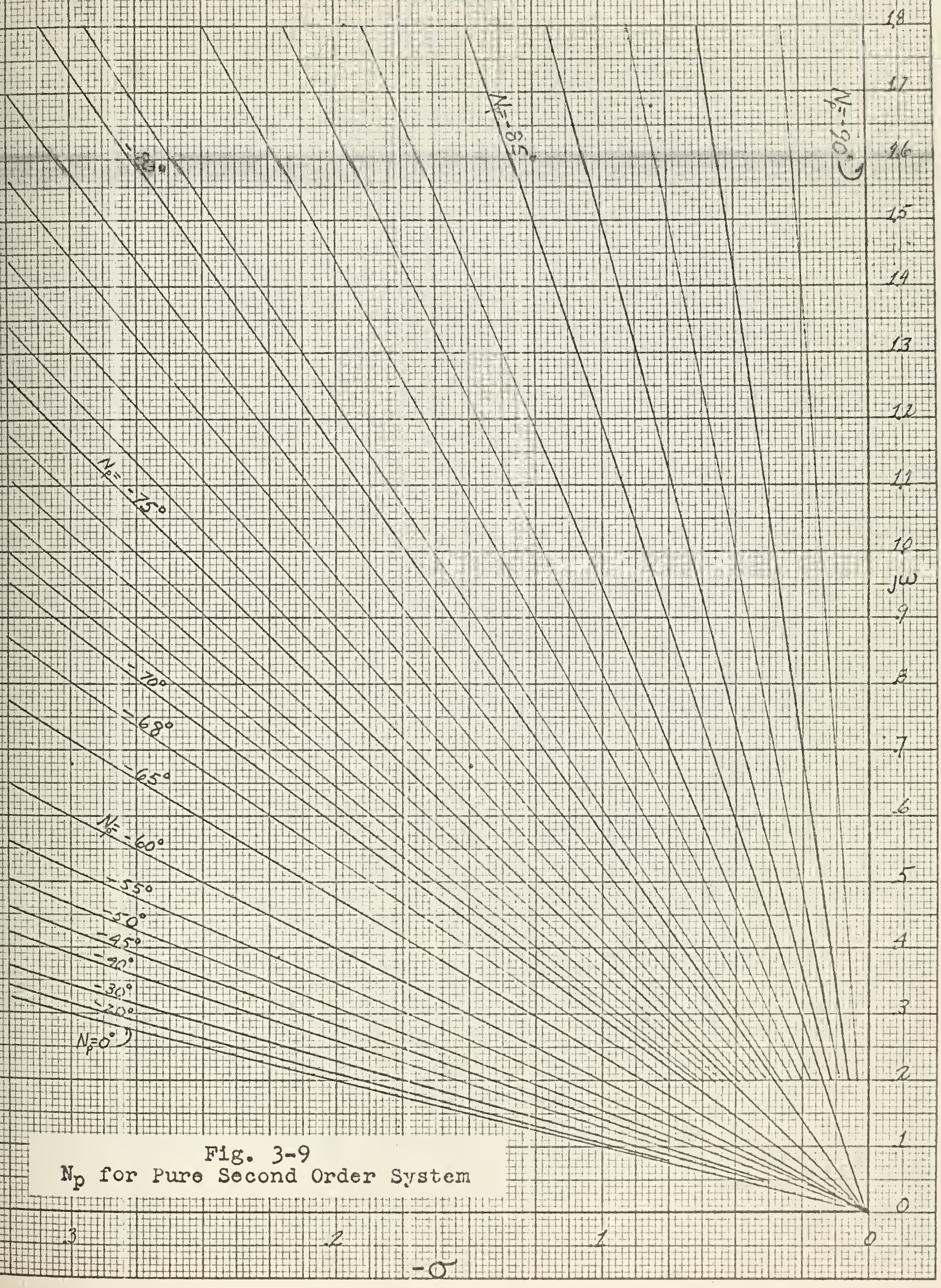

Fig. 3-9
N_p for Pure Second Order System

Fig. 3-10
N_{bw} for Pure Second Order System

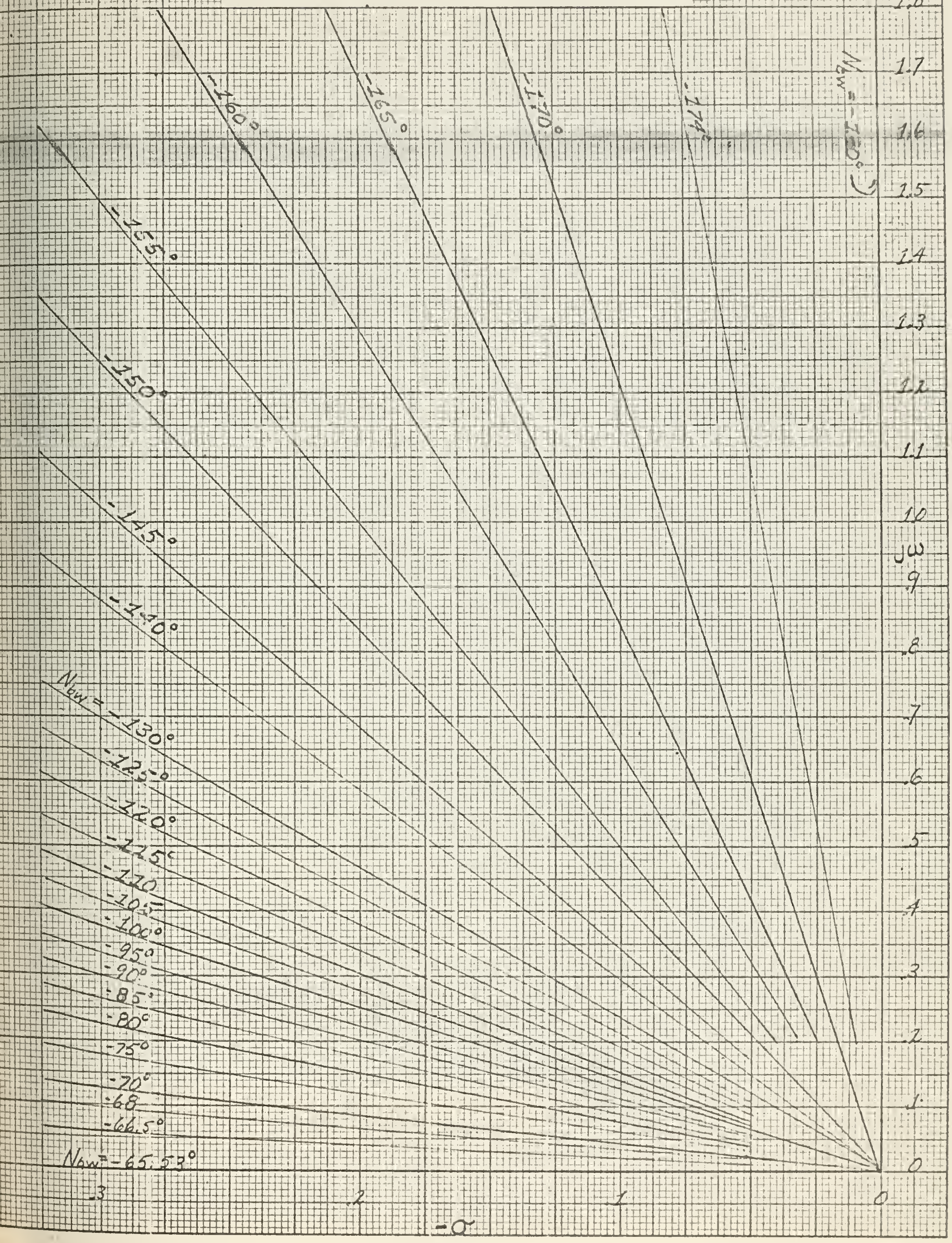

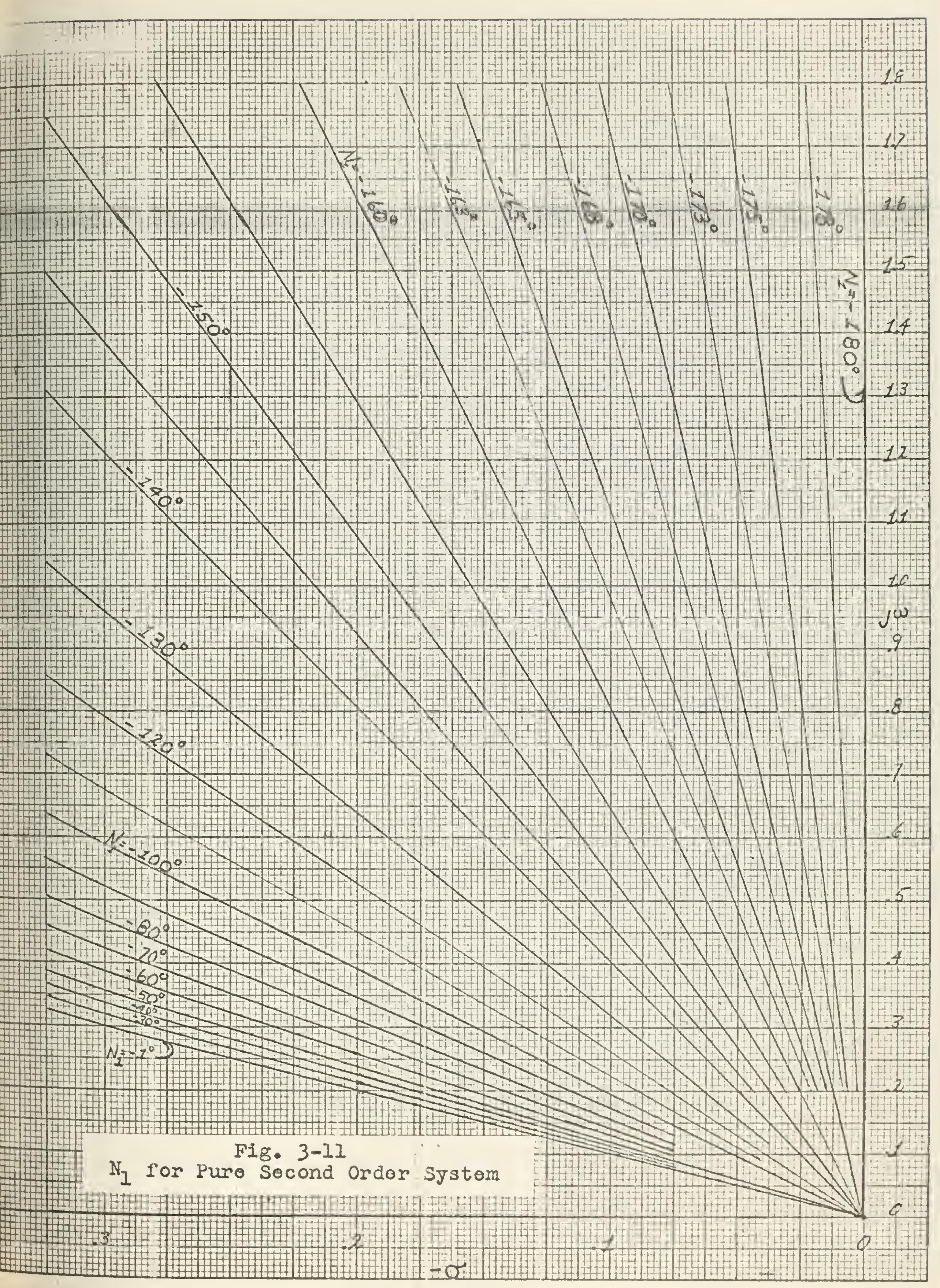

Fig. 3-11
N_1 for Pure Second Order System

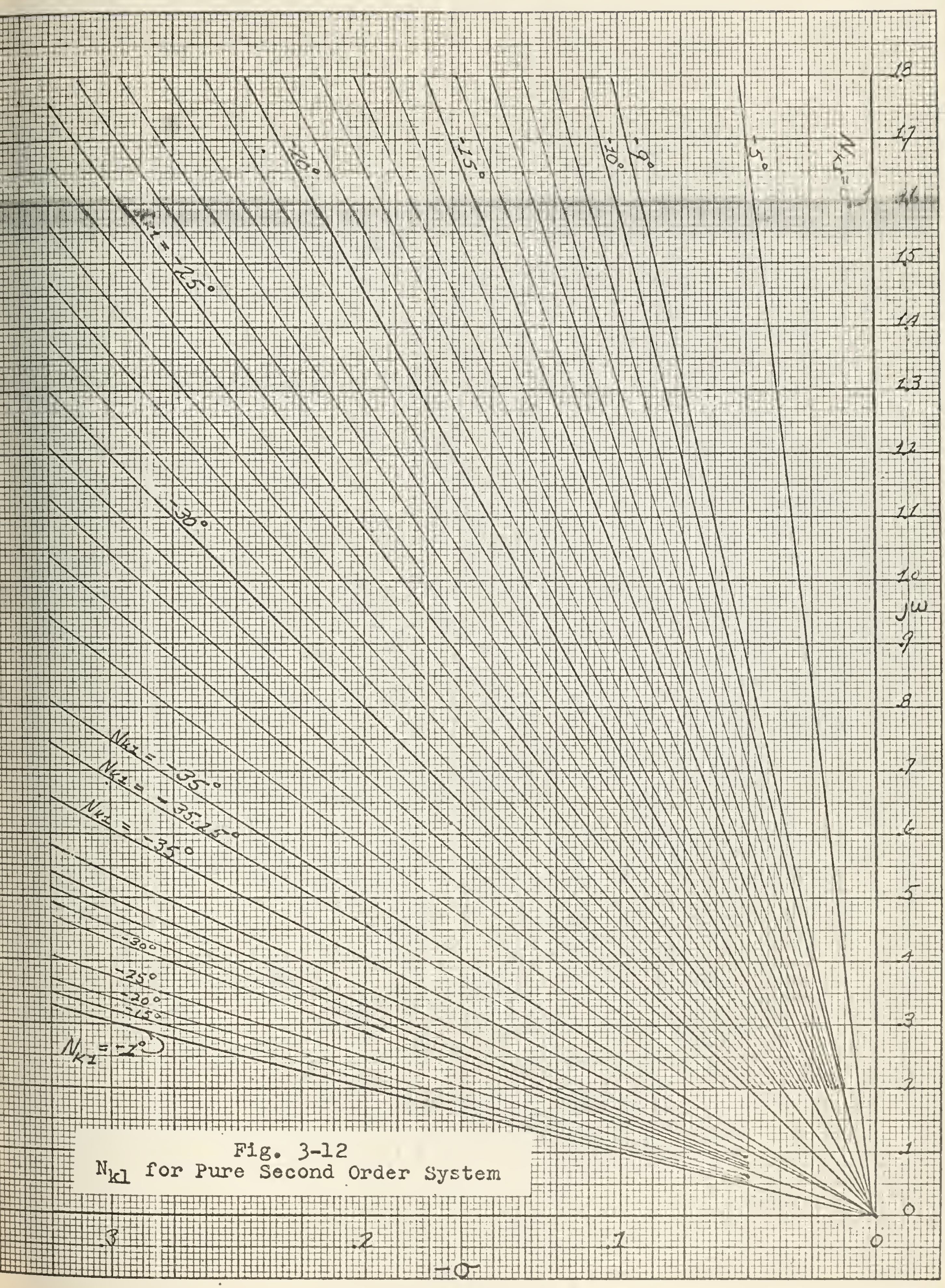

Fig. 3-12
N_{k1} for Pure Second Order System

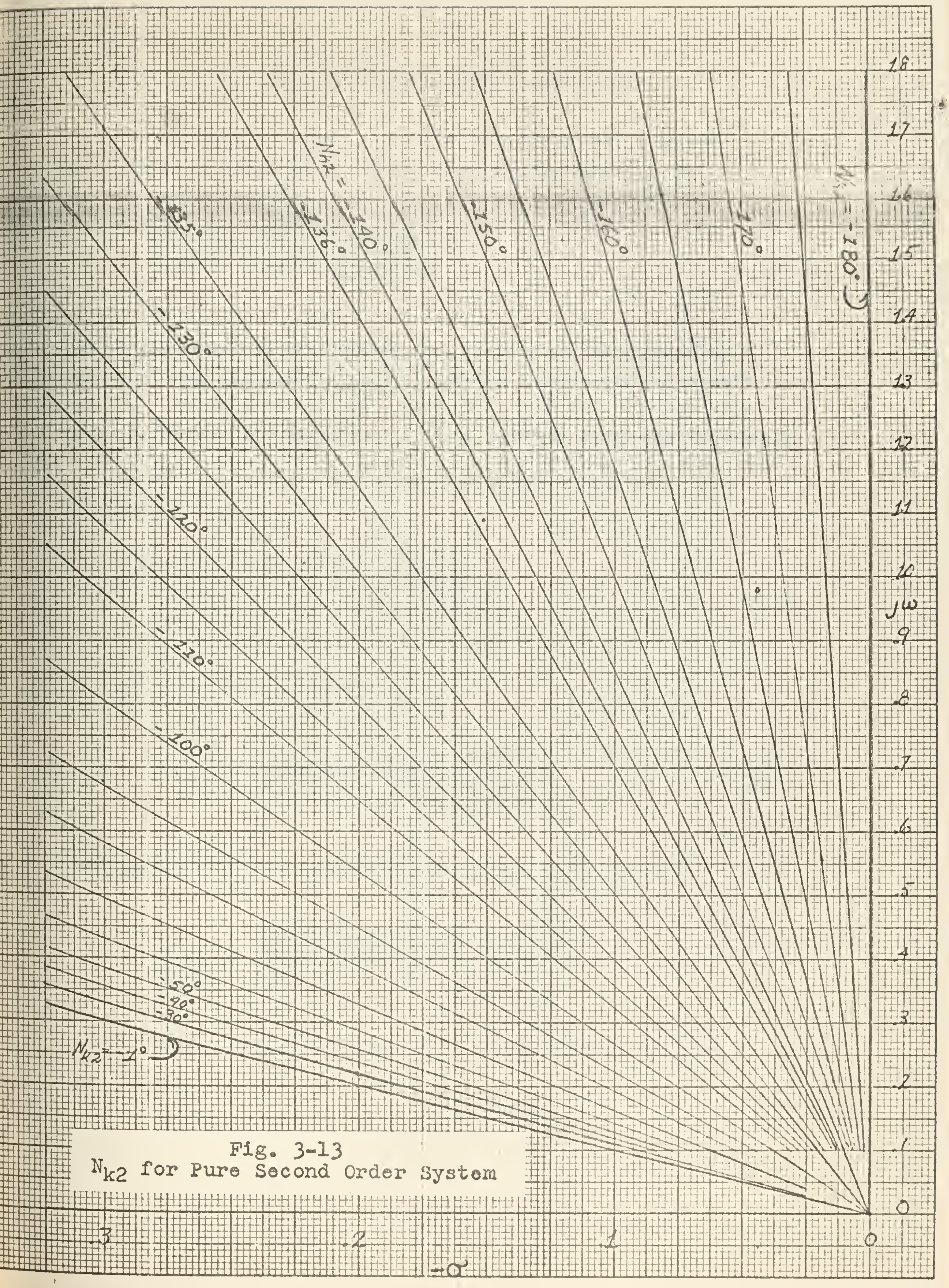

Fig. 3-13
N_{k2} for Pure Second Order System

4. THE SECOND ORDER SYSTEM WITH ONE ZERO

The addition of a real zero to a pure second order system resulted in a system whose closed loop transfer function was

$$F_c(s) = \frac{a^2+b^2}{d} \cdot \frac{(s+d)}{(s+a)^2+b^2} \tag{4.1}$$

The singularities of this system were plotted on the s-plane in Fig. 4-1. The constant $\frac{a^2 + b^2}{d}$, usually interpreted as system gain, reflected the assumption of unity feedback as stated previously.

By letting $s = j\omega$, the frequency response form of Eq. (4.1) resulted in

$$F_c(j\omega) = \frac{a^2+b^2}{d} \cdot \frac{(j\omega+d)}{(j\omega+a)^2+b^2} \tag{4.2}$$

This expanded and rearranged became

$$F_c(j\omega) = \frac{(da^2+db^2)+j(\omega a^2+\omega b^2)}{(da^2+db^2-d\omega^2)+j(2da\omega)} \tag{4.3}$$

Dividing the numerator and denominator of Eq. (4.3) by d^3,

$$F_c(j\omega) = \frac{\left(\frac{a^2}{d^2}+\frac{b^2}{d^2}\right)+j\left(\frac{\omega}{d}\cdot\frac{a^2}{d^2}+\frac{\omega}{d}\cdot\frac{b^2}{d^2}\right)}{\left(\frac{a^2}{d^2}+\frac{b^2}{d^2}-\frac{\omega^2}{d^2}\right)+j\left(2\frac{a}{d}\cdot\frac{\omega}{d}\right)} \tag{4.4}$$

From Eq. (4.4), it was seen that "a", "b", and ω may all be referred to the zero location, d.

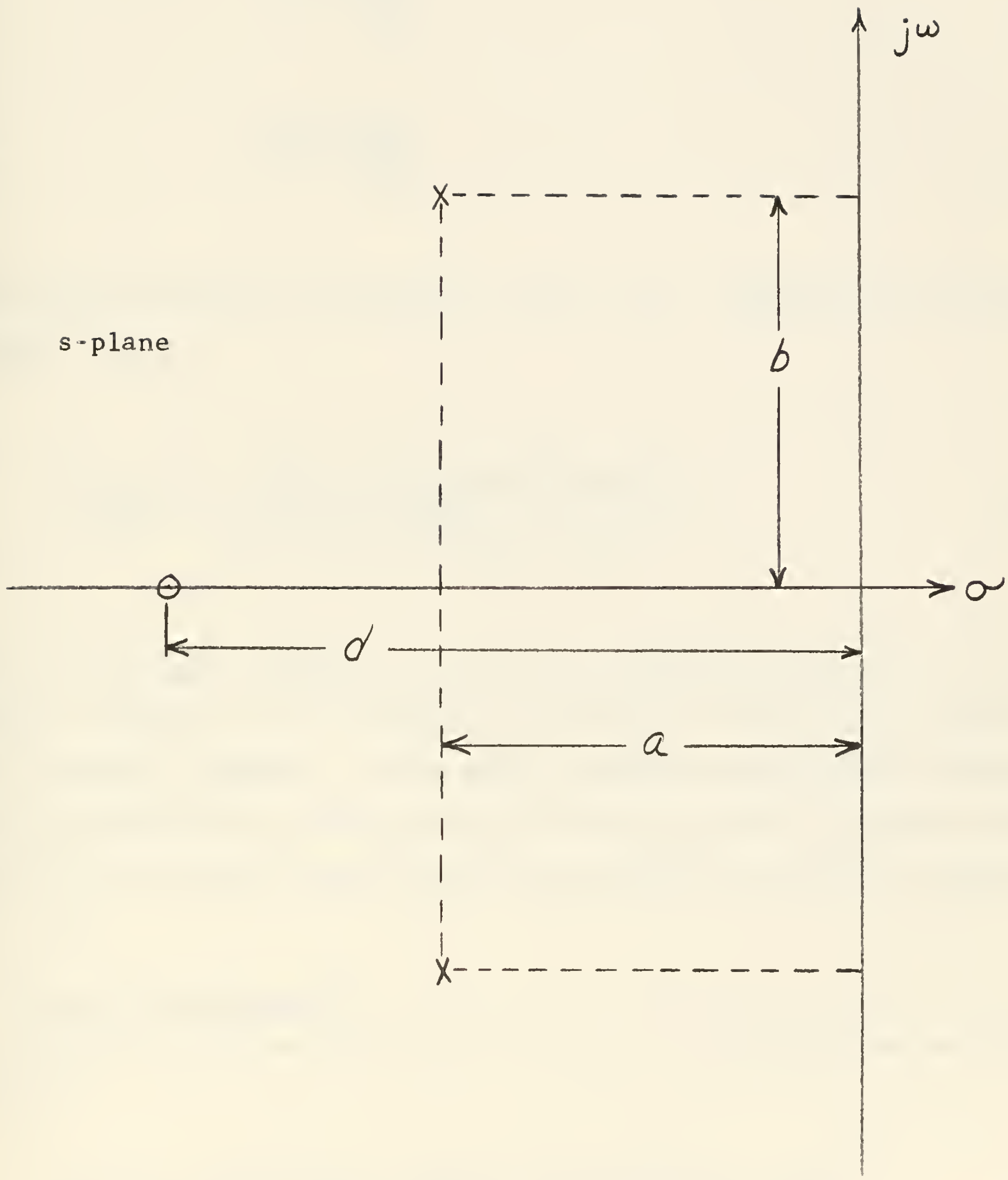

Fig. 4-1 Poles and Zero of the Second Order System with One Zero (s-plane)

From Eq. (4.4),

$$m_1 \triangleq \frac{a}{|d|} \tag{4.5}$$

$$m_2 \triangleq \frac{b}{|d|} \tag{4.6}$$

and

$$\Omega \triangleq \frac{\omega}{|d|} \tag{4.7}$$

These quantities were illustrated in Fig. 4-2. Equation (4.4) then became

$$F_c(j\omega) = \frac{(m_1^2 + m_2^2) + j(\Omega m_1^2 + \Omega m_2^2)}{(m_1^2 + m_2^2 - \Omega^2) + j(2m_1\Omega)} \tag{4.8}$$

Thus the frequency response for the second order system with one zero became a function of the "referred" location of the complex roots and the "referred" frequency. This means then that the frequency response was the same for all systems having the same relative pole-zero configuration when the frequency was also referred to the zero location. (Fig. 4-3)

4.1 M and Ω Calculations

Equation (4.8) was expressed in terms of its magnitude and phase angle by

$$F_c(j\omega) = \frac{(m_1^2 + m_2^2) + j(\Omega m_1^2 + \Omega m_2^2)}{(m_1^2 + m_2^2 - \Omega^2) + j(2m_1\Omega)} \triangleq M\epsilon^{jN} \tag{4.9}$$

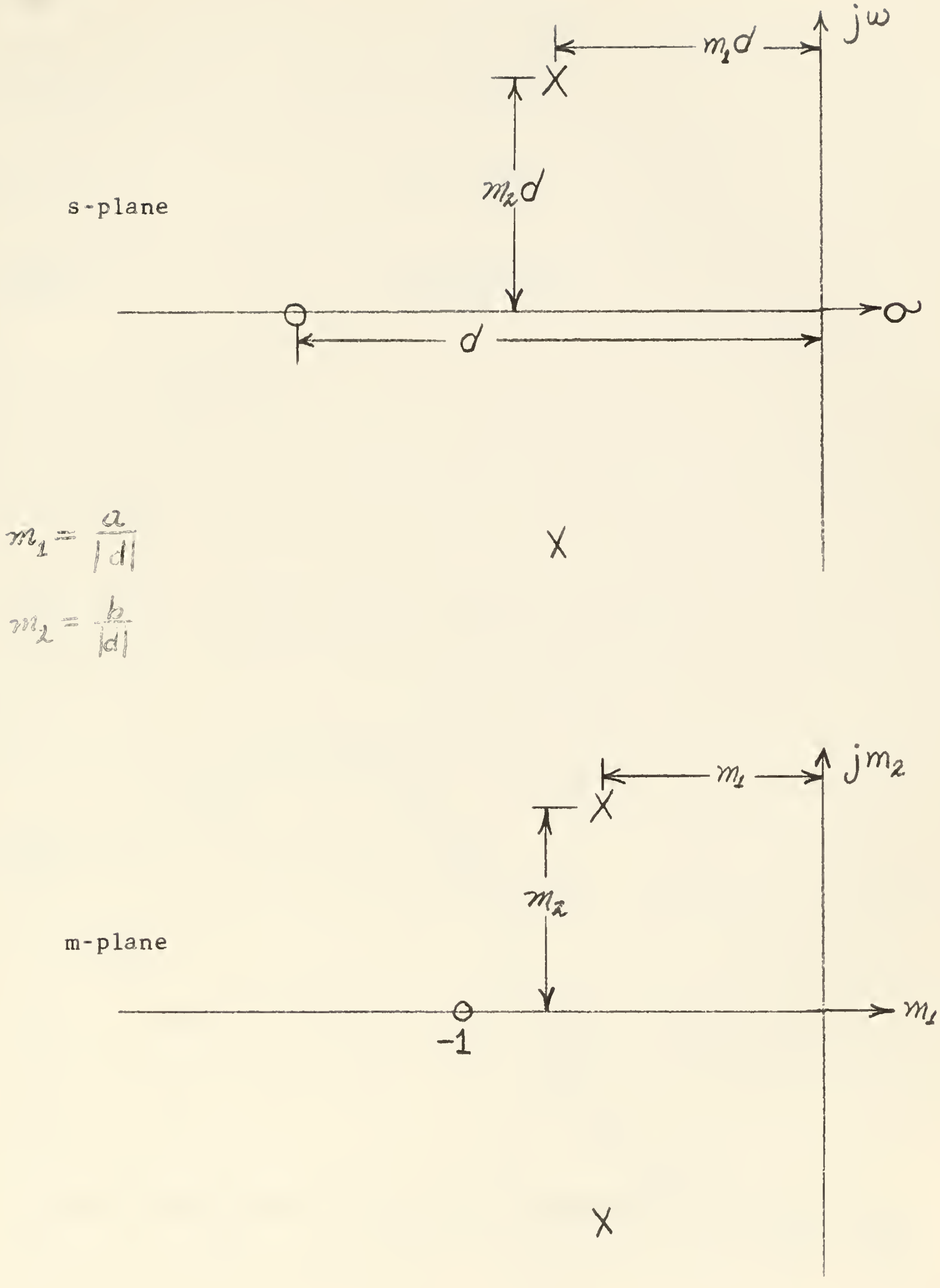

Fig. 4-2 Referred Quantities of m_1 and m_2, Second Order System with One Zero

System A:

$a = 1.0$

$b = 2.0$

$d = 1.0$

$m_1 = \frac{a}{|d|} = 1.0$

$m_2 = \frac{b}{|d|} = 2.0$

System B:

$a = .01$

$b = .02$

$d = .01$

$m_1 = \frac{a}{|d|} = 1.0$

$m_2 = \frac{b}{|d|} = 2.0$

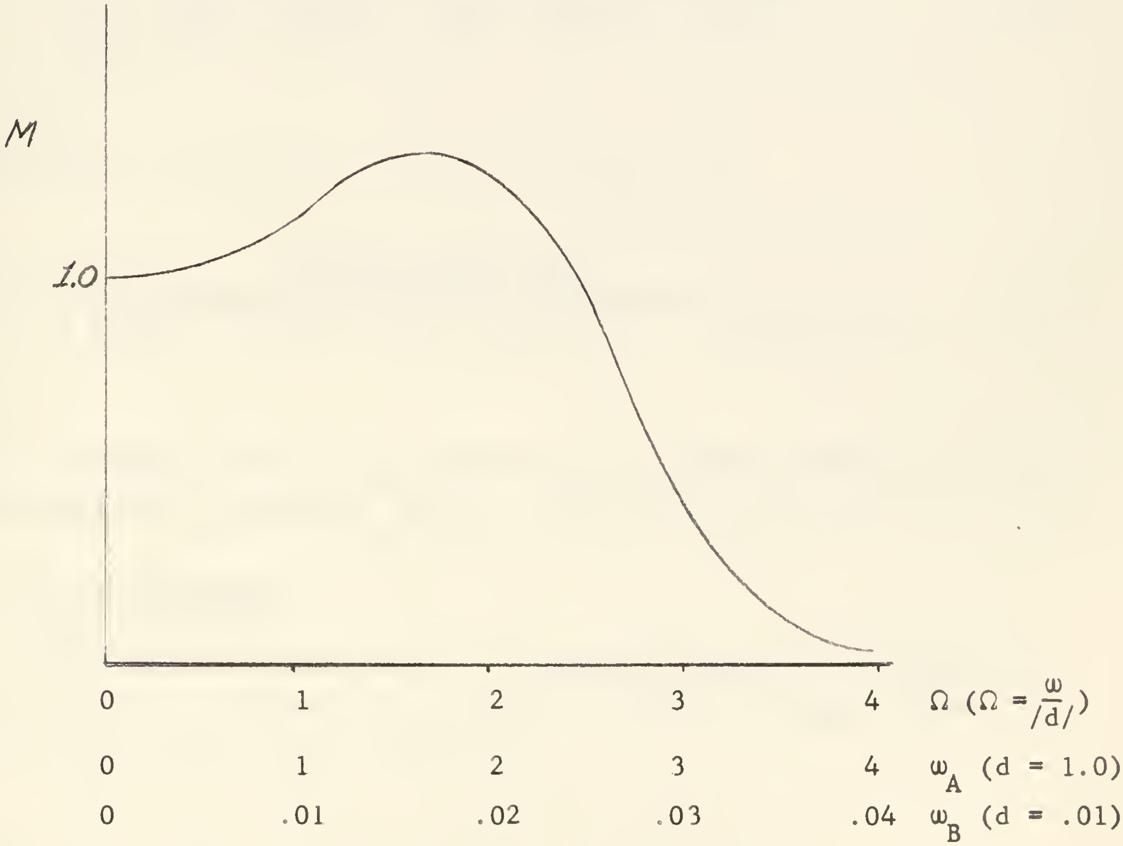

Fig. 4-3 Frequency Response of Two Systems with the Same Relative Pole-Zero Configuration, Second Order System with One Zero

From this,

$$M = \frac{\sqrt{(m_1^2+m_2^2)^2 + \Omega^2 (m_1^2+m_2^2)^2}}{\sqrt{(m_1^2+m_2^2-\Omega^2)^2 + 4 m_1^2 \Omega^2}} \tag{4.10}$$

Equation (4.10) was the basic M equation for the second order system with one zero.

4.2 M_p and Ω_p Determination

The equation for Ω_p was obtained by first squaring Eq. (4.10), then differentiating with respect to Ω and setting the numerator of this equal to zero. This reduced to

$$\Omega_p = \sqrt{-1 + \sqrt{(m_1^2+m_2^2)^2 - 2(m_1^2 - m_2^2) + 1}} \tag{4.11}$$

Substituting this into Eq. (4.10) and simplifying,

$$M_p = \sqrt{\frac{m_1^4 + 2m_1^2 m_2^2 + m_2^4}{2\sqrt{m_1^4 + 2m_1^2 m_2^2 + m_2^4 - 2m_1^2 + 2m_2^2 + 1} \; + 2(m_1^2 - m_2^2 - 1)}} \tag{4.12}$$

Loci of constant values of m_2 were solved by digital computer and were plotted against m_1 versus M_p and Ω_p. (Figs. 4-4 and 4-5).

4.3 Ω_{bw} Determination

The equation for the referred bandwith frequency was obtained by substituting M = .707 into Eq. (4.10) and solving for Ω_{bw}. After considerable algebra, this reduced to

$$\Omega_{bw} = \left\{ (m_1^2+m_2^2)^2 - m_1^2 + m_2^2 + \left[2(m_1^2+m_2^2)^2 \left[m_2^2 - m_1^2 + \frac{(m_1^2+m_2^2)^2}{2} + 1 \right] - 4 m_1^2 m_2^2 \right]^{1/2} \right\}^{1/2} \tag{4.13}$$

(Fig. 4-6)

4.4 $M_{\Omega n}$ and Ω_n Determination

The referred undamped natural frequency was defined for this system as

$$\Omega_n \triangleq \sqrt{m_1^2 + m_2^2} \qquad (4.14)$$

This expressed Ω_n as a function of m_1 and m_2. (Fig. 4-7)

Substituting Eq. (4.14) into Eq. (4.10) and simplifying yielded

$$M_{\Omega n} = \sqrt{\frac{(m_1^2 + m_2^2)^2 + (m_1^2 + m_2^2)}{4 m_1^2}} \qquad (4.15)$$

(Fig. 4-8)

4.5 Ω_1 Determination

As defined previously, Ω_1 was the referred frequency other than zero at which M is unity. The equation for Ω_1 was found by letting M = 1.0 in Eq. (4.10) and solving for Ω_1.

$$\Omega_1 = \sqrt{(m_1^2 + m_2^2)^2 - 2(m_1^2 - m_2^2)} \qquad (4.16)$$

(Fig. 4-9)

4.6 M_k and Ω_k Determination

The use of the curves mentioned up to this point for this class of system provided the four main points required to sketch roughly the M contour. In order to "fill-in" the blank portions of the contour on both sides of Ω_p, it was decided to provide curves for three additional points on the M contour in the same manner as was done for the pure second order system. The use of these additional points was not necessary to sketch the frequency response; however, their use provided a more accurate approximation of the M contour.

As in the pure second order system, the following definition was made

$$\Omega_k \triangleq \sqrt{k}\,\Omega_p \tag{4.17}$$

where k is a constant.

Substituting into Eq. (4.11) for Ω_p,

$$\Omega_k = \sqrt{-k + k\sqrt{(m_1^2+m_2^2)^2 - 2(m_1^2-m_2^2)+1}} \tag{4.18}$$

Values of .5, 1.5 and 2.5 were selected for k. M_k solutions were obtained for each k value by solving Eq. (4.18) for Ω_k and then substituting this value into the basic M equation with the same values of m_1 and m_2. This was accomplished handily by one digital program. (Figs. 4-10, 4-11, 4-12, and 4-13)

4.7 N Calculations

Referring to the basic closed loop transfer function in frequency form, Eq. (4.9), the general phase angle equation for the second order system with one zero, was written as

$$N = \arctan\left[\frac{\Omega(m_1^2 - 2m_1 + m_2^2 - \Omega^2)}{m_1^2 + 2m_1\Omega^2 + m_2^2 - \Omega^2}\right] \tag{4.19}$$

The previously obtained parameter frequency equations (Ω_p, Ω_{bw}, Ω_n, Ω_1, and the three Ω_k's) were solved by digital computer programs. The resulting parameter frequencies were then substituted into the general N equation (4.19) along with the corresponding values of m_1 and m_2. The following figures resulted, all plotted with constant m_2 loci against m_1 versus N:

Fig. 4-14 N_p as function of m_1 and m_2

Fig. 4-15 N_{bw} as function of m_1 and m_2

Fig. 4-16 $N_{\Omega n}$ as function of m_1 and m_2

Fig. 4-17 N_1 as function of m_1 and m_2

Fig. 4-18 N_{k_1} as function of m_1 and m_2 for k_1 = .5

Fig. 4-19 N_{k_2} as function of m_1 and m_2 for k_2 = 1.5

Fig. 4-20 N_{k_3} as function of m_1 and m_2 for k_3 = 2.5

4.8 Example

Given: Complex poles; $-a \pm jb = -2.0 \pm j\,2.0$

Real zero; $-d = -2.0$

Solution:

SPECIFIC DATA

TABLE OF PARAMETER VALUES

x	Ω_x	ω_x*	Ω_x Fig. No.	M_x	M_x Fig. No.	N_x	N_x Fig. No.
p	1.1	2.2	4-4	1.28	4-5	-23.7°	4-14
bw	2.9	5.8	4-6	.707	N.A.	-67.0°	4-15
Ω_n	1.42	2.84	4-7	1.23	4-8	-35.2°	4-16
1	2.0	4.0	4-9	1.0	N.A.	-53.0°	4-17
k_1	0.78	1.56	4-10	1.22	4-11	-10.5°	4-18
k_2	1.35	2.70	4-10	1.24	4-12	-33.2°	4-19
k_3	1.74	3.48	4-10	1.095	4-13	-47.0°	4-20

*Obtain ω_x by $\omega_x = |d|\,\Omega_x$.

GENERAL DATA (for all Second Order plus One Zero Systems)

ω	M	$dM/d\omega$	N	$dN/d\omega$
0	1.0	0	0^o	—
ω_p	M_p	0	—	—
∞	0	0	-90^o	0

Fig 4-21 (page 39) compares the frequency response obtained from this rapid approximation method to the actual M and N contours obtained from a digital computer solution of the general M and N equations.

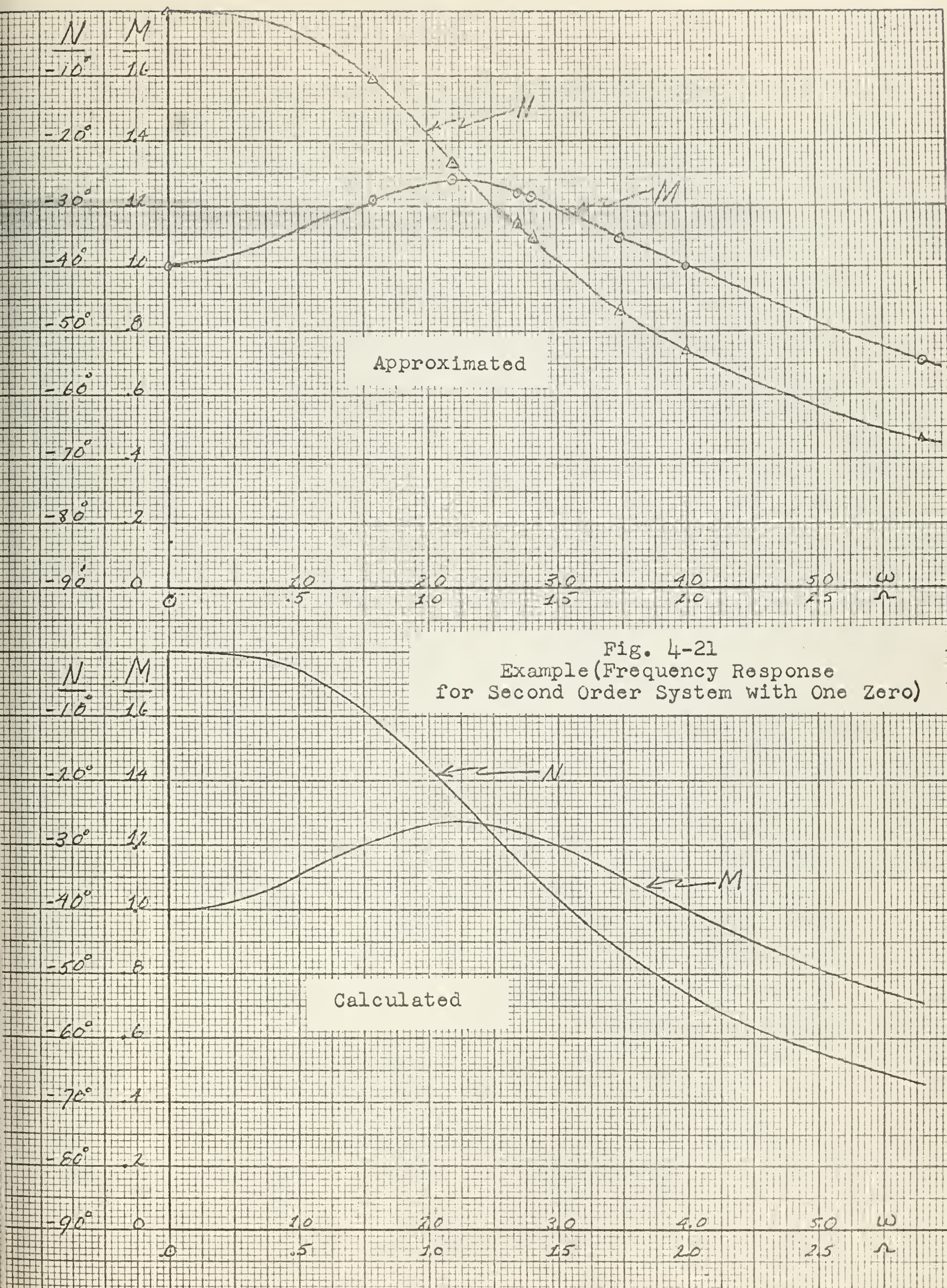

Fig. 4-21
Example (Frequency Response for Second Order System With One Zero)

Fig. 4-4. Ω_p for Second Order System with One Zero

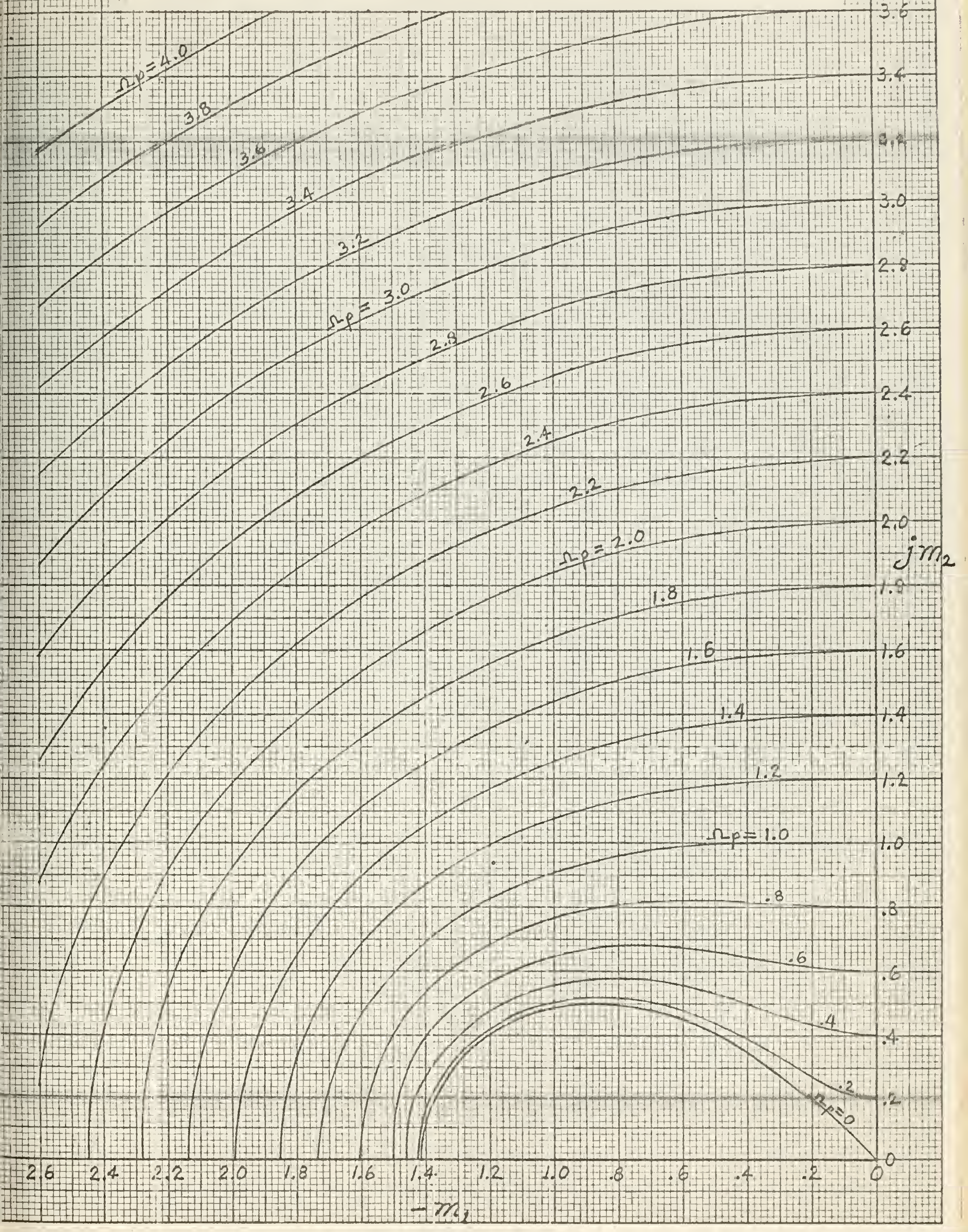

Fig. 4-5. M_p for Second Order System with One Zero

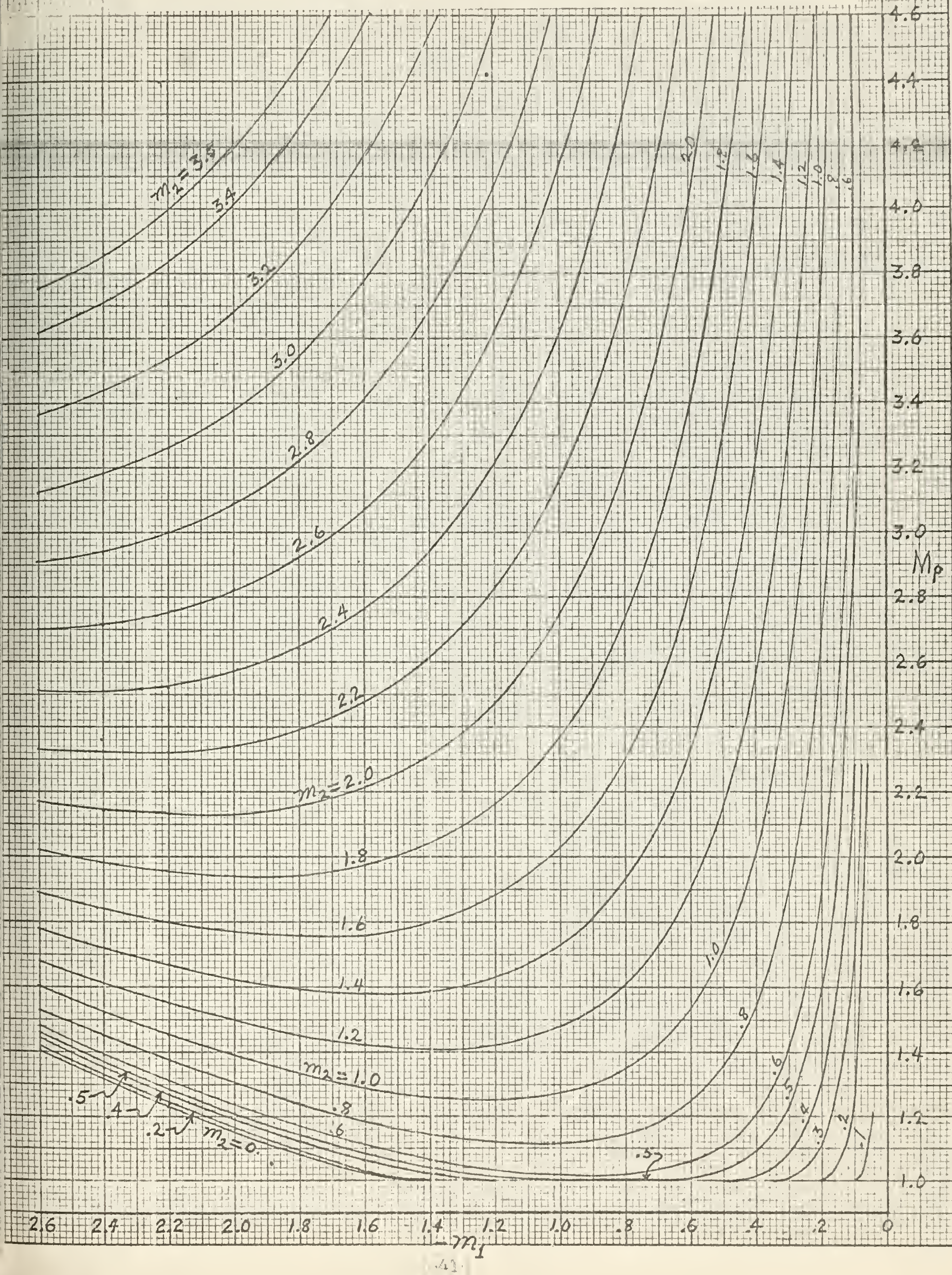

Fig. 4-6. Ω_{bw} for Second Order System with One Zero

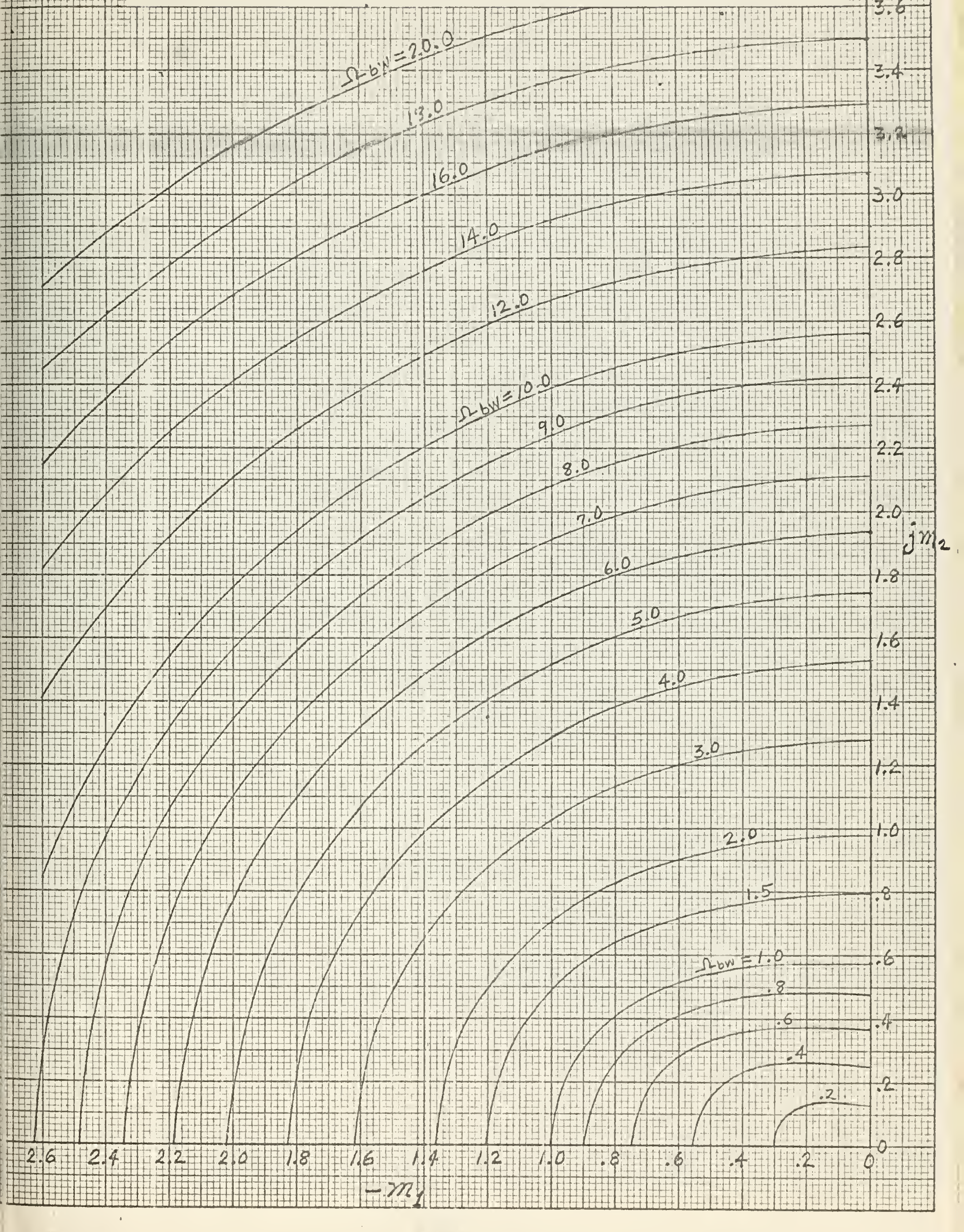

Fig. 4-7. Ω_n for Second Order System with One Zero

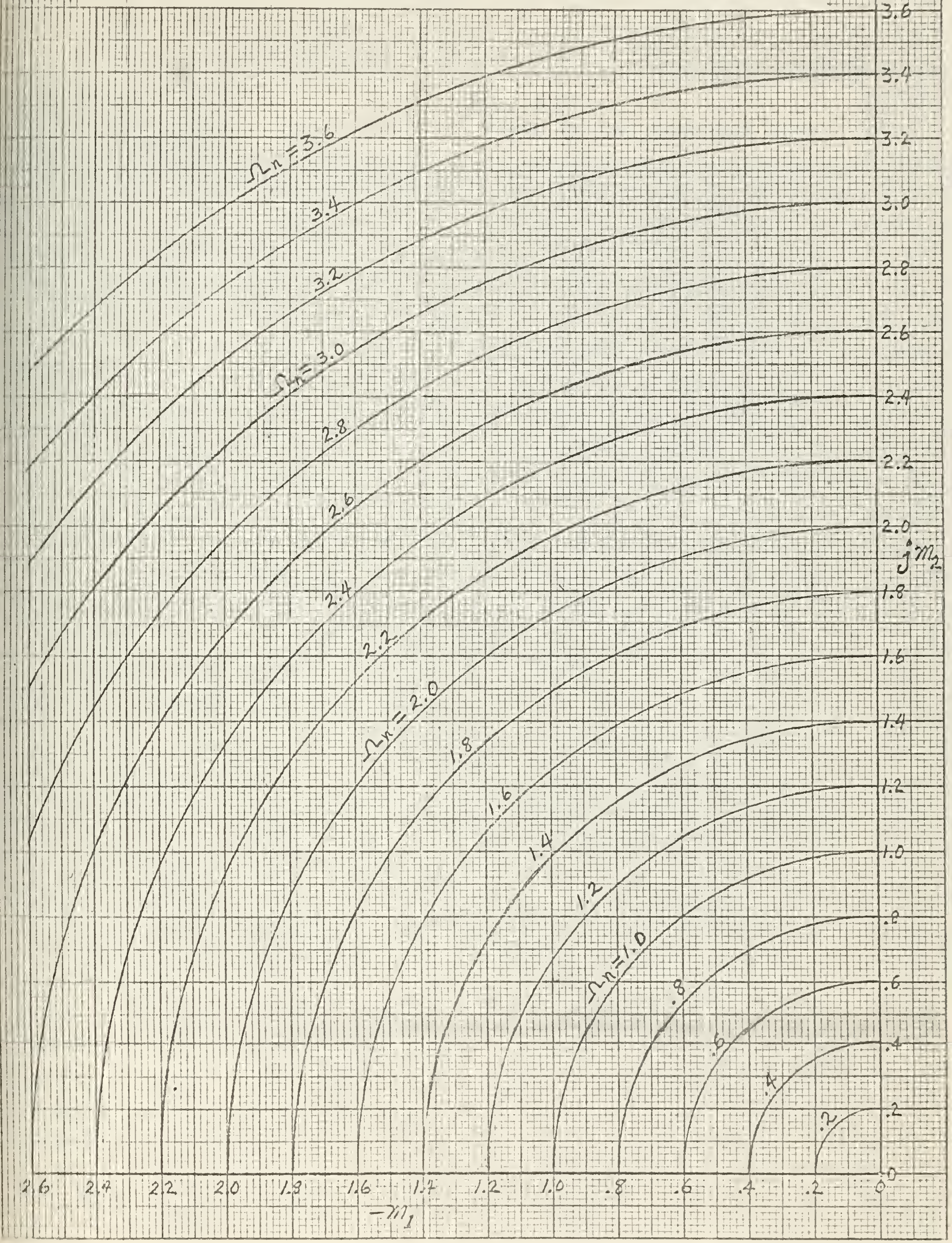

Fig. 4-8
$M_{\Omega n}$ for Second Order System with One Zero

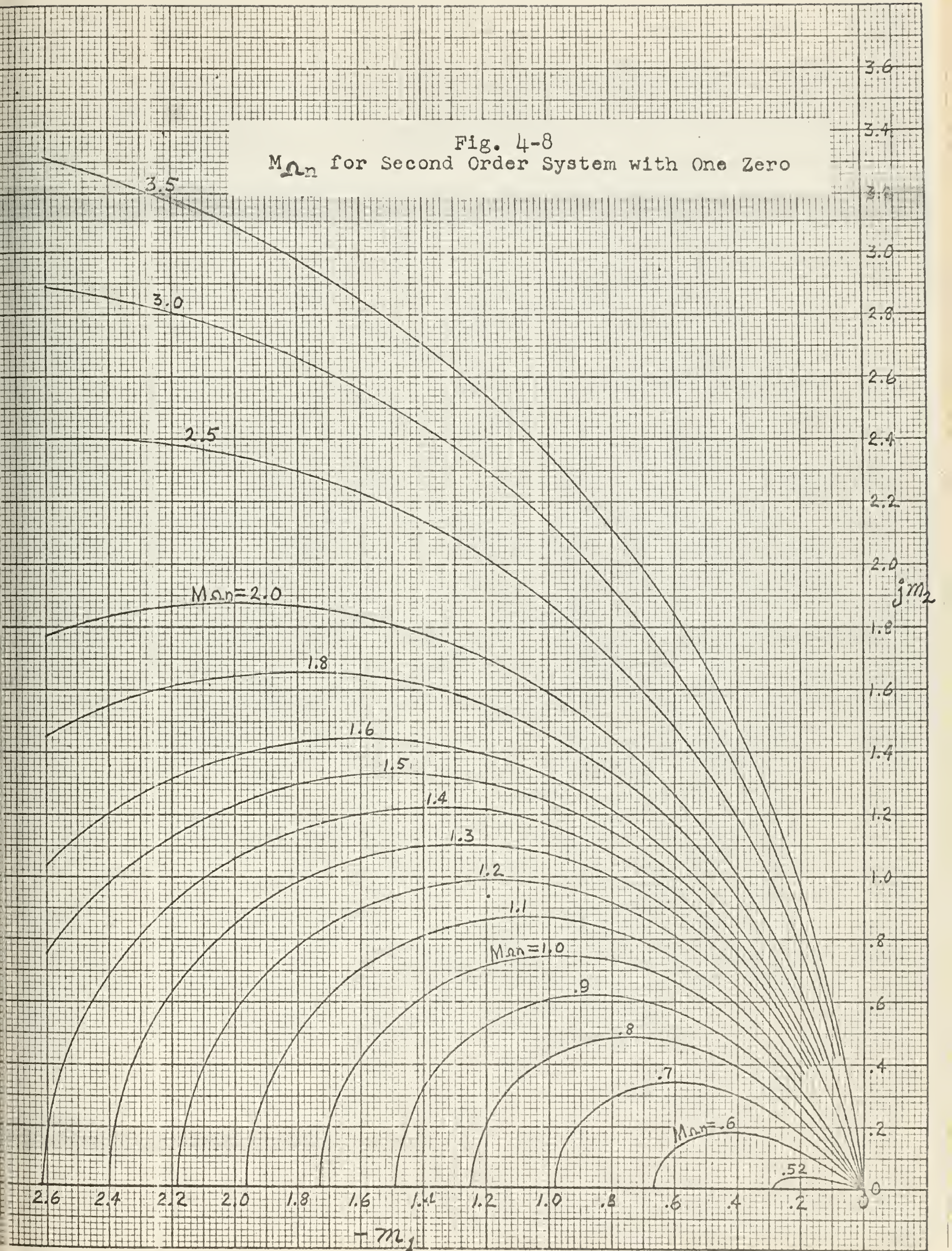

Fig. 4-9. Ω_1 for Second Order System with One Zero

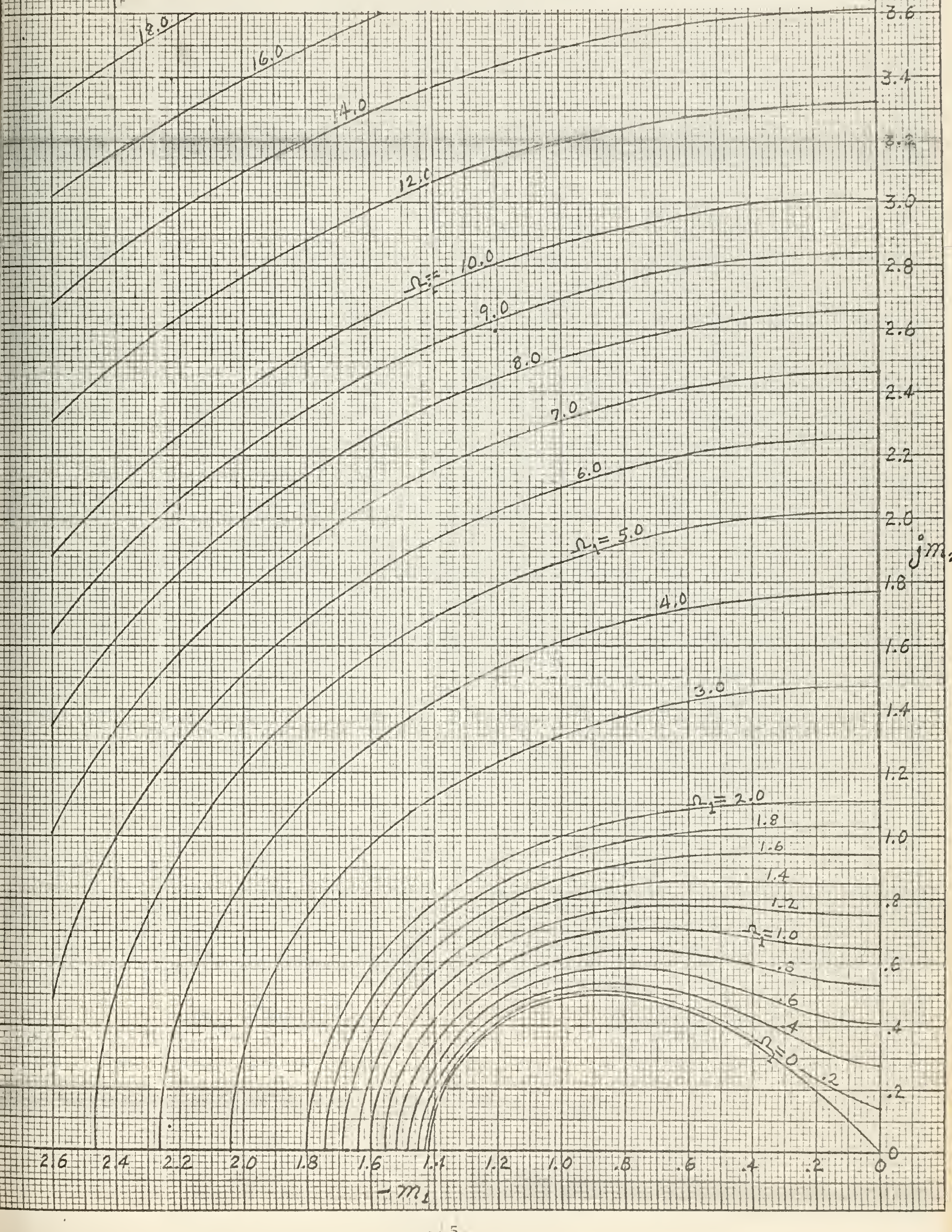

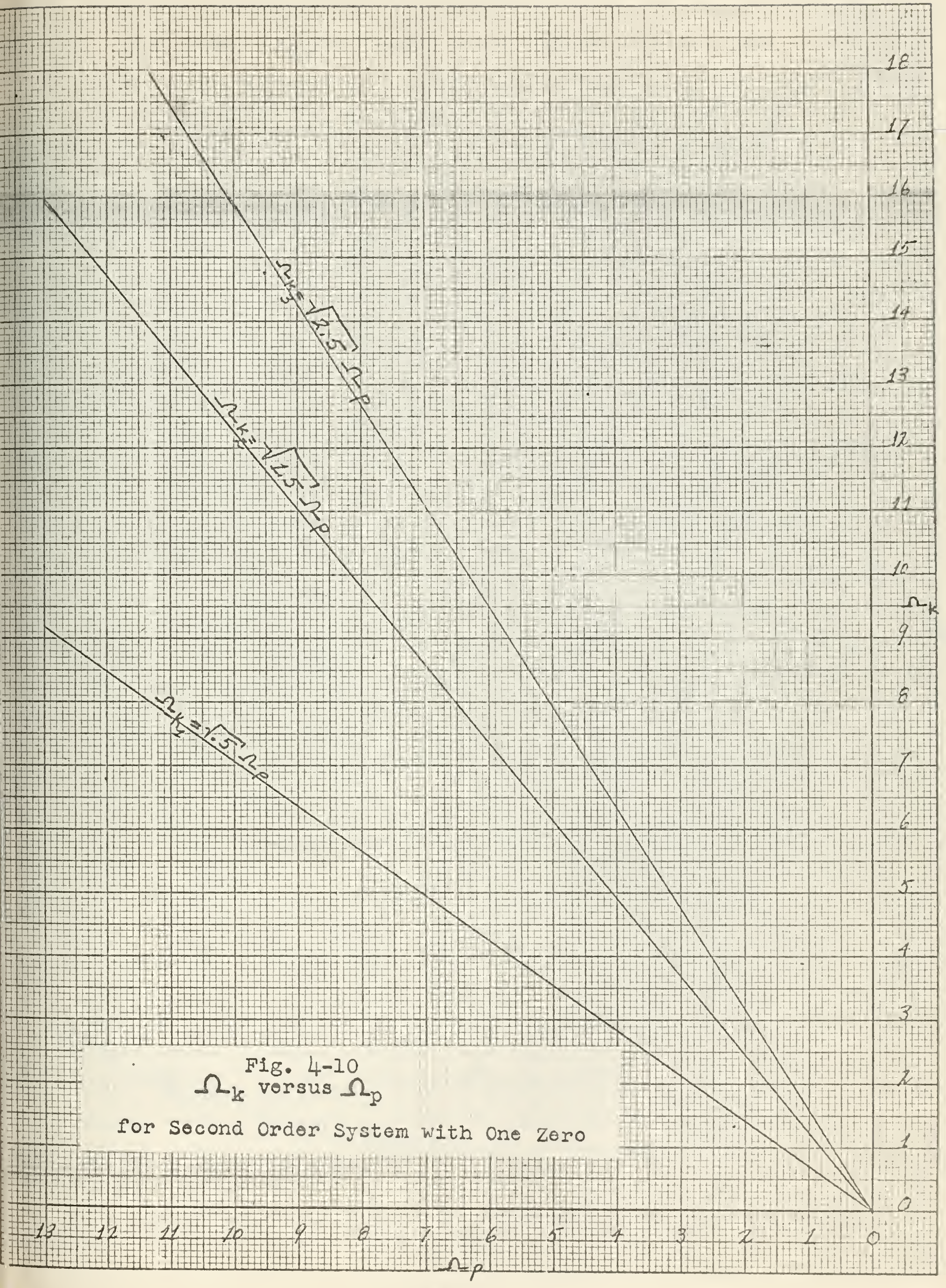

Fig. 4-10
Ω_k versus Ω_p
for Second Order System with One Zero

Fig. 4-11. M_{k1} for Second Order System with One Zero

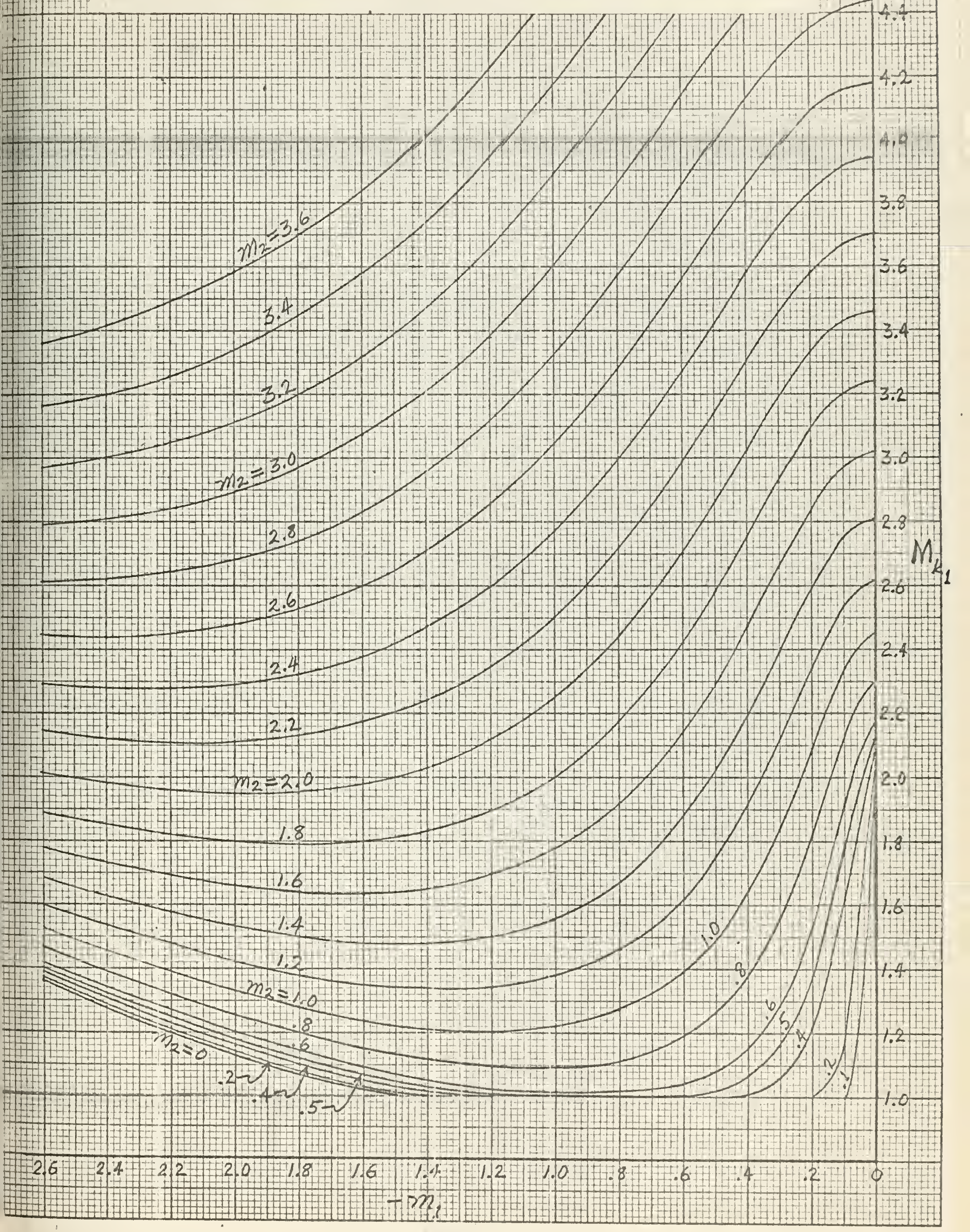

Fig. 4-12. M_{k2} for Second Order System with One Zero

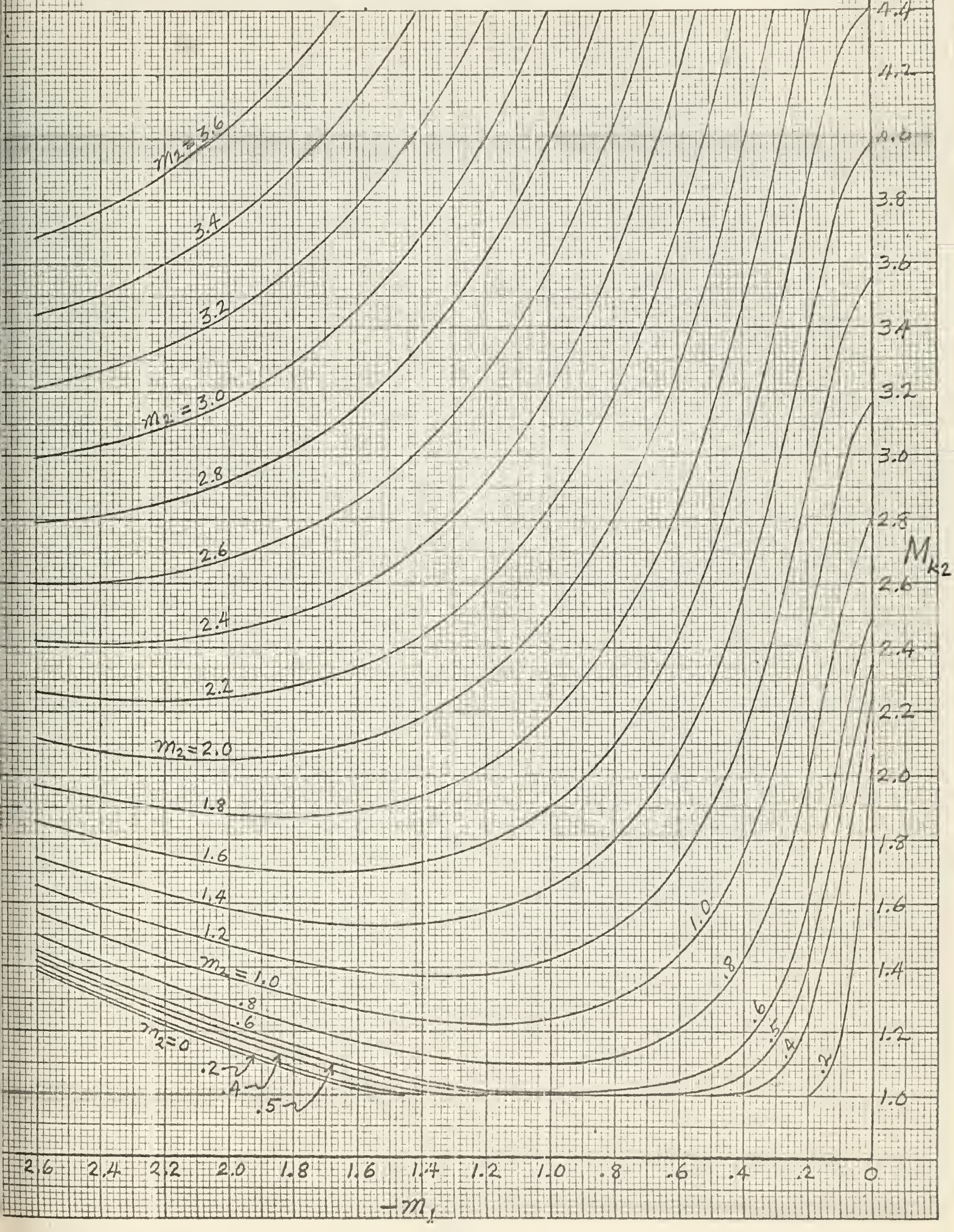

Fig. 4-13. M_{k_3} for Second Order System with One Zero

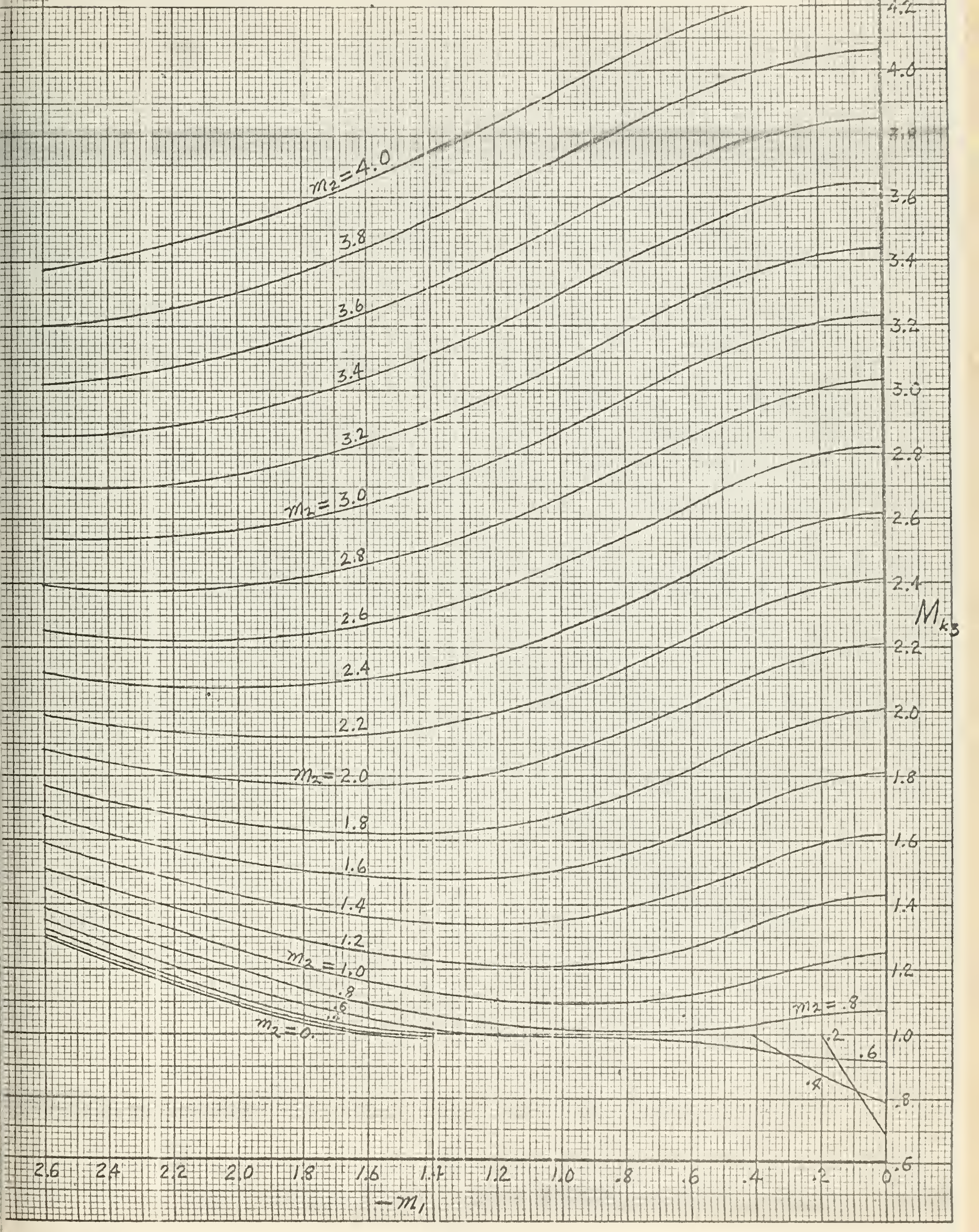

Fig. 4-14

N_p for Second Order System with One Zero

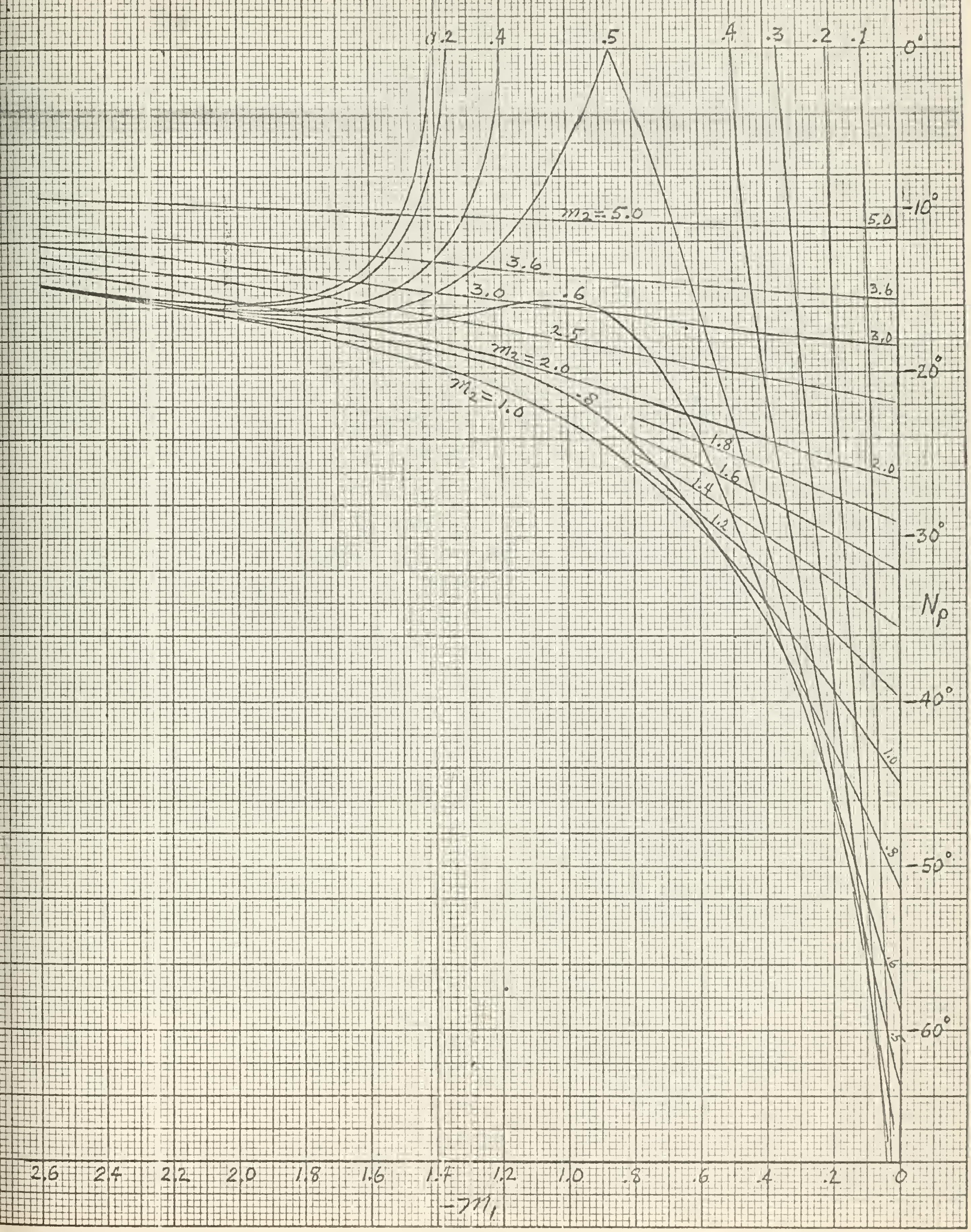

Fig. 4-15
N_{bw} for Second Order System with One Zero

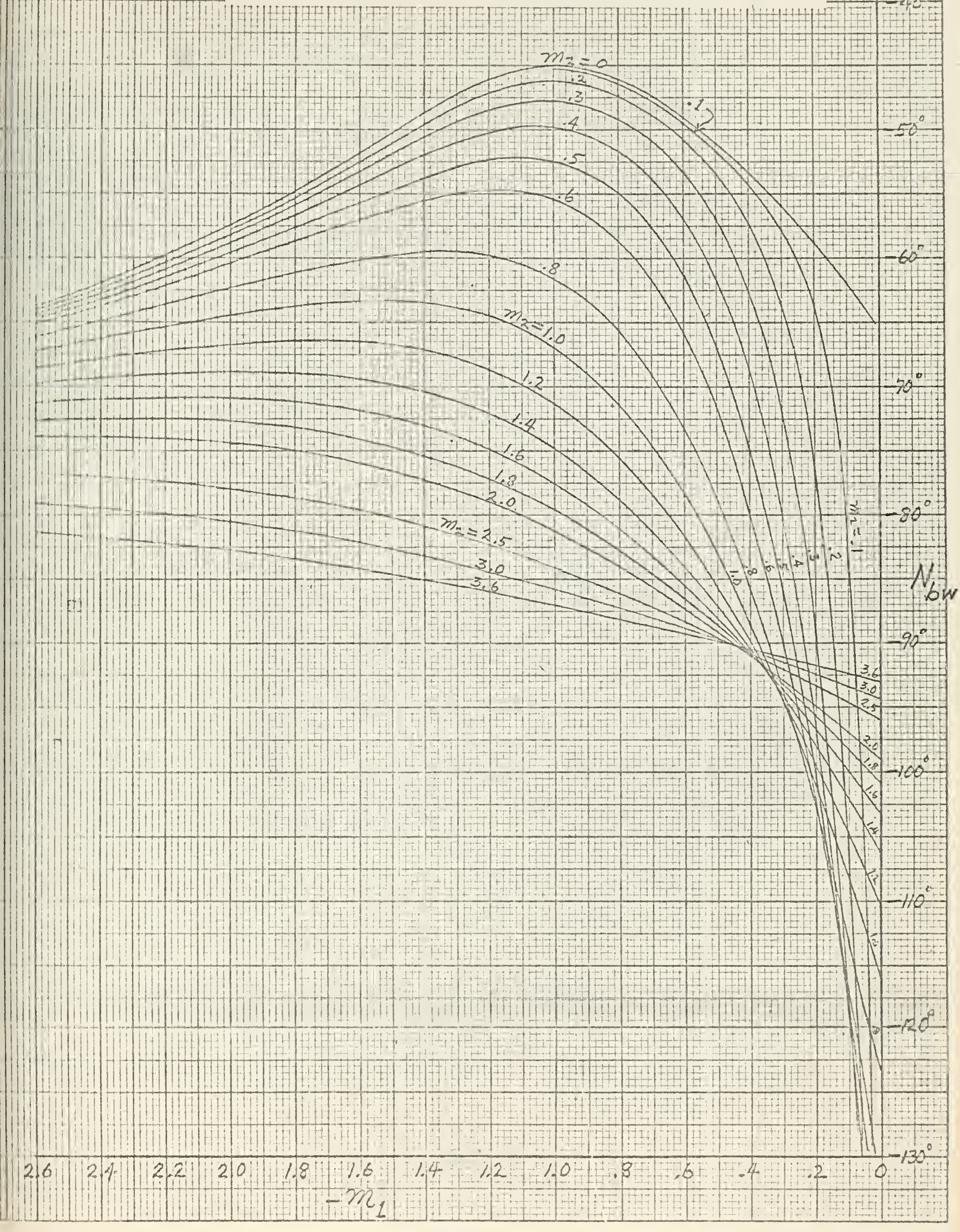

Fig. 4-16

$N_{\Omega n}$ for Second Order System with One Zero

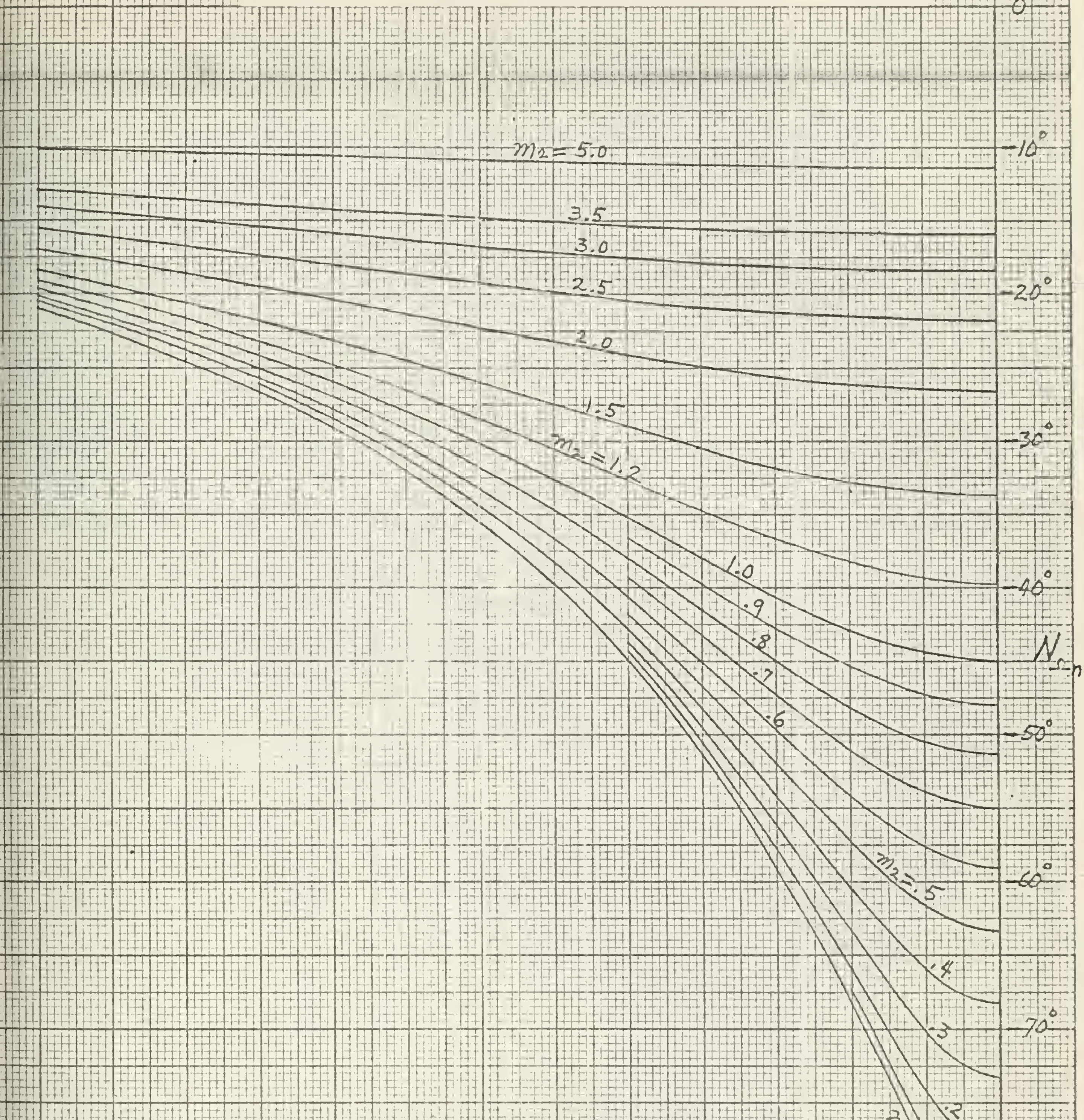

Fig. 4-17

N_1 for Second Order System with One Zero

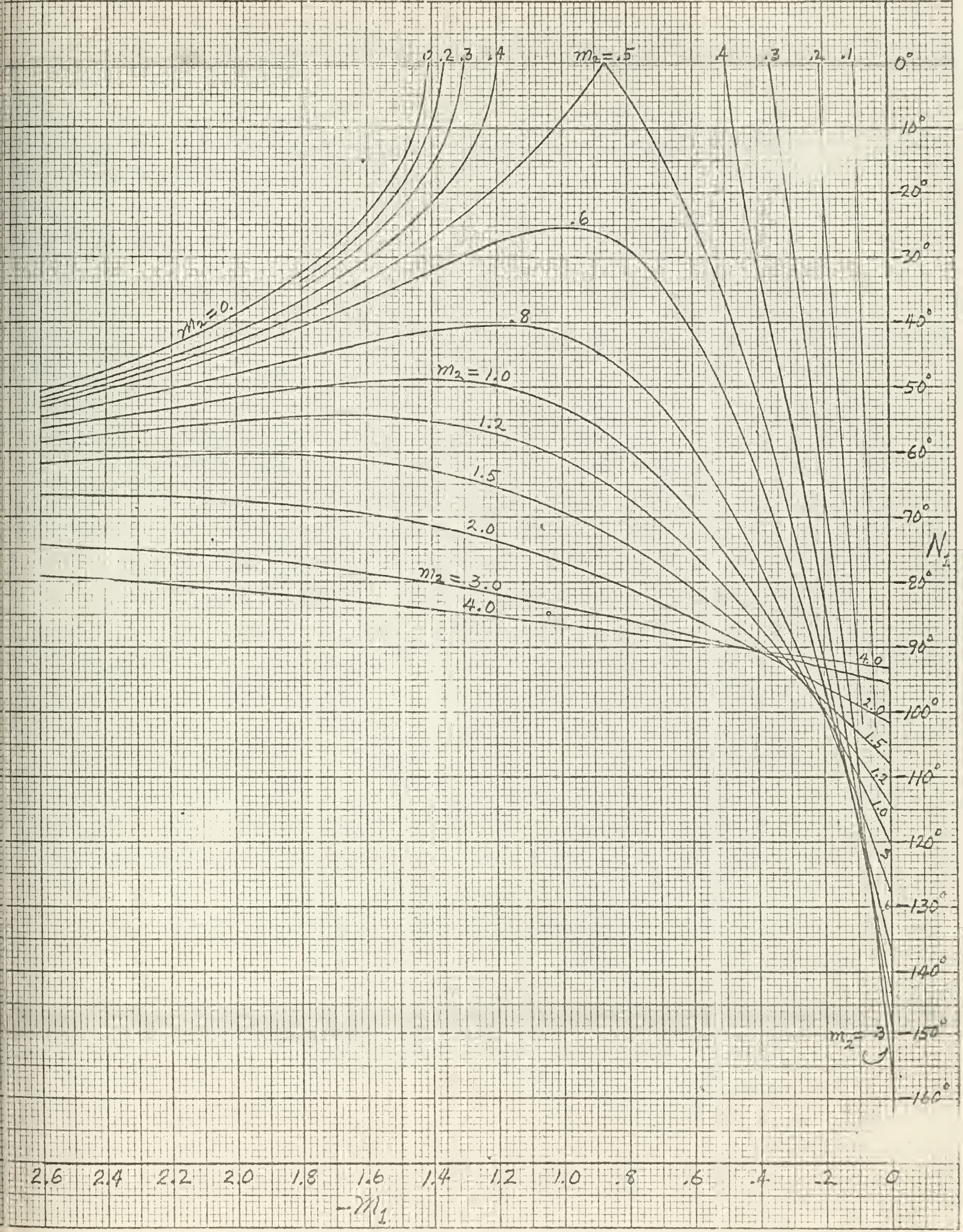

Fig. 4-18
N_{kl} for Second Order System with One Zero

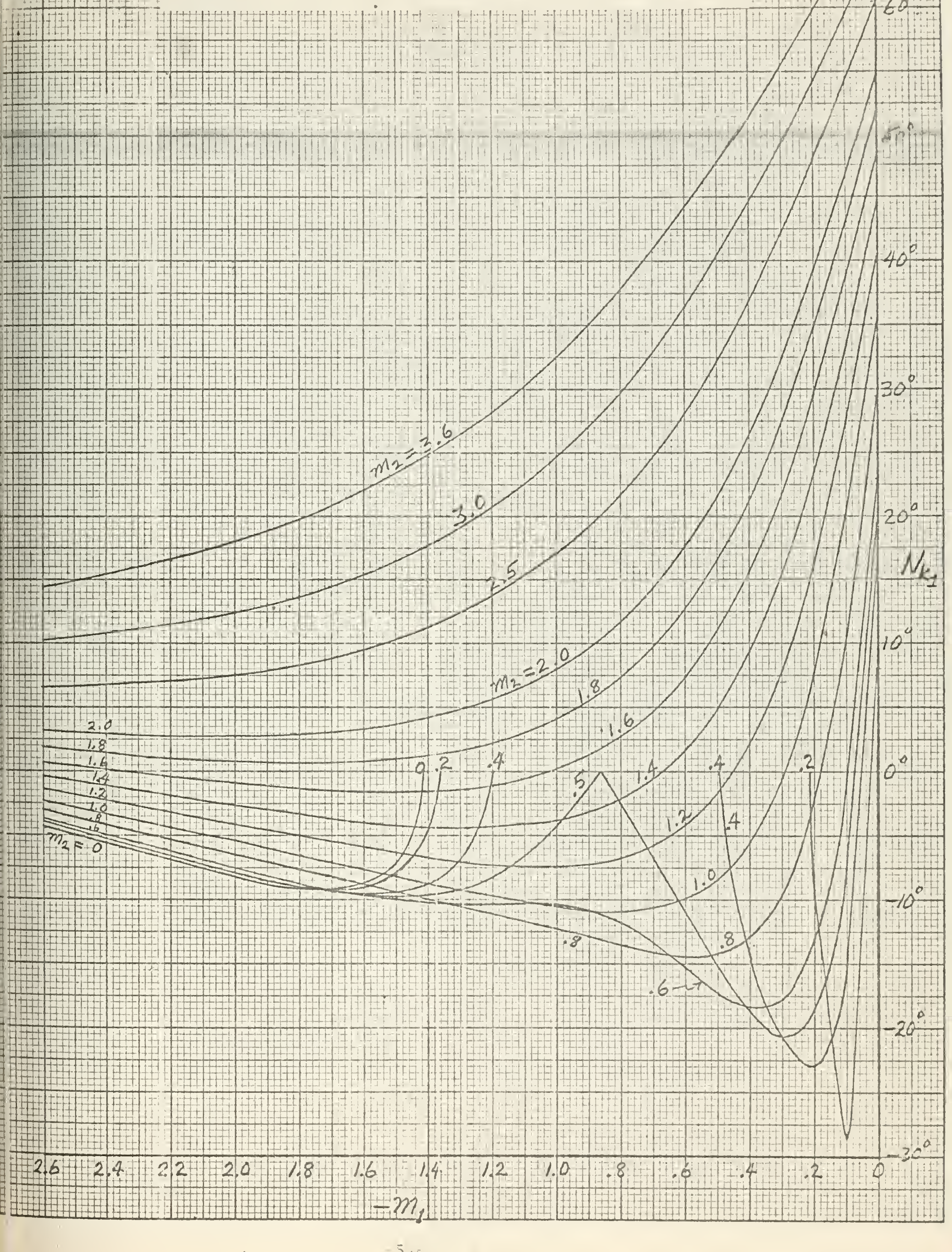

Fig. 4-19
N_{k2} for Second Order System with One Zero

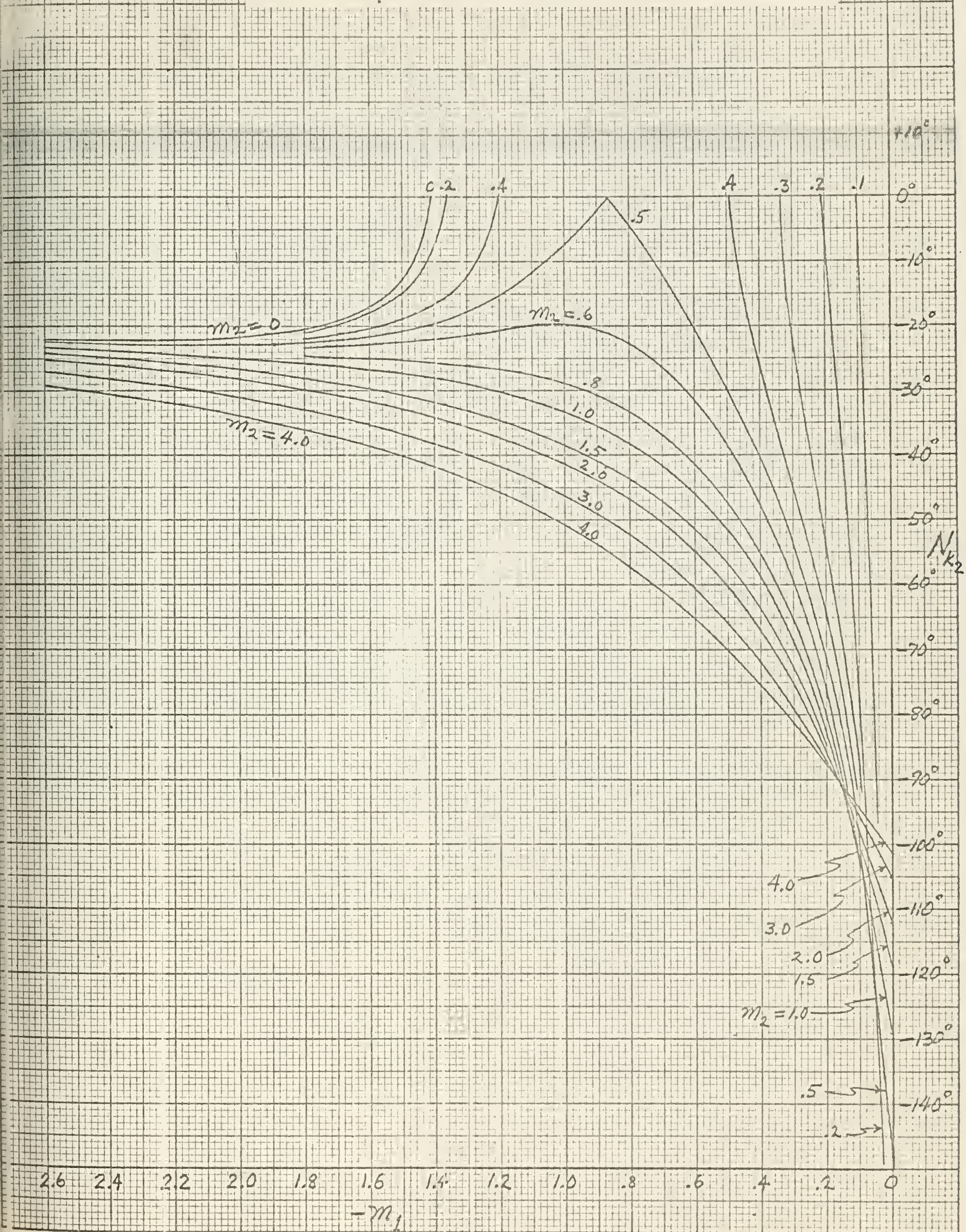

Fig. 4-20
N_{k3} for Second Order System with One Zero

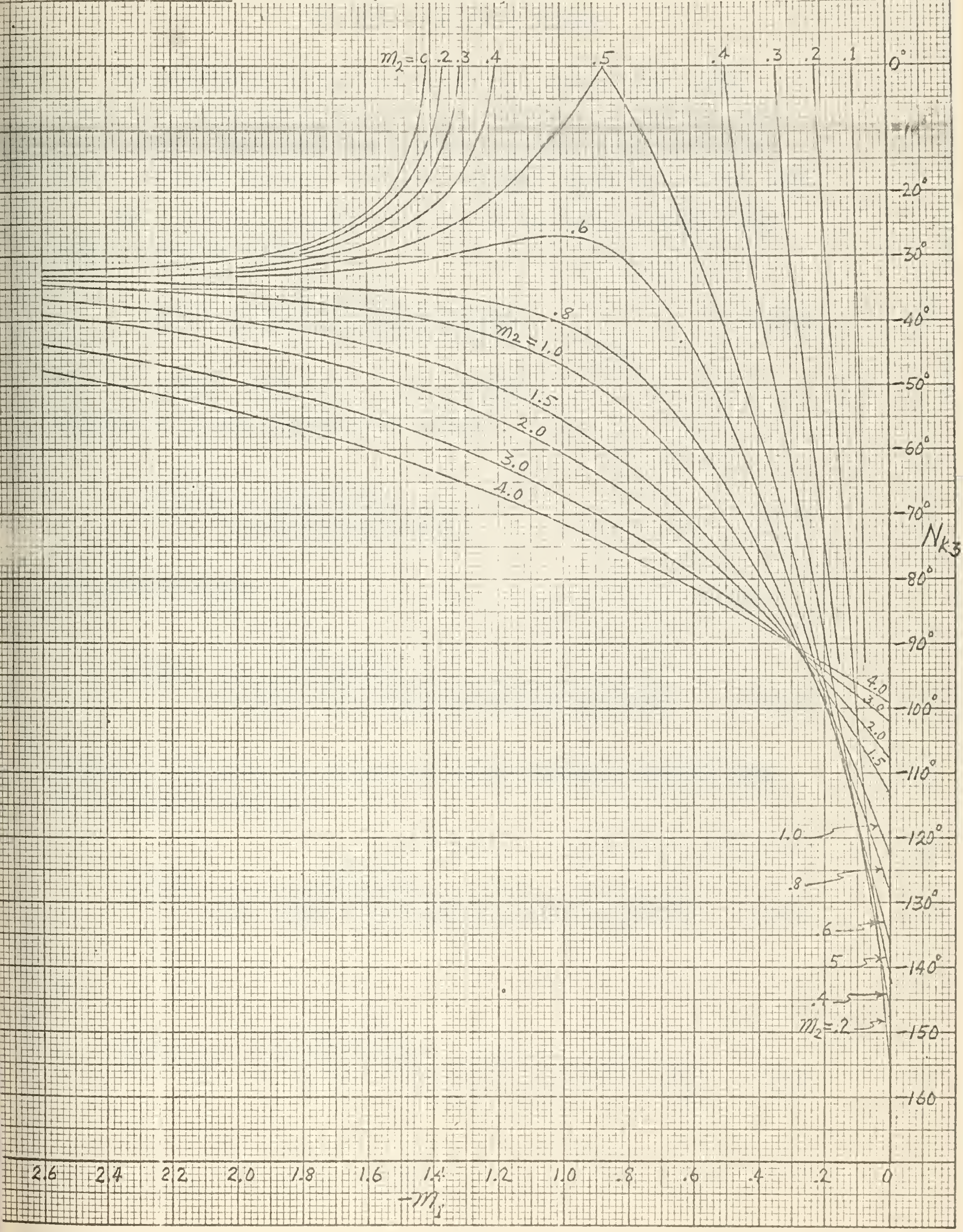

5 THE PURE THIRD ORDER SYSTEM

The addition of a real root to the pure second order system resulted in a new system which will be referred to as the pure third order system. The closed loop transfer function of the pure third order system had one pair of complex conjugate poles and one real pole.

The closed loop transfer function for the unity feedback third order system was written as

$$\Gamma_c(s) = \frac{(a^2+b^2)c}{(s+c)(s+a+jb)(s+a-jb)} \tag{5.1}$$

Fig. 5-1 defined these roots on the s-plane.

Equation (5.1) was simplified as follows:

$$\Gamma_c(s) = \frac{(a^2+b^2)c}{(s+c)\left[(s+a)^2+b^2\right]} \tag{5.2}$$

and expanded became

$$\Gamma_c(s) = \frac{(a^2+b^2)c}{s^3+s^2(2a+c)+s(a^2+2ac+b^2)+c(a^2+b^2)} \tag{5.3}$$

Letting s = jω in Eq. (5.3) resulted in the frequency response form of the transfer function

$$\Gamma_c(j\omega) = \frac{(a^2+b^2)c}{-j\omega^3-\omega^2(2a+c)+j\omega(a^2+2ac+b^2)+c(a^2+b^2)} \tag{5.4}$$

or

$$\Gamma_c(j\omega) = \frac{(a^2+b^2)c}{\left[a^2c+b^2c-\omega^2(2a+c)\right]+j\left[\omega(a^2+2ac+b^2)-\omega^3\right]} \tag{5.5}$$

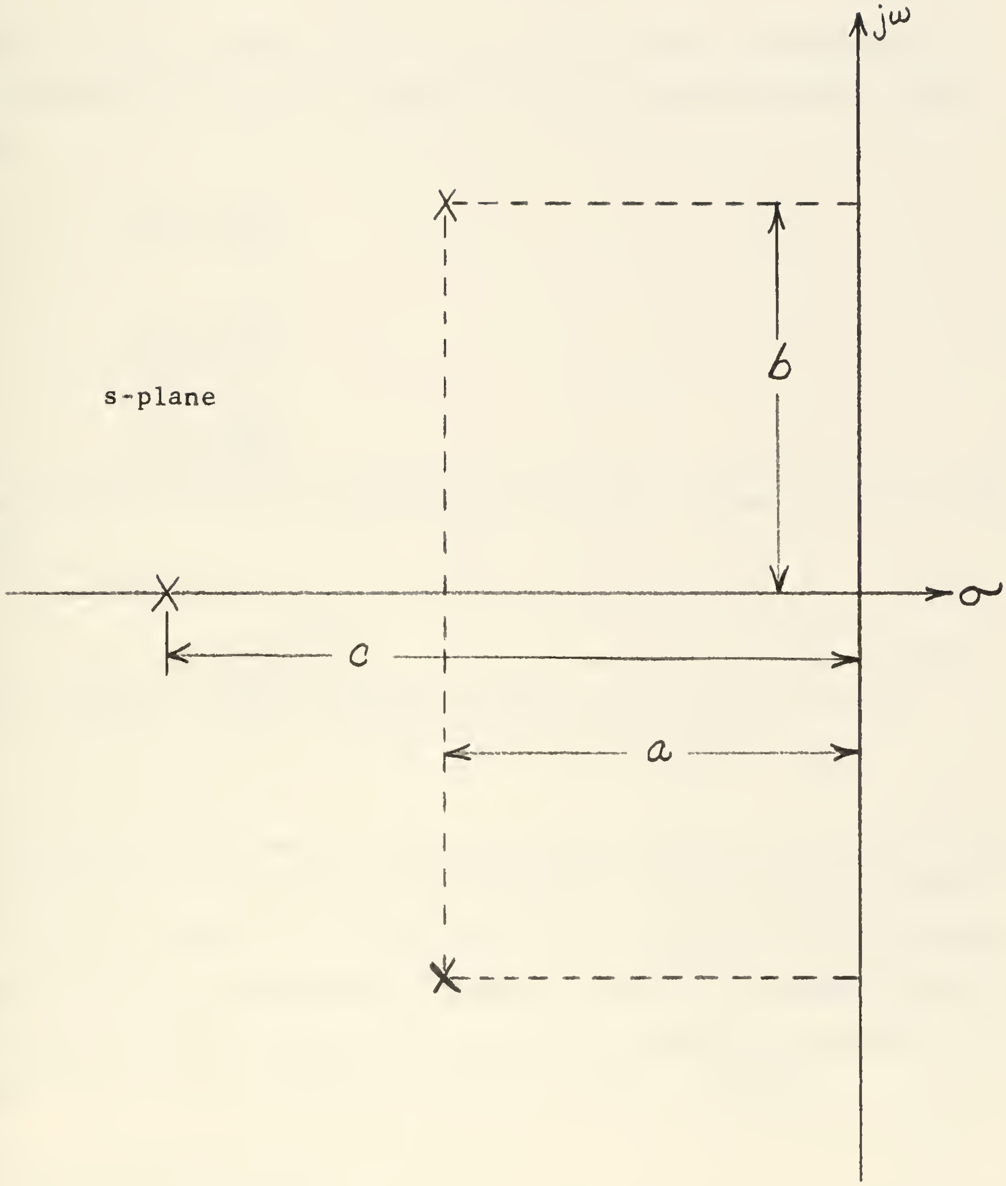

Fig. 5-1 Poles of the Pure Third Order System (s-plane)

Numerator and denominator of Eq. (5.5) divided by c^3:

$$F_c(j\omega) = \frac{\frac{a^2}{c^2} + \frac{b^2}{c^2}}{\left[\frac{a^2}{c^2} + \frac{b^2}{c^2} - \frac{\omega^2}{c^2}\left(\frac{2a}{c} + 1\right)\right] + j\left[\frac{\omega}{c}\left(\frac{a^2}{c^2} + \frac{2a}{c} + \frac{b^2}{c^2}\right) - \frac{\omega^3}{c^3}\right]} \tag{5.6}$$

Observing that a power of "c" exists in all terms corresponding to the same power of "a", "b" and ω; the following definitions were made:

$$n_1 \triangleq \frac{a}{|c|} \tag{5.7}$$

$$n_2 \triangleq \frac{b}{|c|} \tag{5.8}$$

$$\Omega \triangleq \frac{\omega}{|c|} \tag{5.9}$$

These quantities were illustrated in Fig. 5-2. Equation (5.6) then became

$$F_c(j\omega) = \frac{n_1^2 + n_2^2}{\left[n_1^2 + n_2^2 - \Omega^2(2n_1 + 1)\right] + j\left[\Omega\left(n_1^2 + n_1 + n_2^2\right) - \Omega^3\right]} \triangleq M e^{jN} \tag{5.10}$$

n_1 and n_2 were the complex pole locations referred to the real pole location and Ω was the referred frequency. The frequency response for the pure third order system was then a function of the referred complex pole and the referred frequency. Thus all systems having the same relative pole configuration will have identical response if the frequency were also referred to the real pole location.

5.1 <u>M and Ω Calculations</u>

The magnitude portion of Eq. (5.10), after algebraic manipulation, reduced to

$$M = \frac{n_1^2 + n_2^2}{\sqrt{\Omega^6 + \Omega^4\left[2(n_1^2 - n_2^2) + 1\right] + \Omega^2\left[(n_1^2 + n_2^2)^2 + 2(n_1^2 - n_2^2)\right] + \left[(n_1^2 + n_2^2)^2\right]}} \tag{5.11}$$

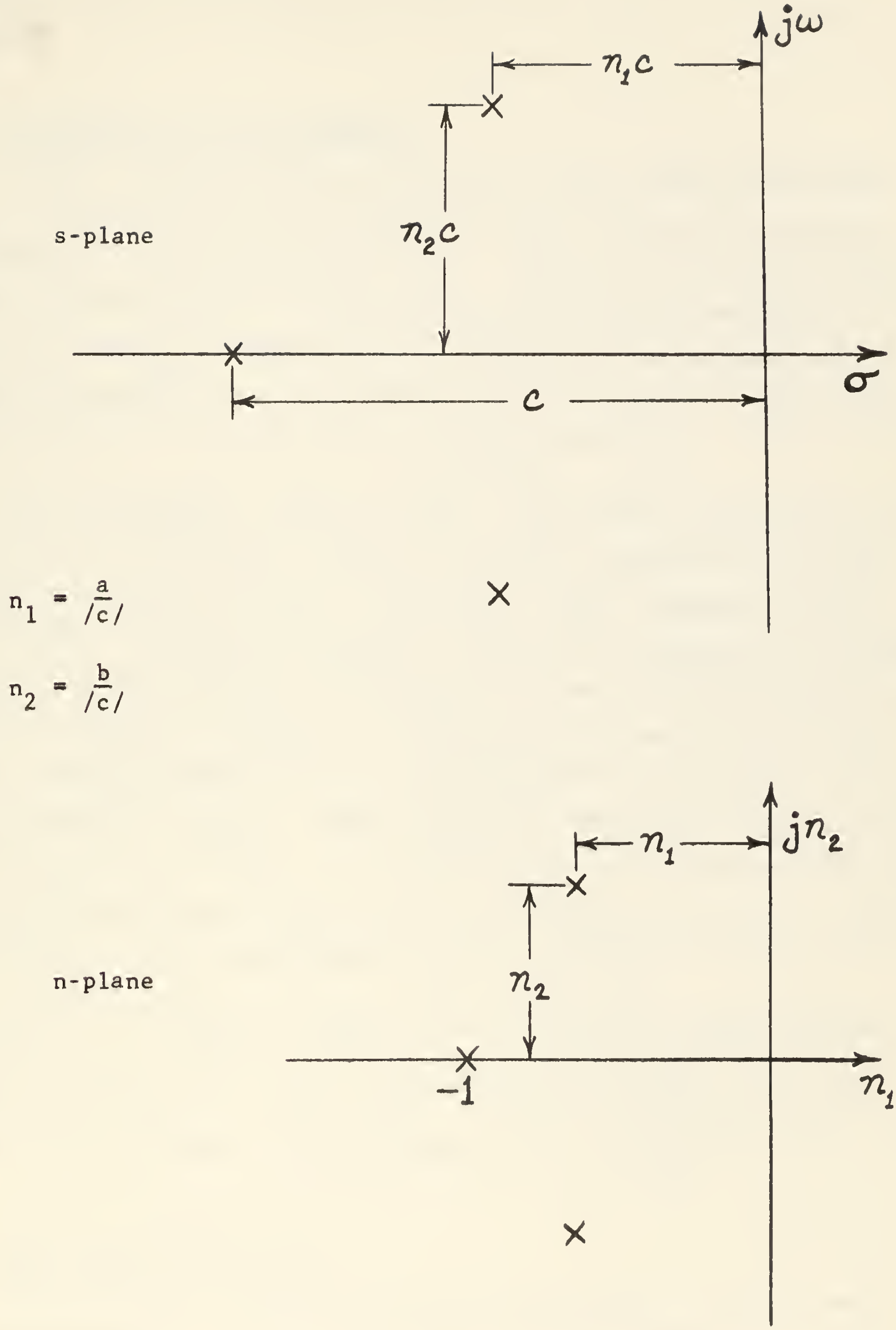

Fig. 5-2 Referred Quantities n_1 and n_2, Pure Third Order System

Equation (5.11) was the basic M equation for the pure third order system.

5.2 Discussion of the M Contours

It was found that the M contour for a pure third order system will be one of three basic "shapes" as shown in Fig. 5-3a, b and c, depending on the values of n_1 and n_2. Figure 5-3a was the situation when there was no peak. No value of Ω_p was obtained and hence no values for Ω_1 or the Ω_k's. Figure 5-3b was similar to the second order M contour shape and had a single peak. For this general "shape" points were obtained for Ω_p, Ω_{bw}, Ω_n, Ω_1, Ω_{k_1}, Ω_{k_2}, and Ω_{k_3}.

The third general "shape" is Fig. 5-3c, which resulted from the Ω_p equation (5.12) which yielded two non-zero frequencies at which the M contour slope was zero, one being a "peak" frequency and the other being a "minimum" frequency. This latter frequency was designated Ω_m to avoid being confused with the Ω_p. It was also discovered that with this shape of M contour, it was possible to have M_p less than unity. Another possibility was to have M_m less than M_{bw} and at the same time M_p greater than one. This resulted in two values of Ω_1, two values of Ω_{k_1}, M_{k_1}, Ω_{k_2}, and M_{k_2} (one relative to M_p and the other relative to M_m), and three values of Ω_{bw} (one for each crossing of the M = .707 line), in addition to the usual points at Ω_p, Ω_m, and Ω_n.

Figure 5-4 might be thought of as the complex n-plane and shows the regions in which certain n_1 and n_2 combinations produce one of the three above M contours. This figure indicates the general shape of the M contours that result from the known n_1 and n_2 values.

5.3 M_p and Ω_p Determination

The equation for Ω_p was obtained by squaring Eq. (5.11), then differentiating with respect to Ω and setting the numerator of this equal to zero. This reduced to

$$\Omega_p = \sqrt{-\frac{2}{3}(n_1^2 - n_2^2 + .5) \pm \frac{1}{3}\sqrt{n_1^2(n_1^2 - 14n_2^2 - 2) + n_2^2(n_2^2 + 2) + 1}} \qquad (5.12)$$

Fig. 5-3 The Three Basic M Curve Shapes for Pure Third Order System

(a)

(b)

(c)

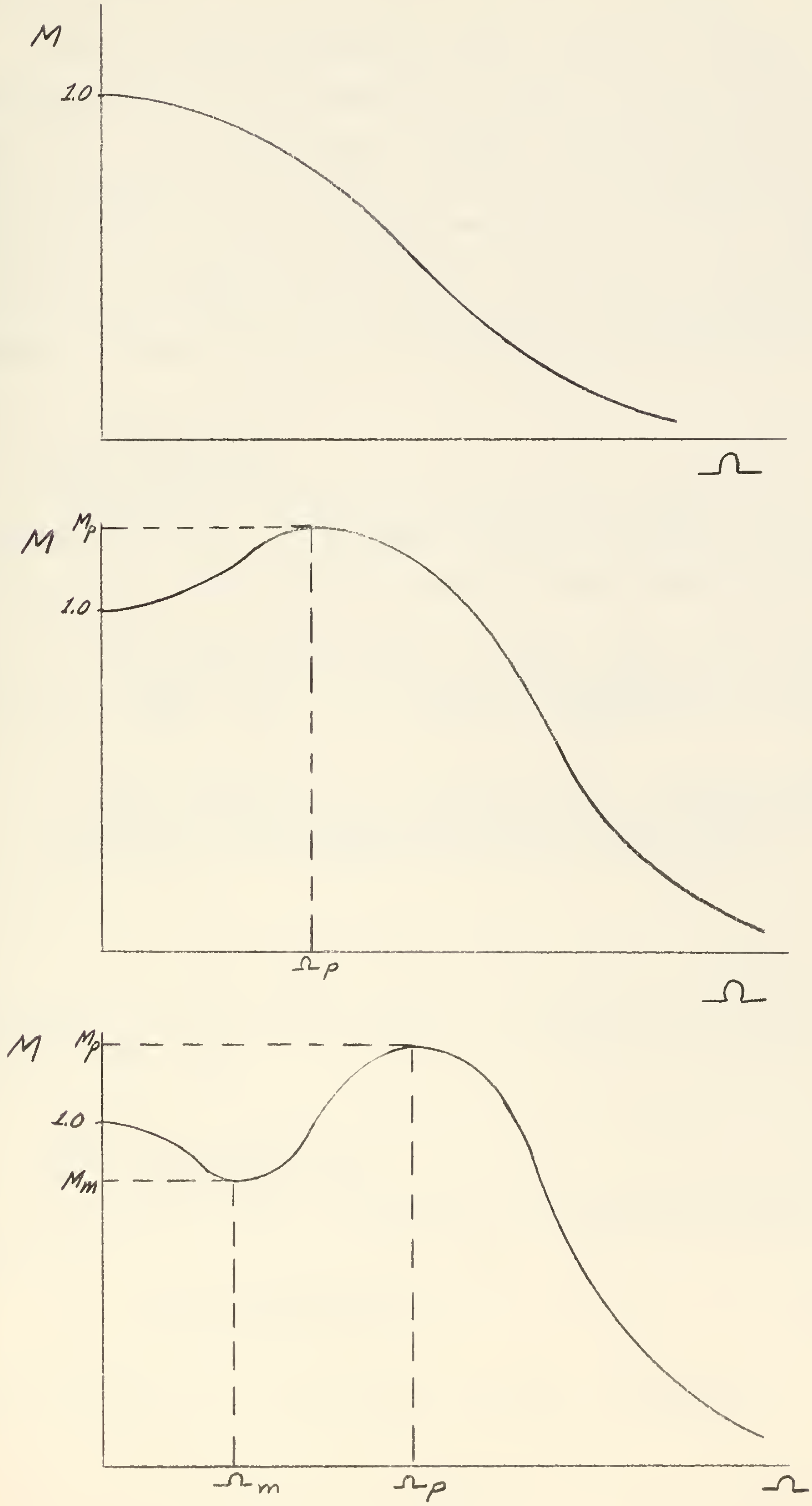

The plus and minus values of the inner square root quantity were both valid and resulted in two possible solutions for Ω_p. The consequences of two solutions were discussed in detail in paragraph 5.2 above.

Loci of constant values of n_2 were solved by a digital computer program and were plotted against n_1 versus Ω_p and Ω_m in Figs. 5-5a and 5-5b. In the same computer program, values of M_p were obtained for corresponding values of n_1, Ω_p, and n_2 by substituting these known quantities into the basic M equation, Eq. (5.11). Figures 5-6a, 5-6b, and 5-6c contain M_p plotted as a function of n_1 and n_2. No specific M_p equation was derived due to the obvious complexity involved in substituting Eq. (5.12) into Eq. (5.11) for Ω.

5.4 Ω_{bw} Determination

The equation for the referred bandwidth frequency was obtained by substituting M = .707 into Eq. (5.11) and solving for n_1 as a function of Ω_{bw} and n_2. This involved extensive algebra which reduced to

$$n_1 = \left\{ -\left[\frac{\Omega_{bw}^4 + \Omega_{bw}^2(1+n_2^2) - n_2^2}{\Omega_{bw}^2 - 1} \right] \pm \left[\left(\frac{\Omega_{bw}^4 + \Omega_{bw}^2(1+n_2^2) - n_2^2}{\Omega_{bw}^2 - 1} \right)^2 - \left(\frac{\Omega_{bw}^6 + \Omega_{bw}^4(-2n_2^2+1) + \Omega_{bw}^2(n_2^4 - 2n_2^2) - n_2^4}{\Omega_{bw}^2 - 1} \right) \right]^{1/2} \right\}^{1/2} \tag{5.13}$$

The $\pm$ signs were both valid here also and their effect will be discussed later. (Fig. 5-7)

5.5 $M_{\Omega n}$ and Ω_n Determination

The undamped natural frequency for the pure third order system was defined as

$$\Omega_n \triangleq \sqrt{n_1^2 + n_2^2} \tag{5.14}$$

Ω_n was expressed as a function of n_1 and n_2. (Fig. 5-8)

Substituting this into Eq. (5.11) and simplifying yielded

$$M_{\Omega n} = \frac{n_1^2 + n_2^2}{\sqrt{4n_1^2(n_1^2+n_2^2)(n_1^2+n_2^2+1)}} \qquad (5.15)$$

$M_{\Omega n}$ was thus expressed as a function of n_1 and n_2. (Figs. 5-9a and 5-9b)

5.6 Ω_1 Determination

The referred frequency, other than zero, at which M = 1.0 was defined as Ω_1.

Letting M = 1.0 in Eq. (5.11) and solving for Ω_1 resulted in

$$\Omega_1 = \sqrt{-n_1^2+n_2^2-.5 \pm \sqrt{n_2^2-n_1^2-4n_1^2n_2^2+.25}} \qquad (5.16)$$

(Figs. 5-10 a, b, c, and d)

5.7 M_k and Ω_k Determination

For the same reasons as discussed in Section 2.4, it was found desirable to obtain "fill-in" points on both sides of Ω_p. This was done by defining

$$\Omega_k = k\Omega p \qquad (5.17)$$

which eliminated the square root of k as used for the previous two classes of systems.

The values of k chosen were .8, 1.4, and 1.8; therefore

$$\Omega_{k_1} = .8\ \Omega p \qquad (5.18)$$

$$\Omega_{k_2} = 1.4\ \Omega p \qquad (5.19)$$

$$\Omega_{k_3} = 1.8\ \Omega p \qquad (5.20)$$

Fig. 5-11 was the almost trivial plot of these three equations, included for optional use in determining the Ω_k values once Ω_p has been determined.

Loci for the three M_k's were calculated by a digital program which utilized Eqs. (5.11), (5.12), (5.18), (5.19), and (5.20); thus it was not necessary to attempt to obtain any specific M_k equations. (Figs. 5-12 a,b, 5-13 a,b, 5-14)

5.8 Determination of N Curves

Referring to the basic closed loop transfer function in frequency form, Eq. (5.10), the general phase angle equation for the pure third order system was written as

$$N = -\arctan\left[\frac{-\Omega^3 + \Omega(n_1^2 + 2n_1 + n_2^2)}{-\Omega^2(2n_1+1) + n_1^2 + n_2^2}\right] \tag{5.21}$$

The previously obtained parameter frequency equations (Ω_p, Ω_{bw}, Ω_1, and Ω_k) were solved by digital computer programs. The resulting parameter frequencies were then substituted into the general N equation, Eq. (5.21), along with the corresponding values of n_1 and n_2. The following figures resulted, all plotted with constant n_2 loci against n_1 versus N:

Fig. 5-15 a	N_p as a function of n_1 and n_2
Fig. 5-15 b	N_m as a function of n_1 and n_2
Fig. 5-16 a	N_{bw} as a function of n_1 and n_2
Fig. 5-16 b	N_{bw} (extended) as a function of n_1 and n_2
Fig. 5-17 a	N_1 as a function of n_1 and n_2
Fig. 5-17 b	N_1 (expanded) as a function of n_1 and n_2
Fig. 5-17 c	N_1 (2nd value)as a function of n_1 and n_2
Fig. 5-18 a	N_{k_1} for maximum (Ω_p)

Fig. 5-18 b $\quad N_{k_1}$ for minimum (Ω_m)

Fig. 5-19 a $\quad N_{k_2}$ for maximum (Ω_p)

Fig. 5-19 b $\quad N_{k_2}$ for minimum (Ω_m)

Fig. 5-20 $\quad N_{k_3}$ for maximum (Ω_p)

An equation for $N_{\Omega n}$ was obtained by substituting Eq. (5.14) into the basic N equation, Eq. (5.21),

$$N_{\Omega n} = -\arctan\left[-\frac{1}{\Omega_n}\right]$$

$$= -\arctan\left[\frac{-1}{\sqrt{n_1^2+n_2^2}}\right] \qquad (5.22)$$

Loci of $N_{\Omega n}$ were plotted as a function of n_1 and n_2. (Fig. 5-21)

5.9 Example

Given Complex poles: $-a \pm jb = -.8 \pm j\,4.0$

Real pole: $-c = -2.0$

Solution:

SPECIFIC DATA

$$n_1 = \frac{a}{/c/} = .4$$

$$n_2 = \frac{b}{/c/} = 2.0$$

TABLE OF PARAMETER VALUES

x	Ω_x	ω_x ***	Ω_x Fig.No.	M_x	M_x Fig.No.	N_x	N_x Fig.No.
p	1.88	3.70	5-5a	1.19	5-6a,b	-130°	5-15a
m	0.93	1.86	5-5b	0.91	5-6c	-56.5°	5-15b
bw	2.34	4.68	5-7	.707	N.A.	-192.5°	5-16b
bw	N A.	——	——	.707	N.A.	N.A.	——
bw	N.A.	——	——	.707	N.A.	N.A.	——
n	2.04	4.08	5-8	1.12	5-9b	-154°	5-21
l	2.14	4.28	5-10a,b	1.0	N.A.	-168.5°	5-17a,b
l	1.45	2.90	5-10c,d	1.0	N.A.	-85°	5-17c
k_1 *	1.52	3.04	5-11	1.025	5-12a	-89°	5-18a
k_1 **	0.76	1.52	5-11	0.912	5-12b	-47°	5-18b
k_2 *	2.64	5.28	5-11	0.42	5-13a	-212°	5-19a
k_2 **	1.33	2.66	5-11	0.955	5-13b	-77°	5-19b
k_3 *	3.4	6.80	5-11	0.15	5-14	-233°	5-20

* Relative to Ω_p ** Relative to Ω_m *** $\omega_x = /c/\ \Omega_x$

GENERAL DATA (for all pure third order)

ω (or Ω)	M	dM/dω	N	dN/dω
0	1.0	0	0^o	—
ω_p	M_p	0	—	—
ω_n	M_m	0	—	—
∞	0	0	-270^o	0

Fig. 5-22 (page 69) compares the frequency response obtained from this rapid approximation method to the actual M and N contours obtained from a digital computer program of the general M and N equations.

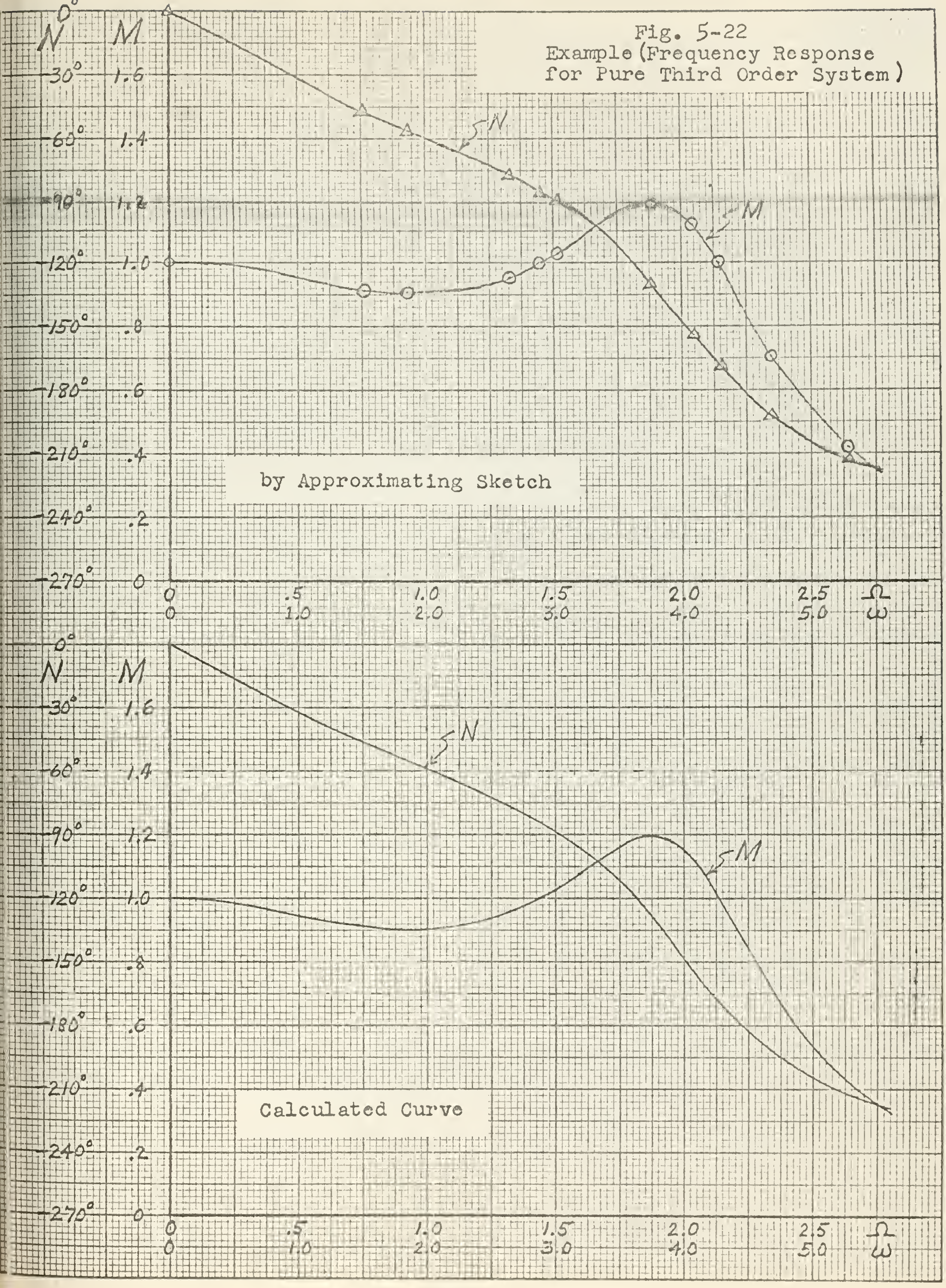

Fig. 5-22
Example (Frequency Response for Pure Third Order System)

Fig. 5-4
Determination of General M Curve Shape
for Pure Third Order System

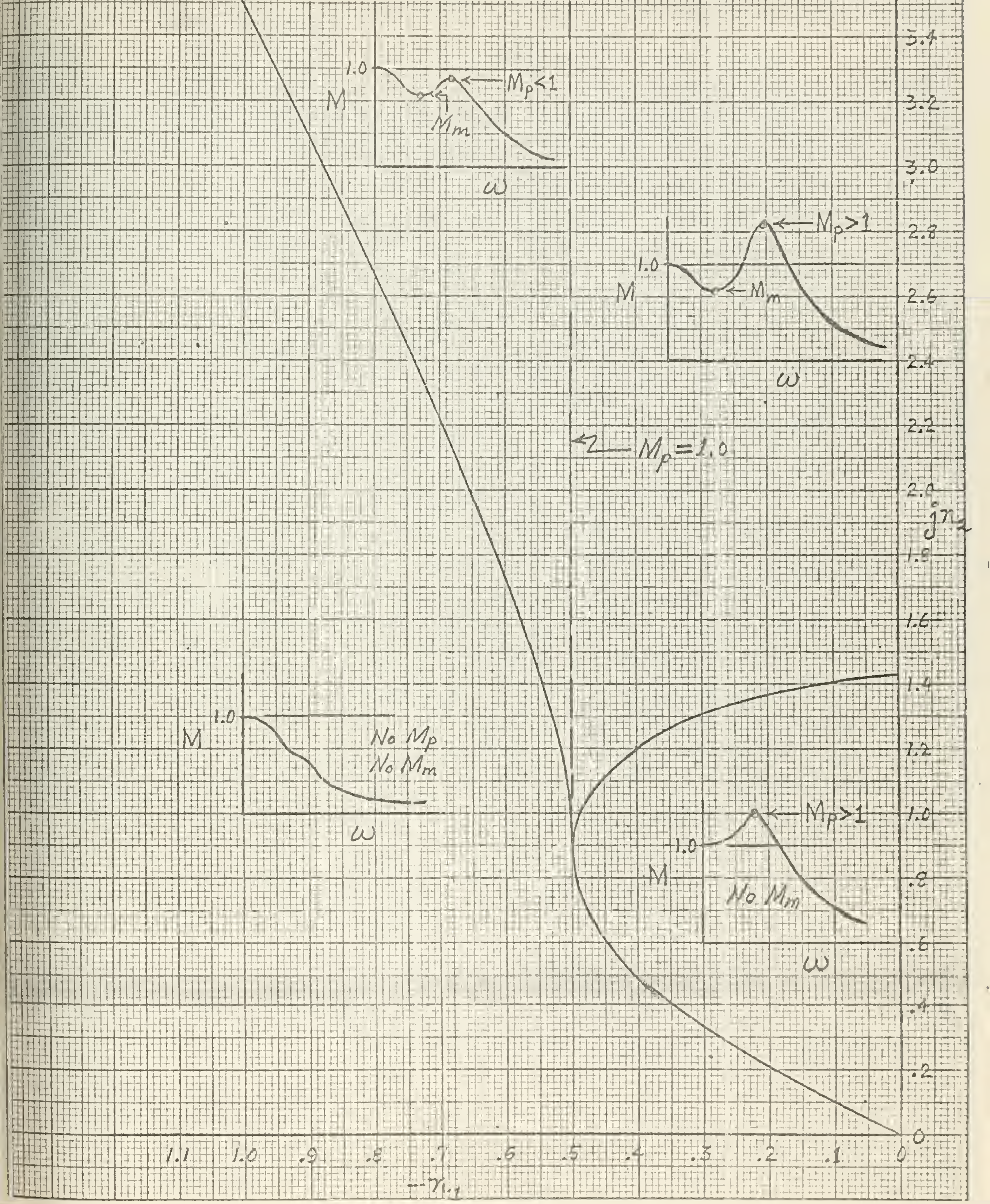

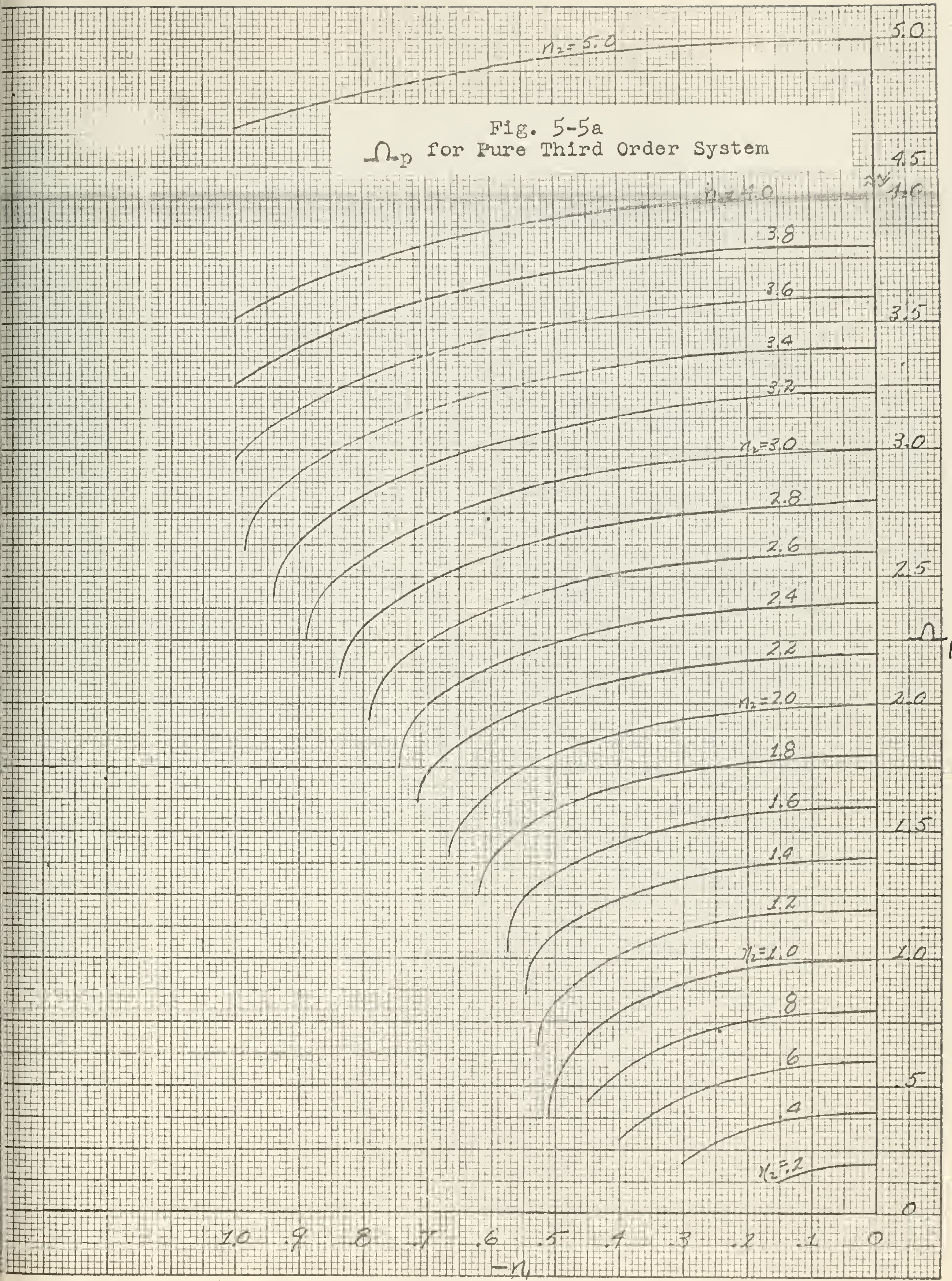

Fig. 5-5a
Ω_p for Pure Third Order System
$n_2=5.0$
$n_2=4.0$
3.8
3.6
3.4
3.2
$n_2=3.0$
2.8
2.6
2.4
2.2
$n_2=2.0$
1.8
1.6
1.4
1.2
$n_2=1.0$
.8
.6
.4
$n_2=.2$
5.0
4.5
4.0
3.5
3.0
2.5
Ω_p
2.0
1.5
1.0
.5
0
1.0 .9 .8 .7 .6 .5 .4 .3 .2 .1 0
$-n_1$

Fig. 5-5b

Ω_m for Pure Third Order System

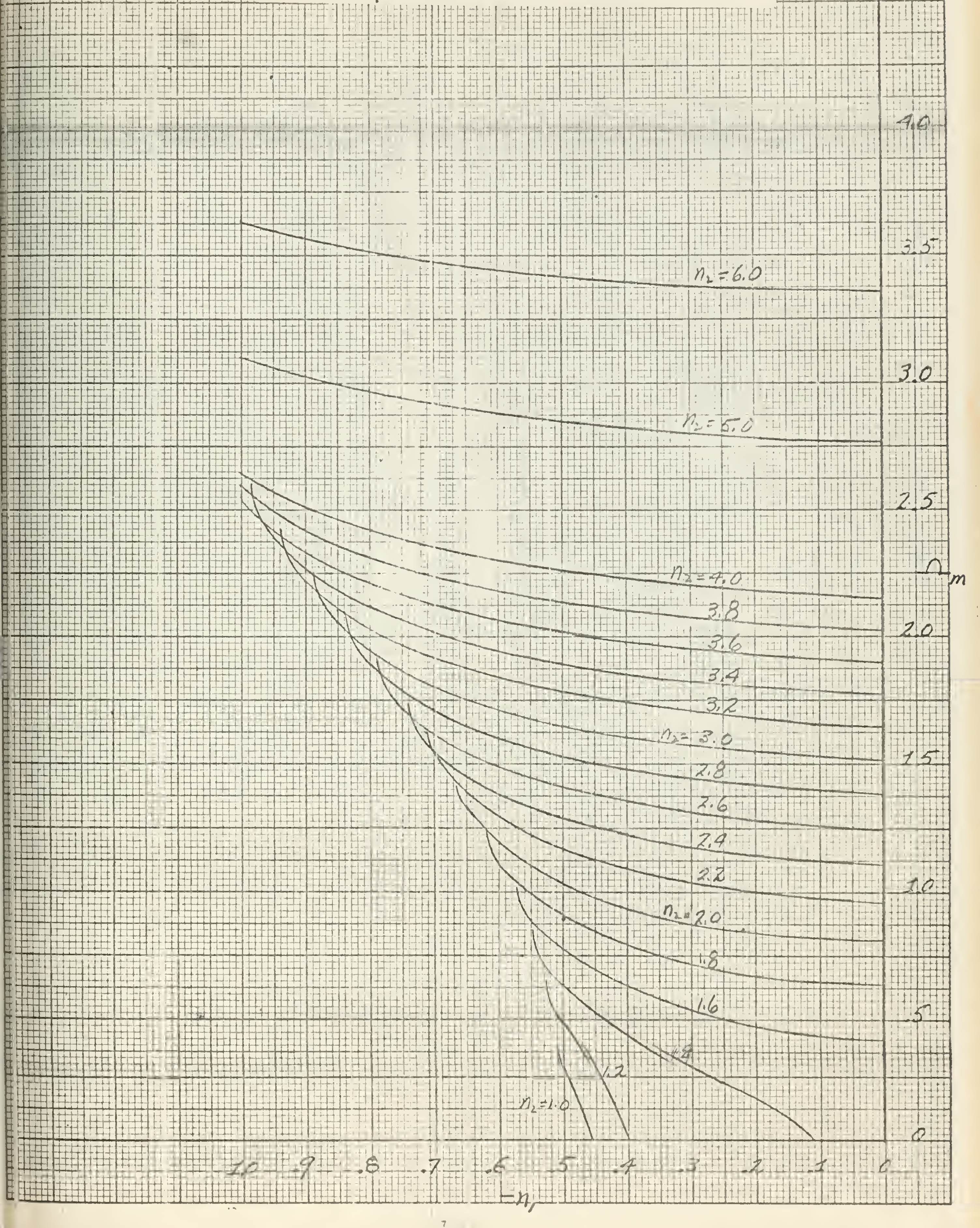

Fig. 5-6a
M_p for Pure Third Order System

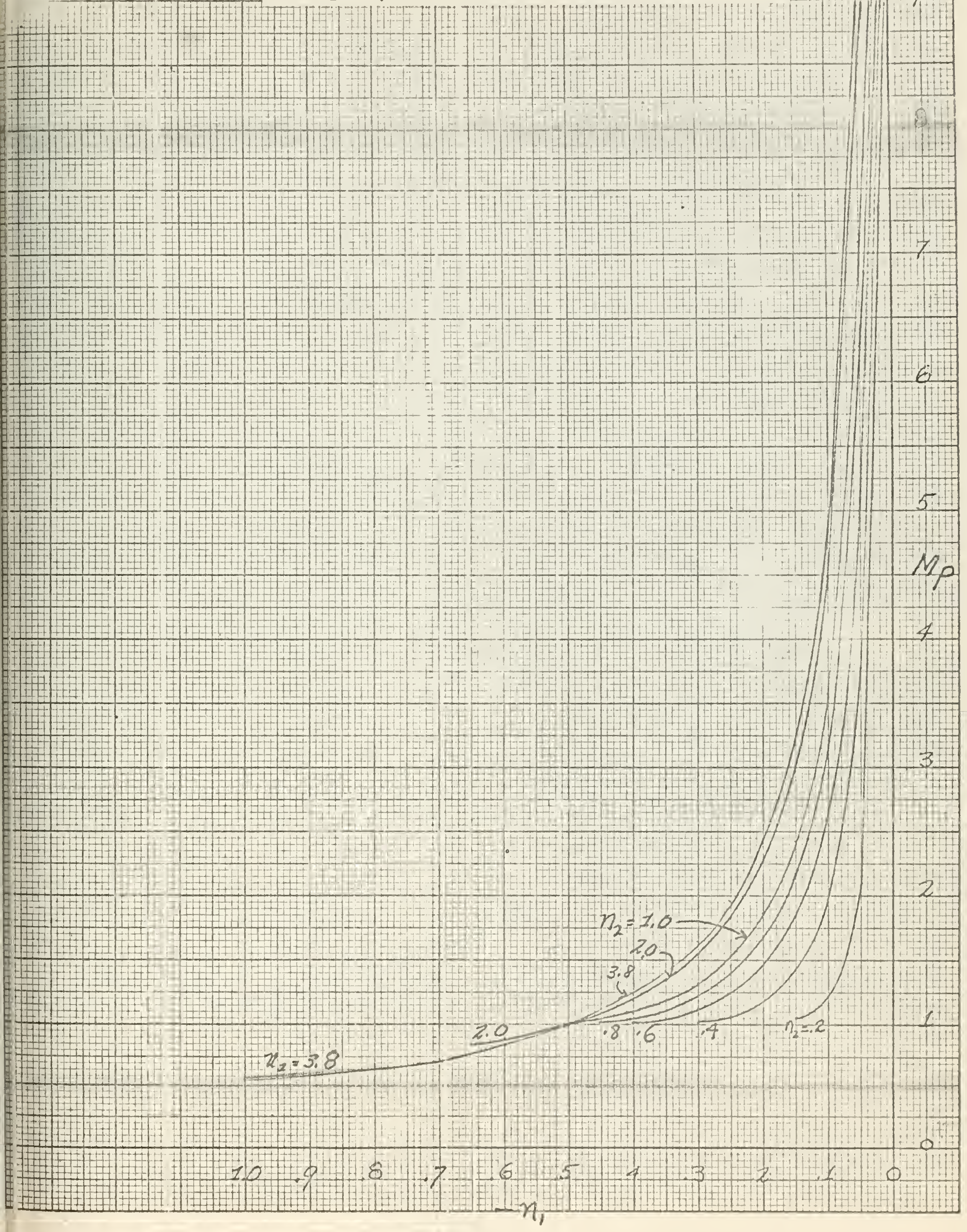

Fig. 5-6b
M_p for Pure Third Order System
Expanded

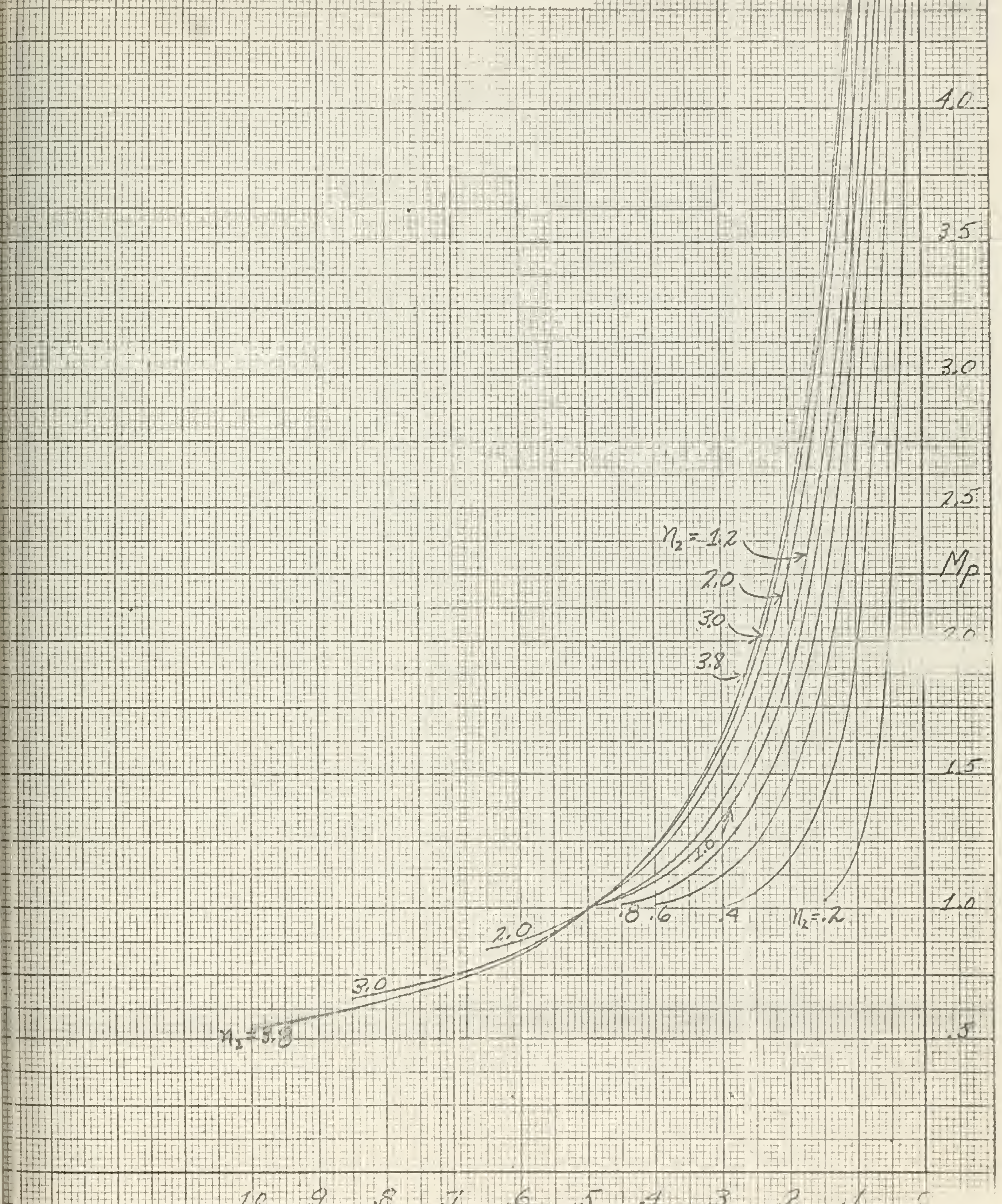

Fig. 5-6c
M_m for Pure Third Order System

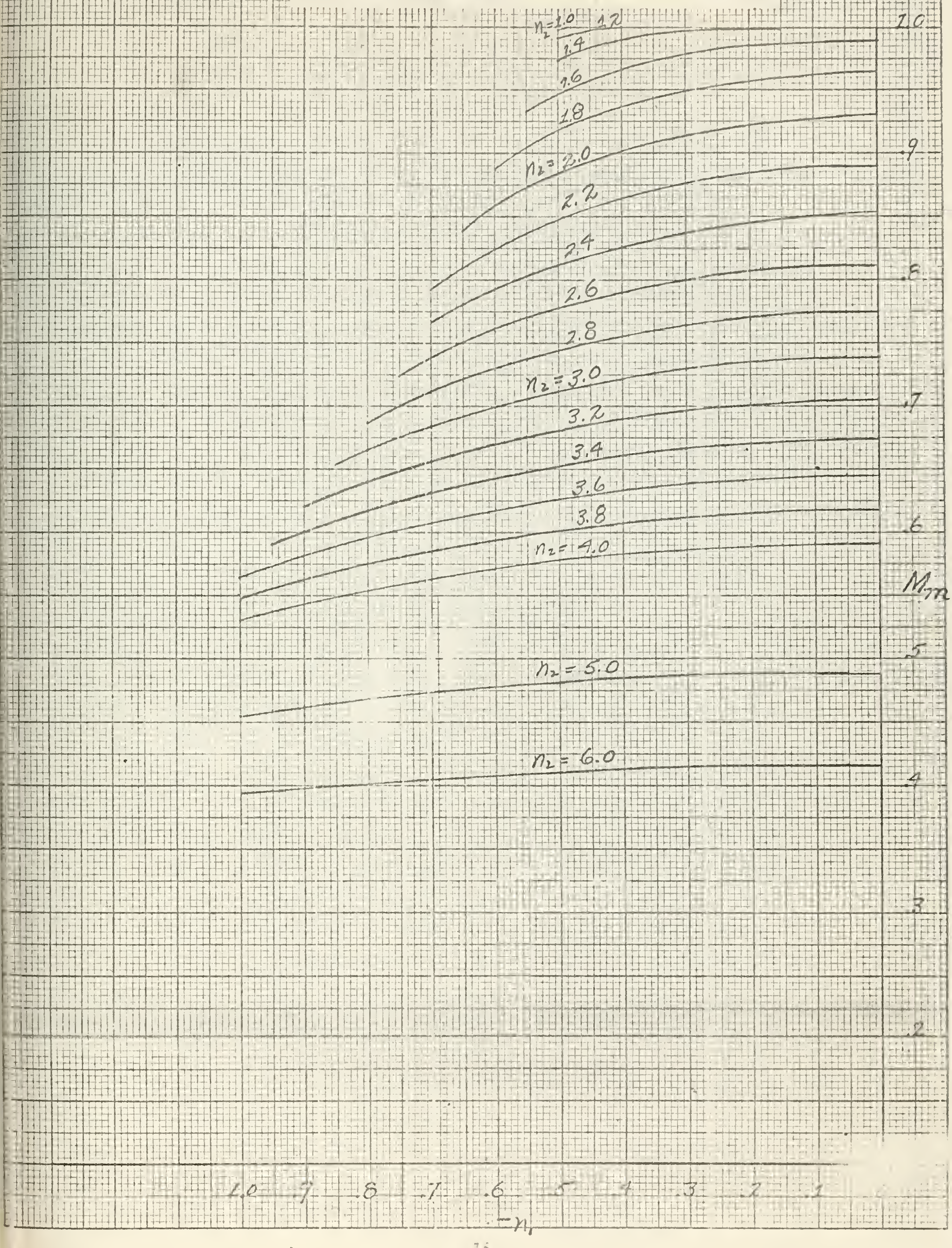

Fig. 5-7
Ω_{bw} for Pure Third Order System

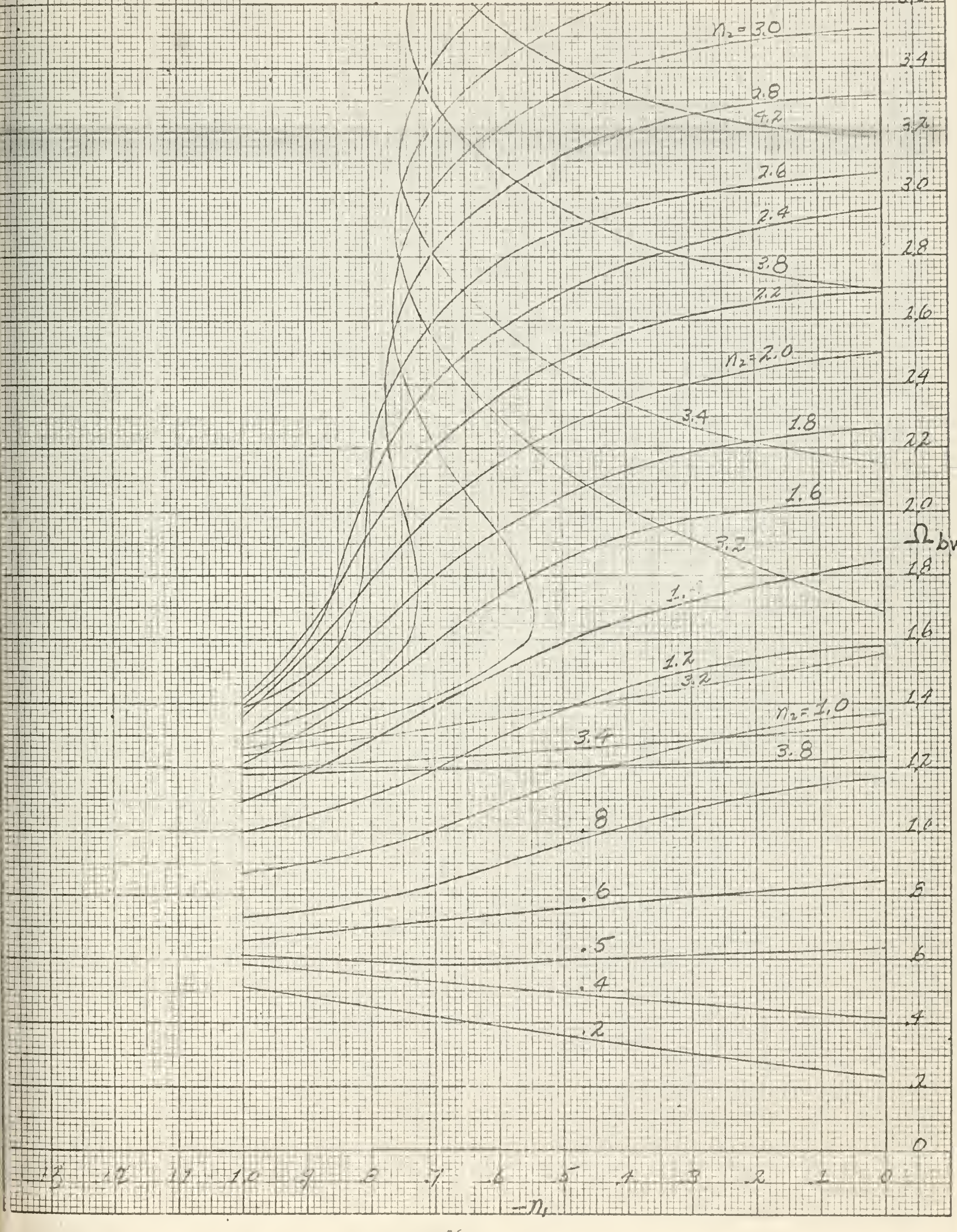

Fig. 5-8
Ω_n for Pure Third Order System

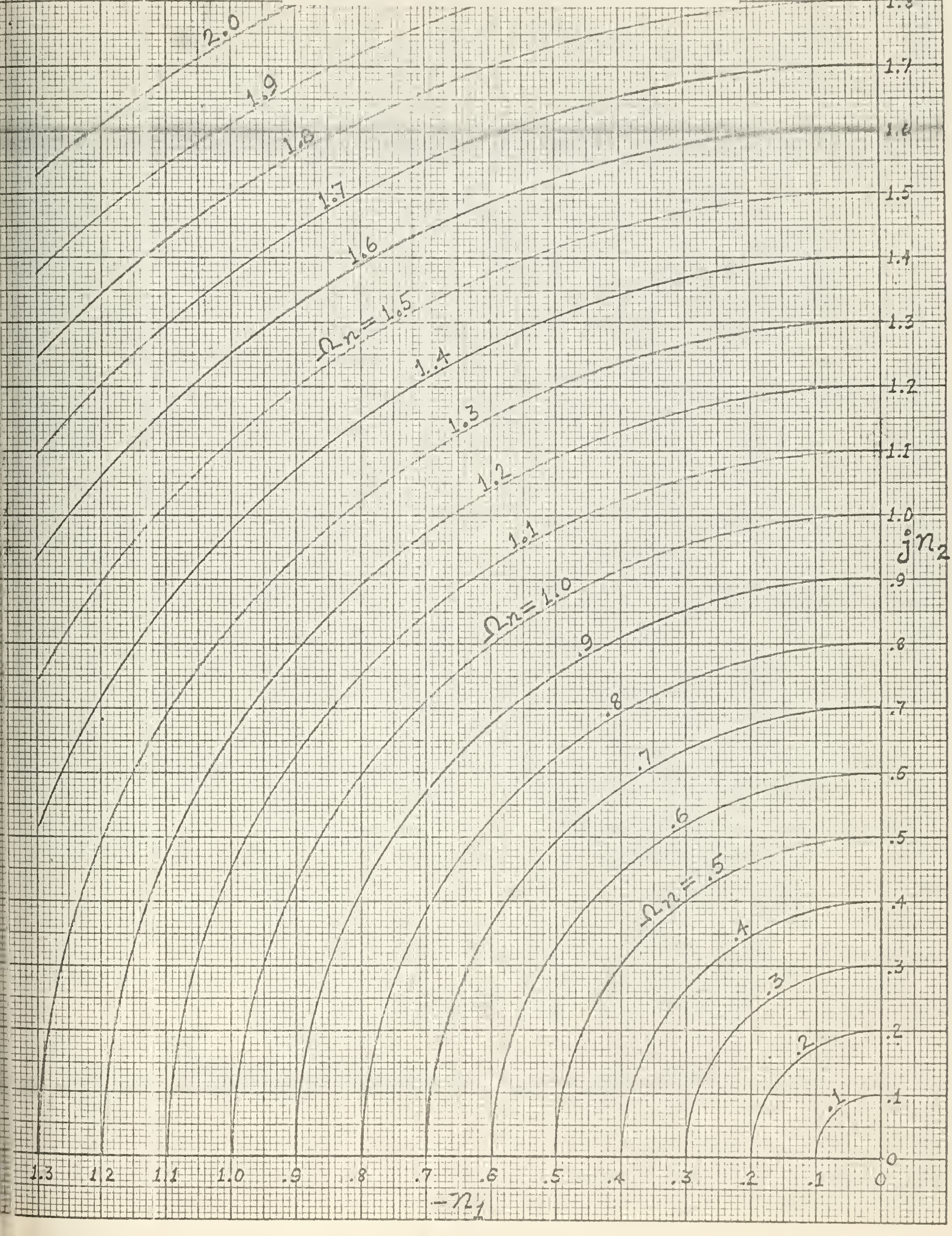

Fig. 5-9a
M_{Ω_n} for Pure Third Order System

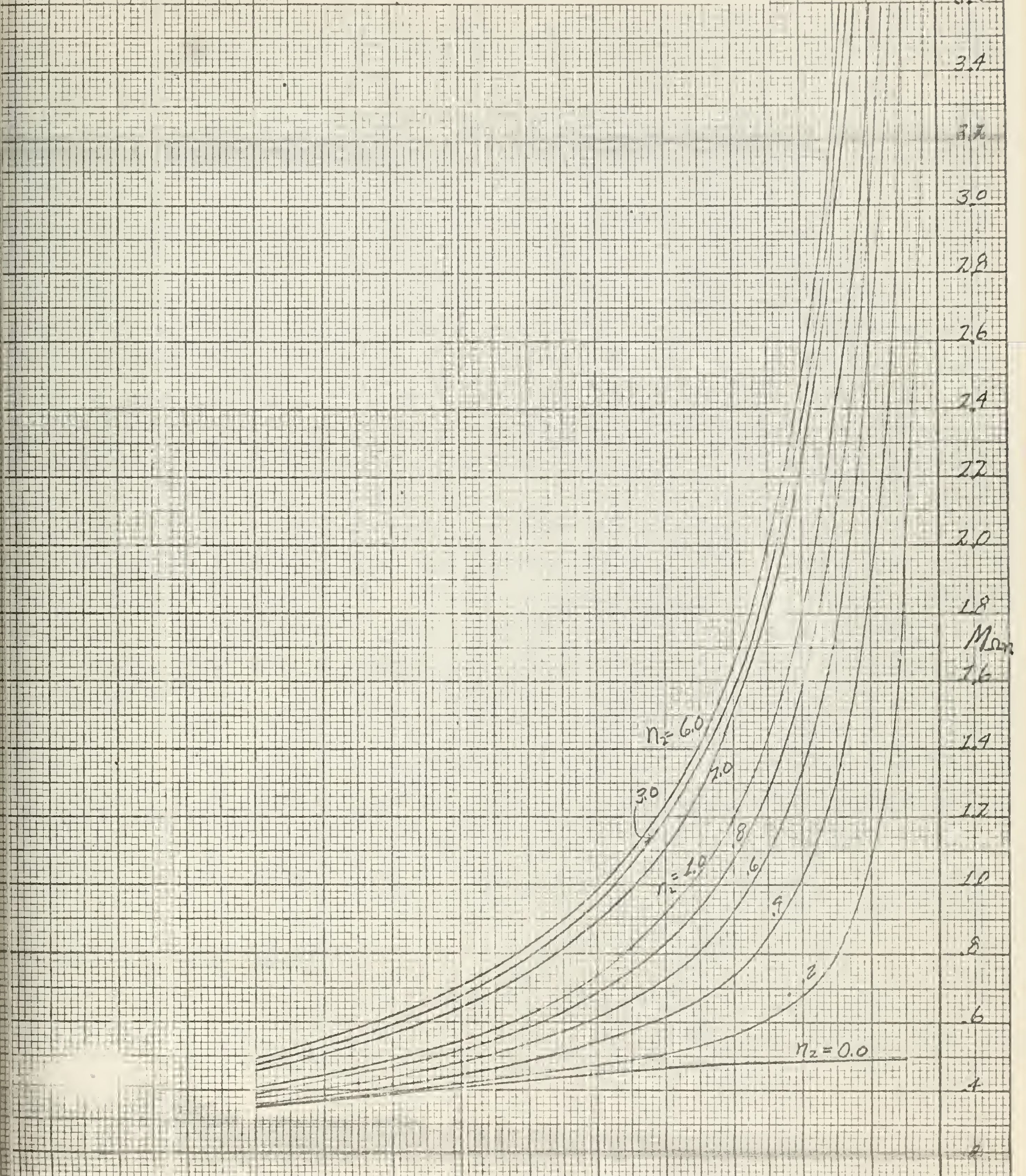

Fig. 5-9b
$M_{\Omega n}$ for Pure Third Order System
Expanded

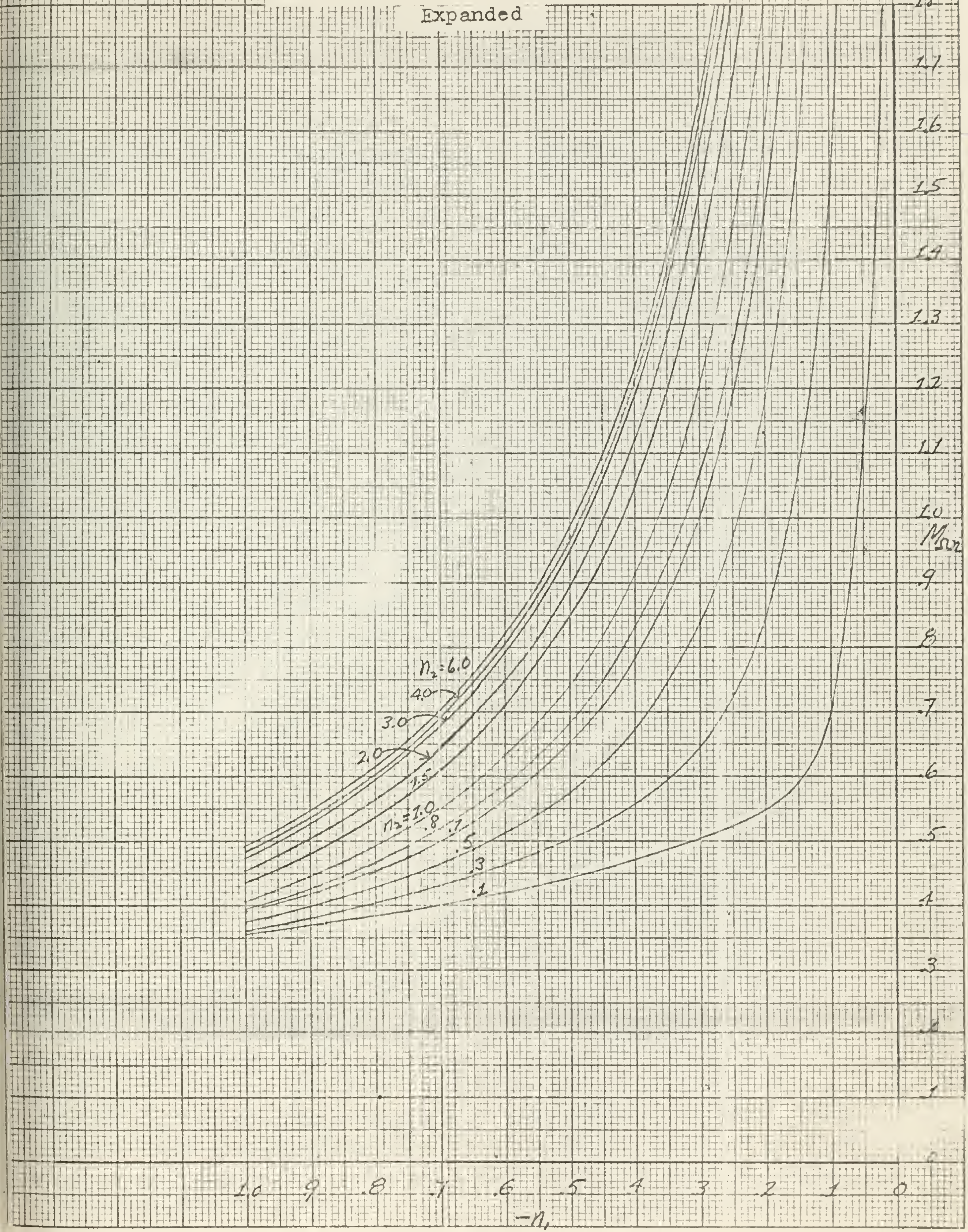

Fig. 5-10a. Ω_1 for Pure Third Order System

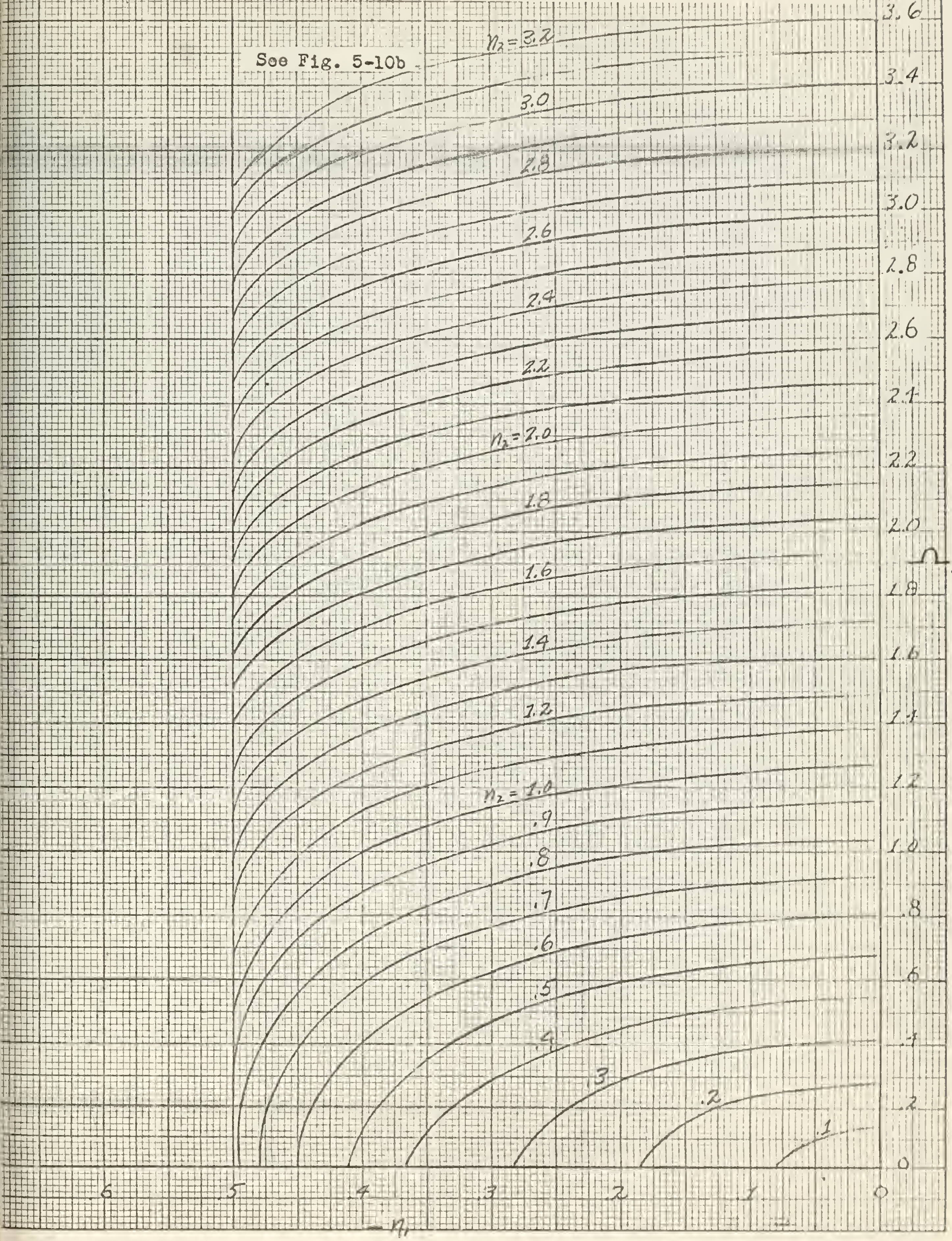

Fig. 5-10b

Ω_1 for Pure Third Order System

Extended

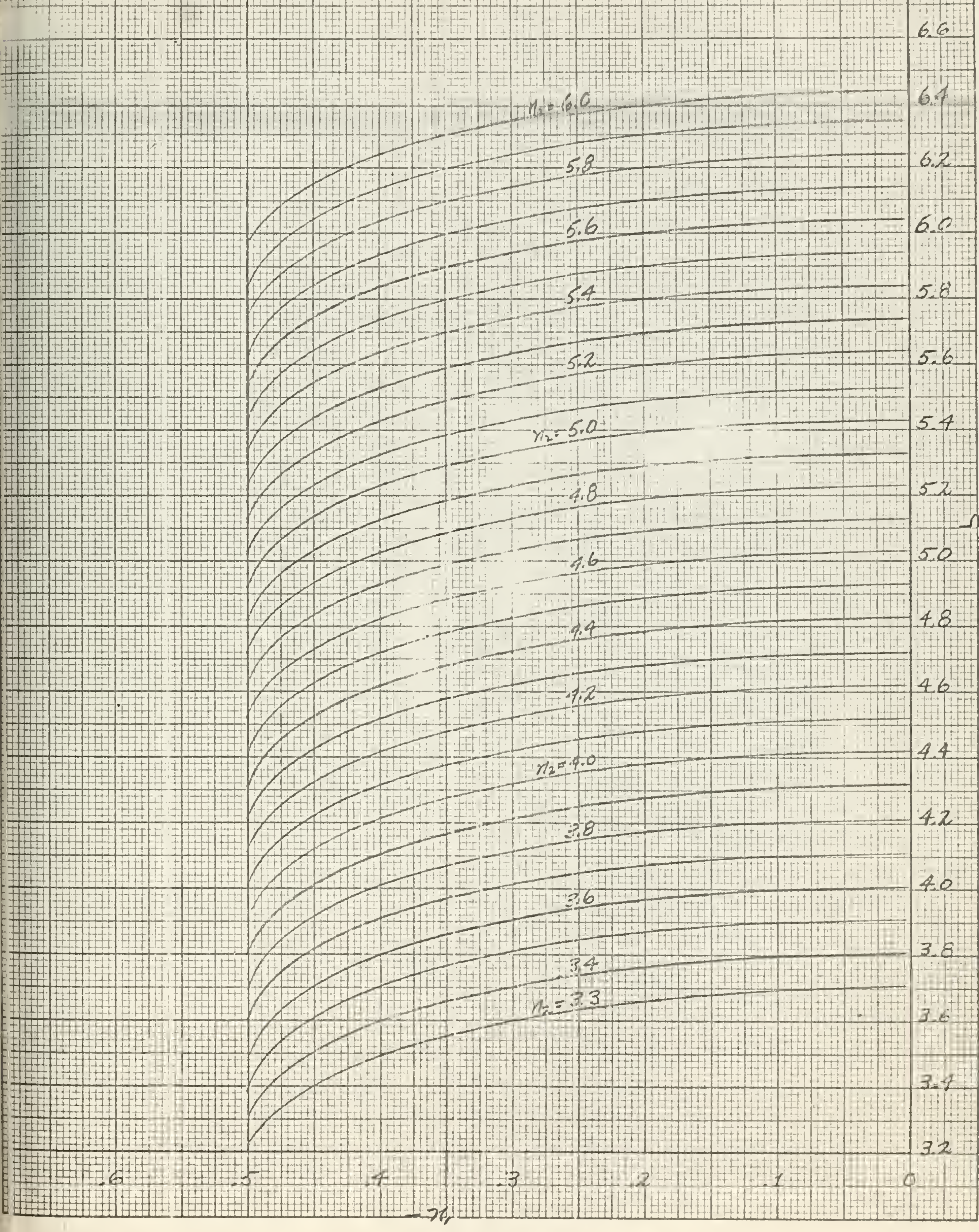

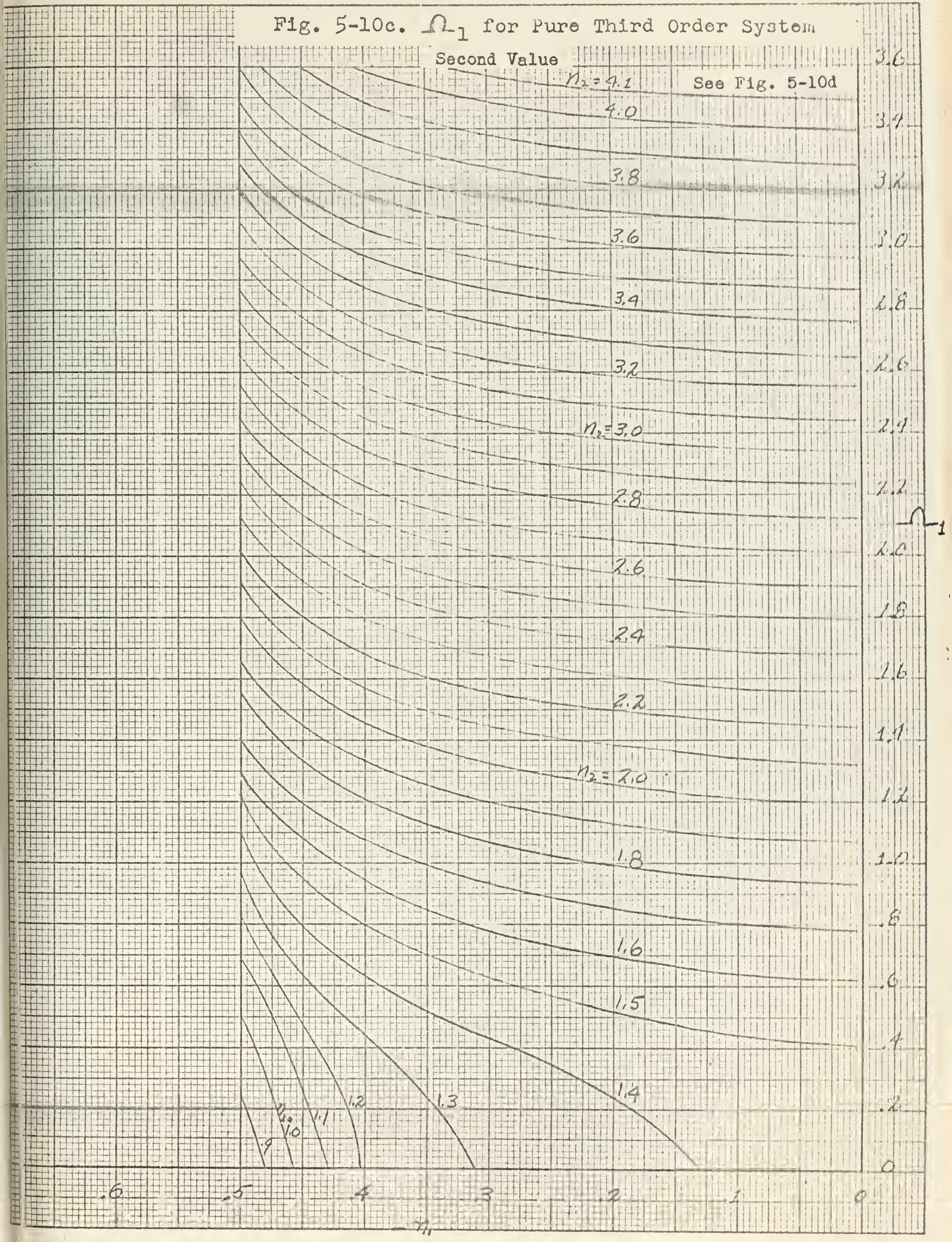
Fig. 5-10c. Ω_1 for Pure Third Order System
Second Value
See Fig. 5-10d
n_2=4.1
4.0
3.8
3.6
3.4
3.2
n_2=3.0
2.8
2.6
2.4
2.2
n_2=2.0
1.8
1.6
1.5
1.4
1.3
1.2
1.1
n_2=1.0
.9
3.6
3.4
3.2
3.0
2.8
2.6
2.4
2.2
2.0
1.8
1.6
1.4
1.2
1.0
.8
.6
.4
.2
0
Ω_1
.6
.5
.4
.3
.2
.1
0
n_1

Fig. 5-10d

Ω_1 for Pure Third Order System

Second Value, Extended

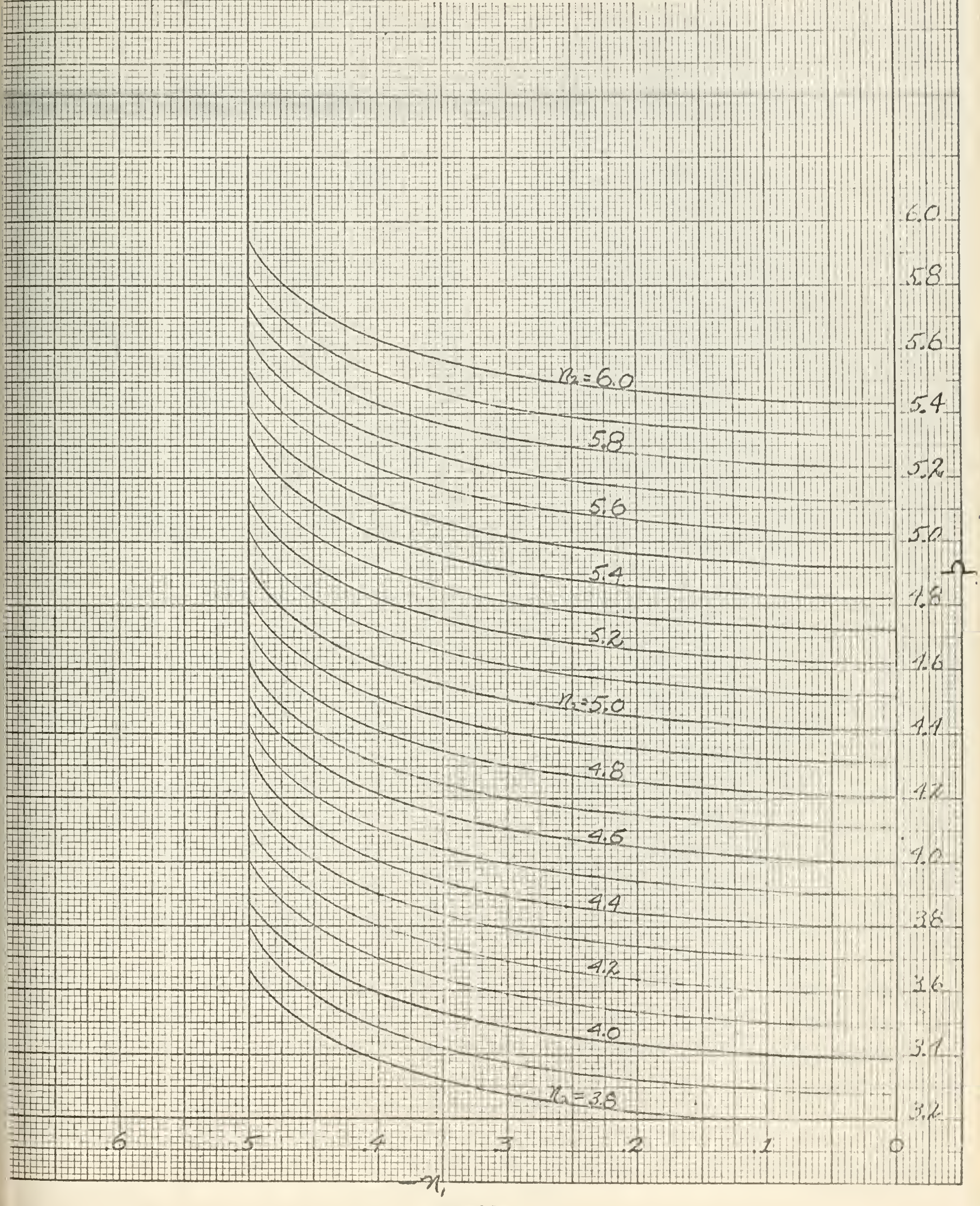

Fig. 5-11

Ω_k versus Ω_p and Ω_m

for Pure Third Order System

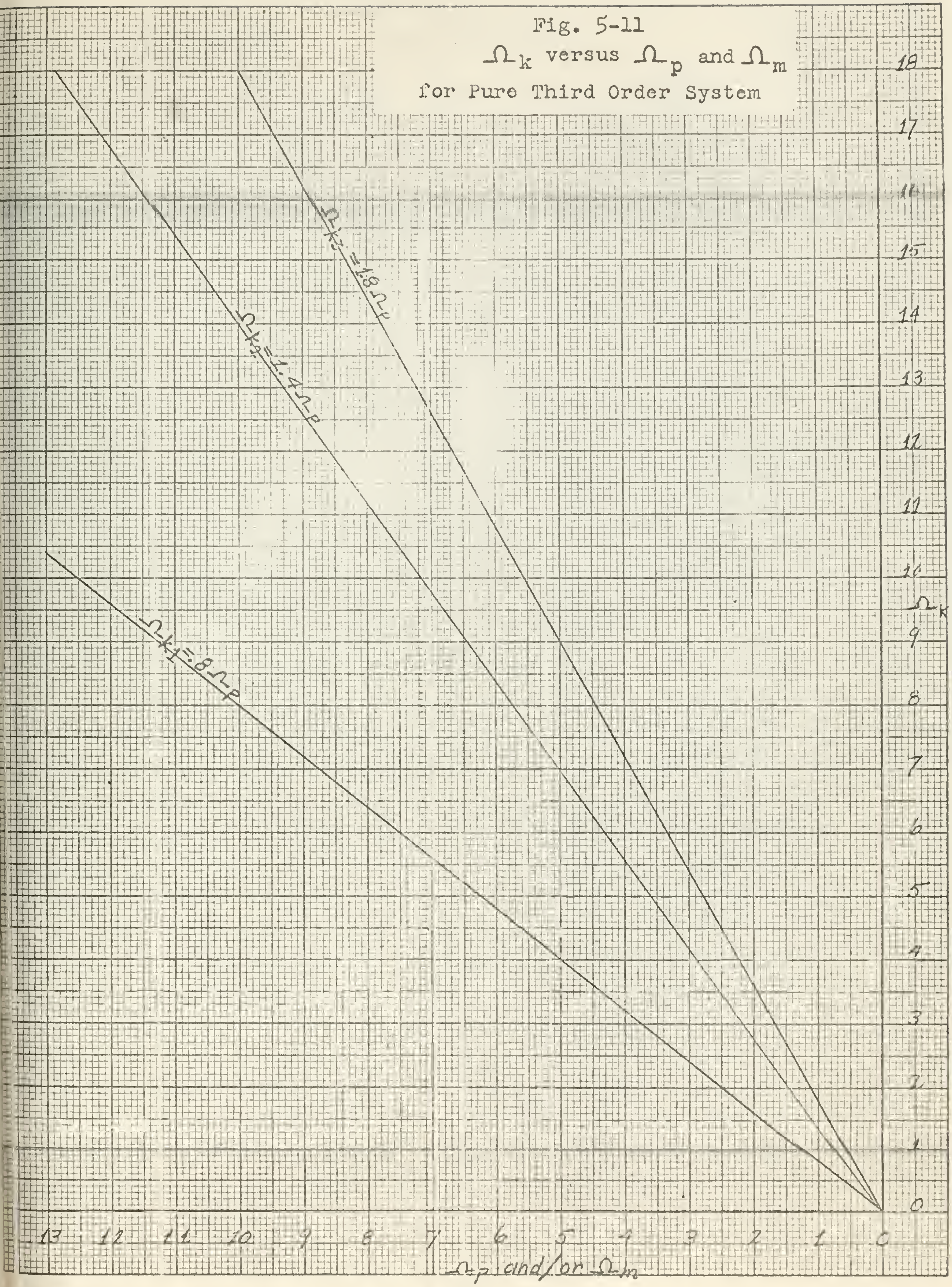

Fig. 5-12a
M_{k_1} for Pure Third Order System
Relative to Ω_p

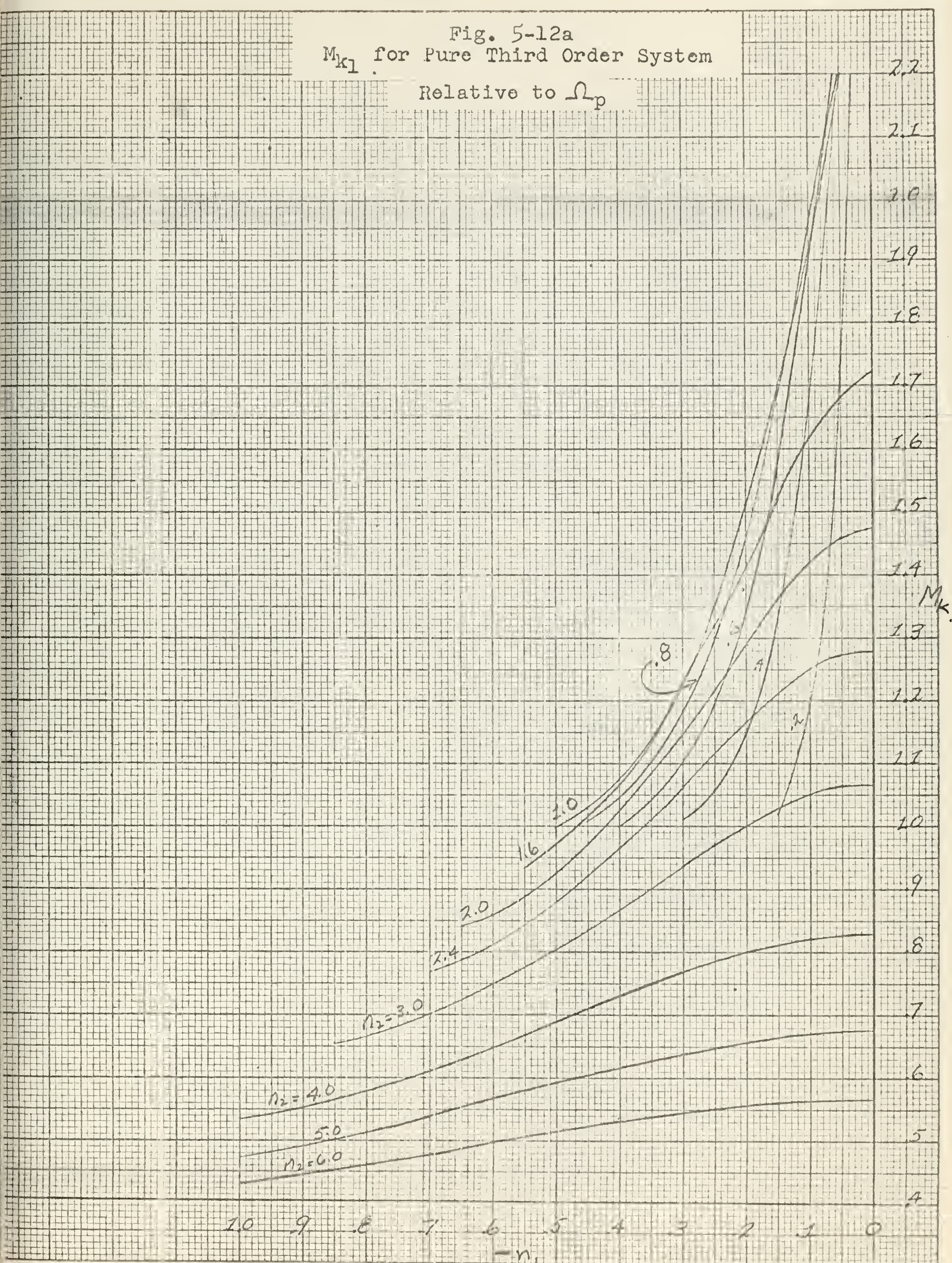

Fig. 5-12b
M_{k1} for Pure Third Order System

Relative to Ω_m

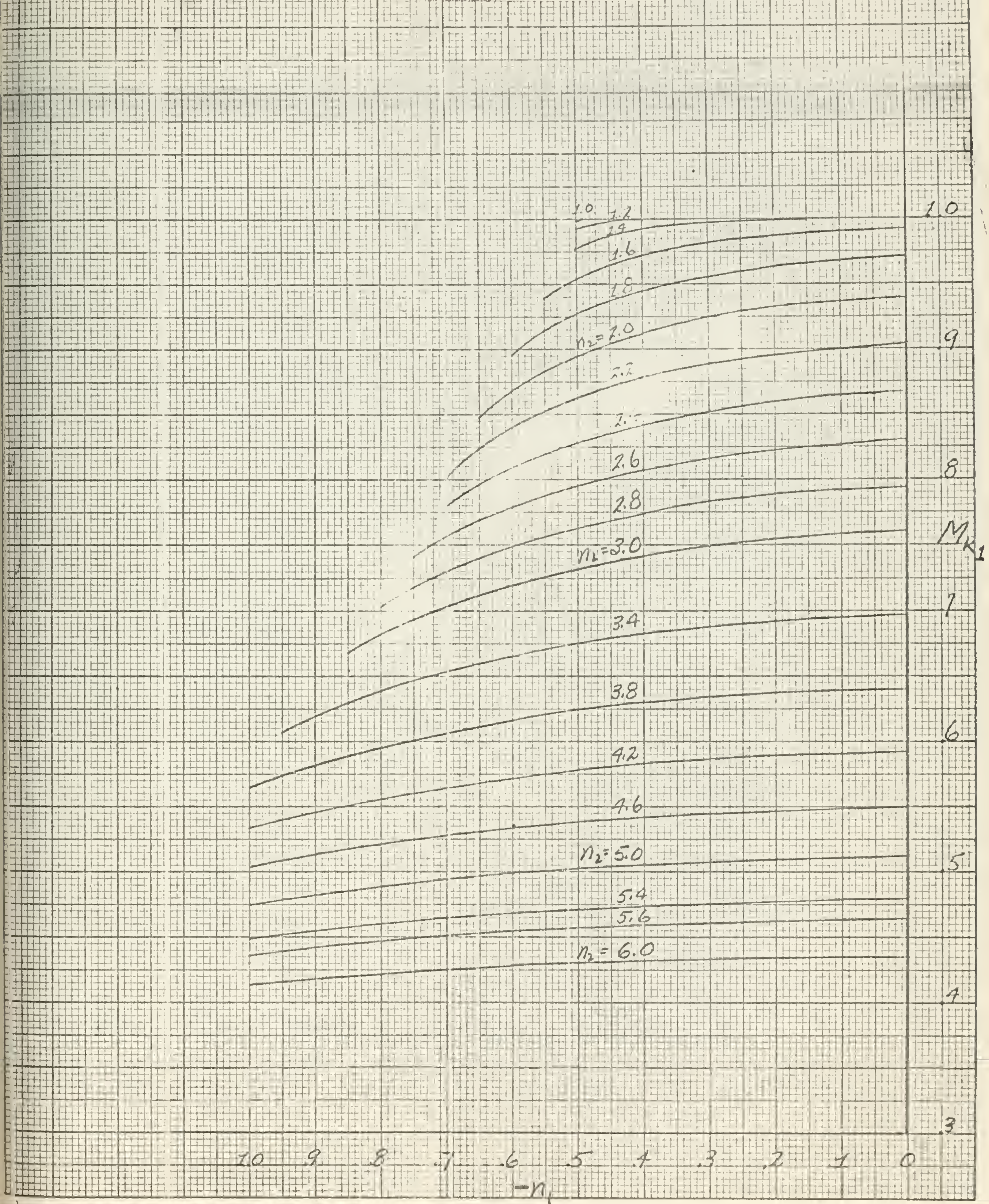

Fig. 5-13a
M_{k2} for Pure Third Order System
Relative to Ω_p

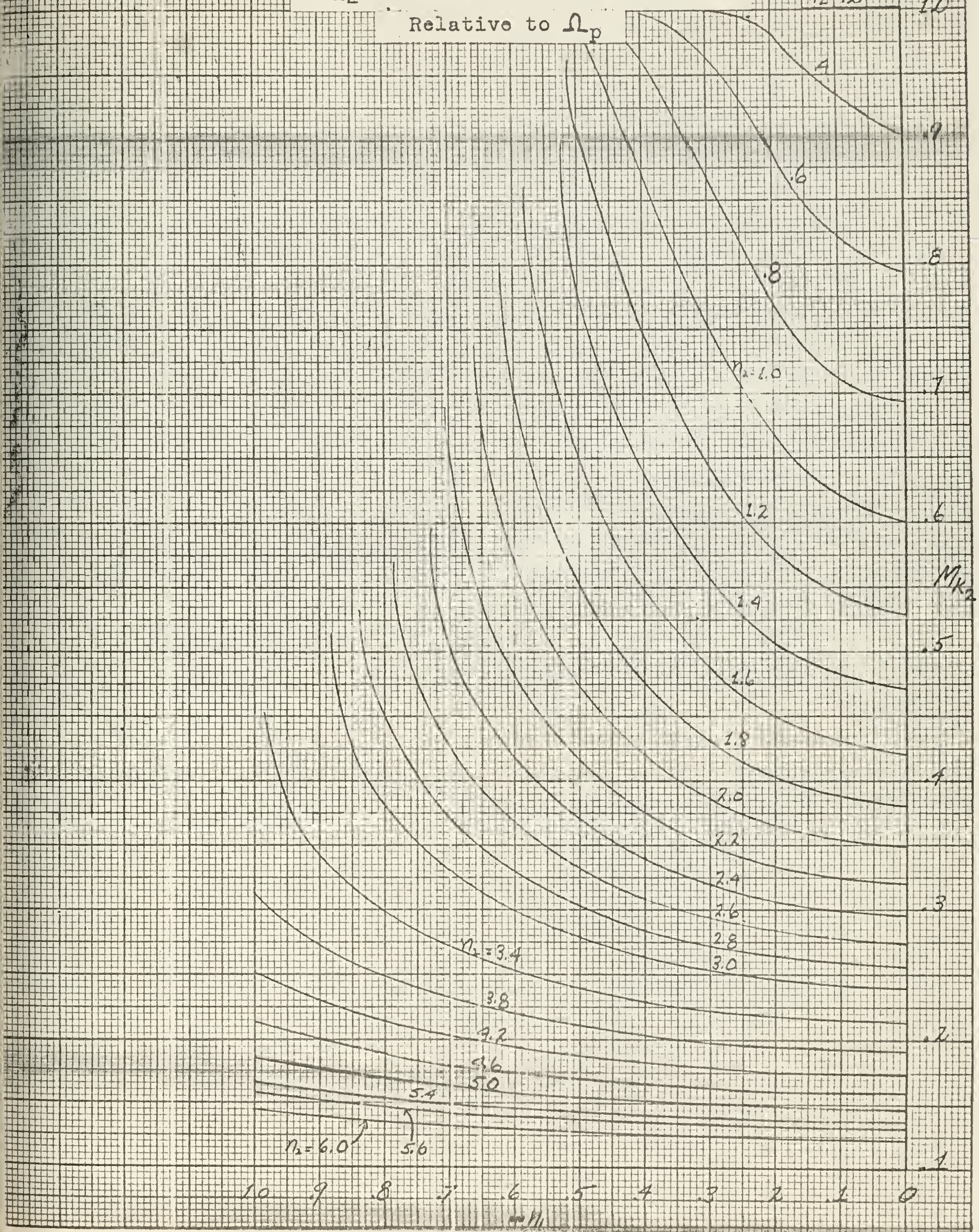

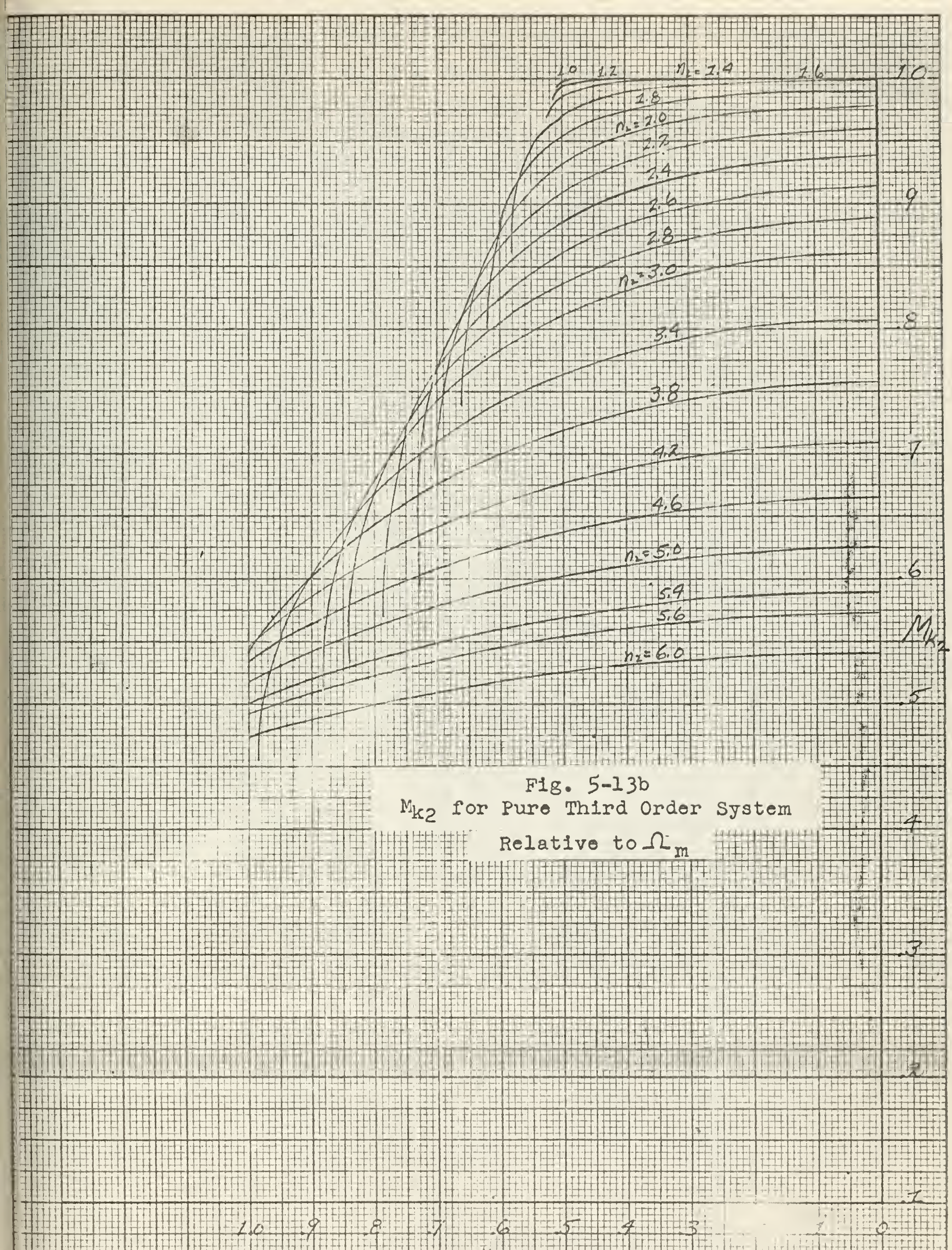

Fig. 5-13b
M_{k2} for Pure Third Order System
Relative to Ω_m

Fig. 5-14
M_{k3} for Pure Third Order System
Relative to Ω_p

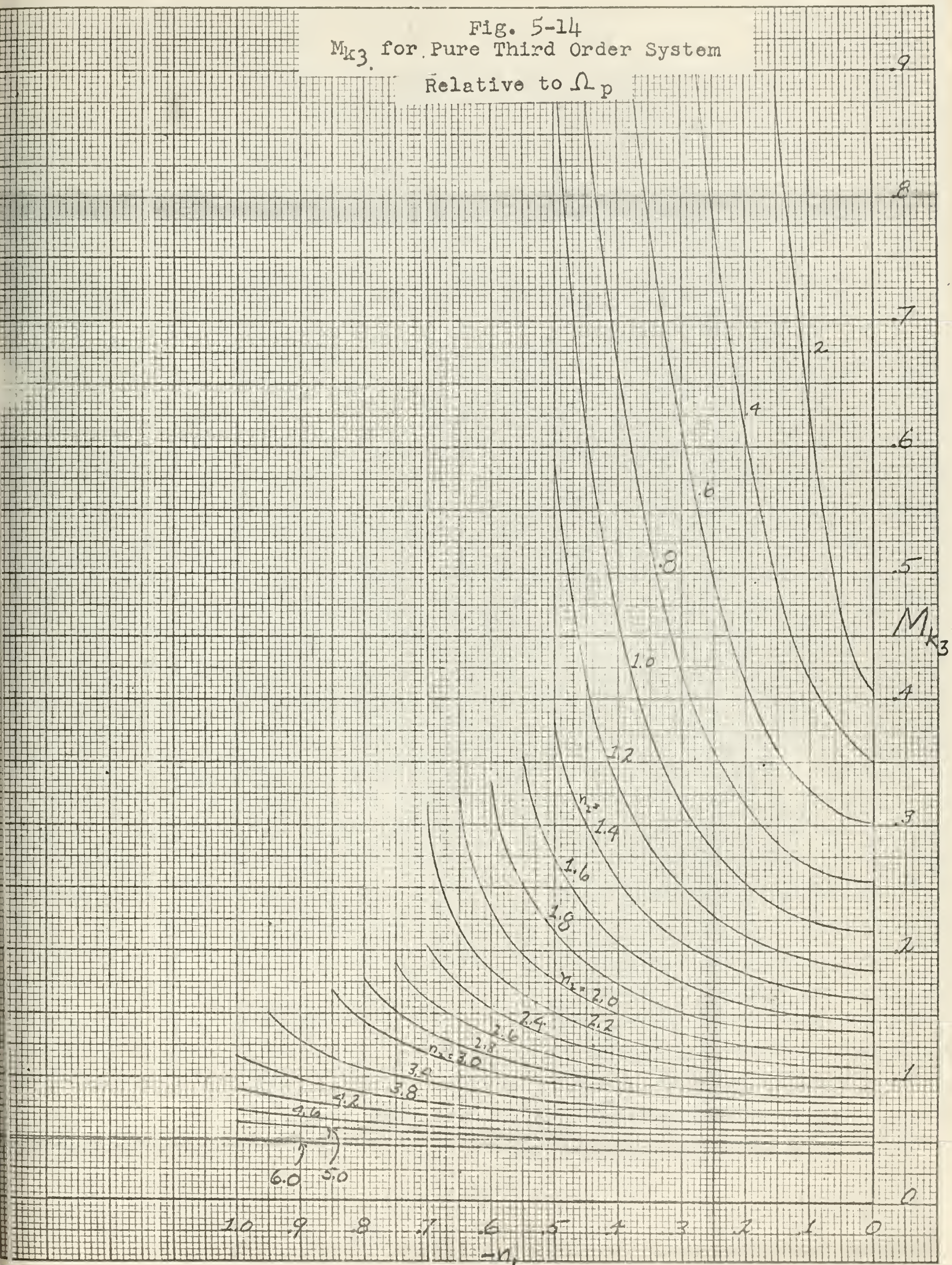

Fig. 5-15a
N_p for Pure Third Order System

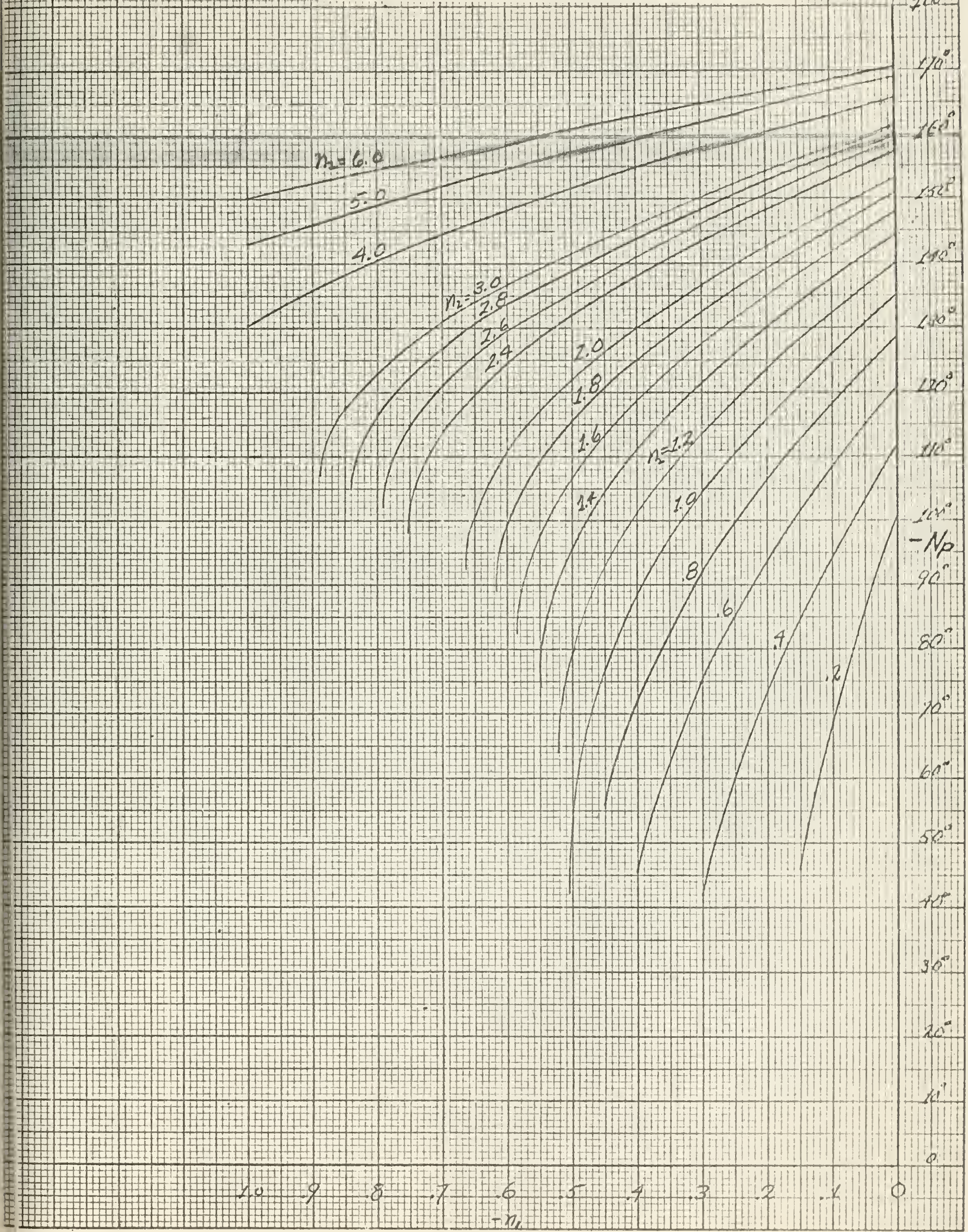

Fig. 5-15b
N_m for Pure Third Order System

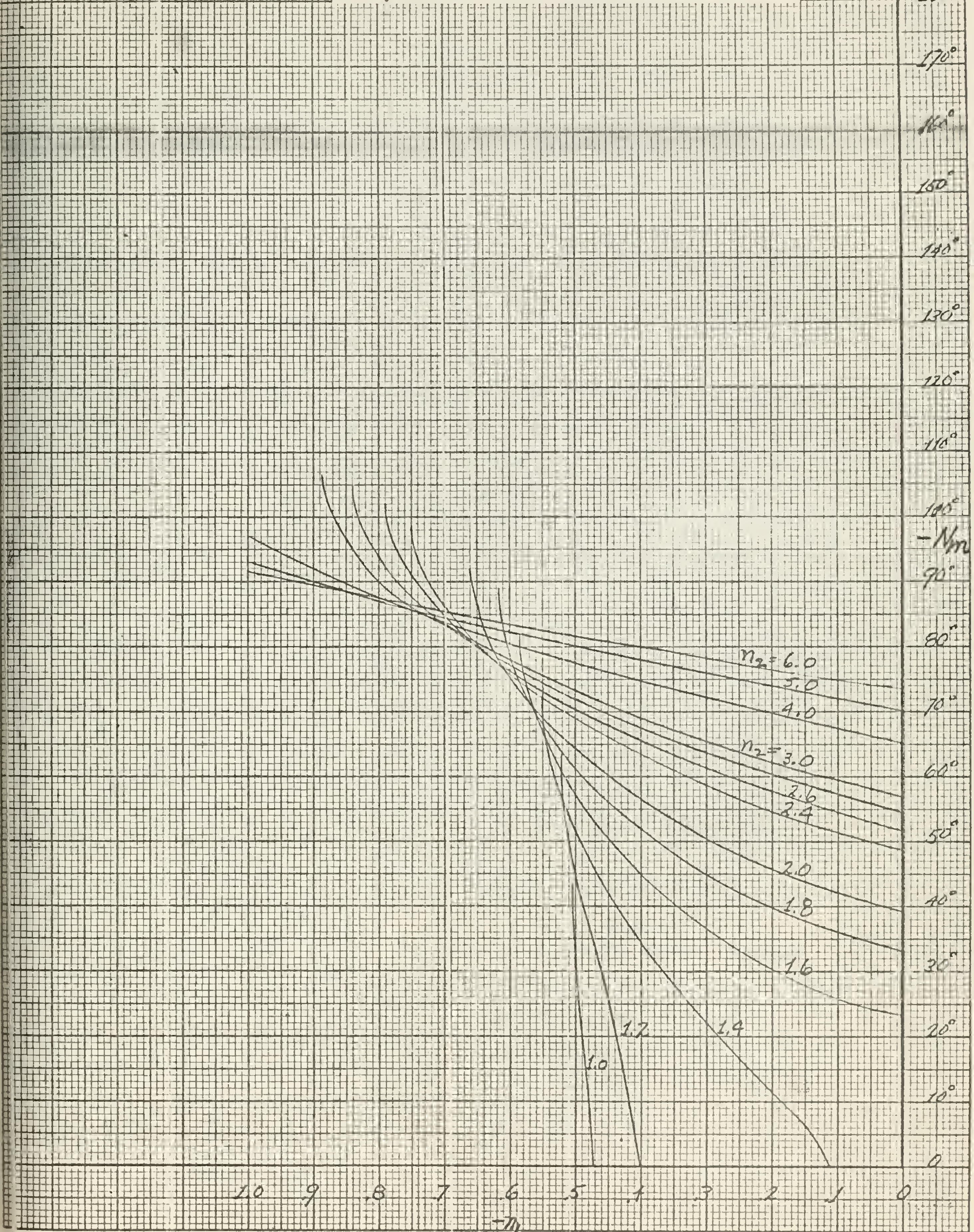

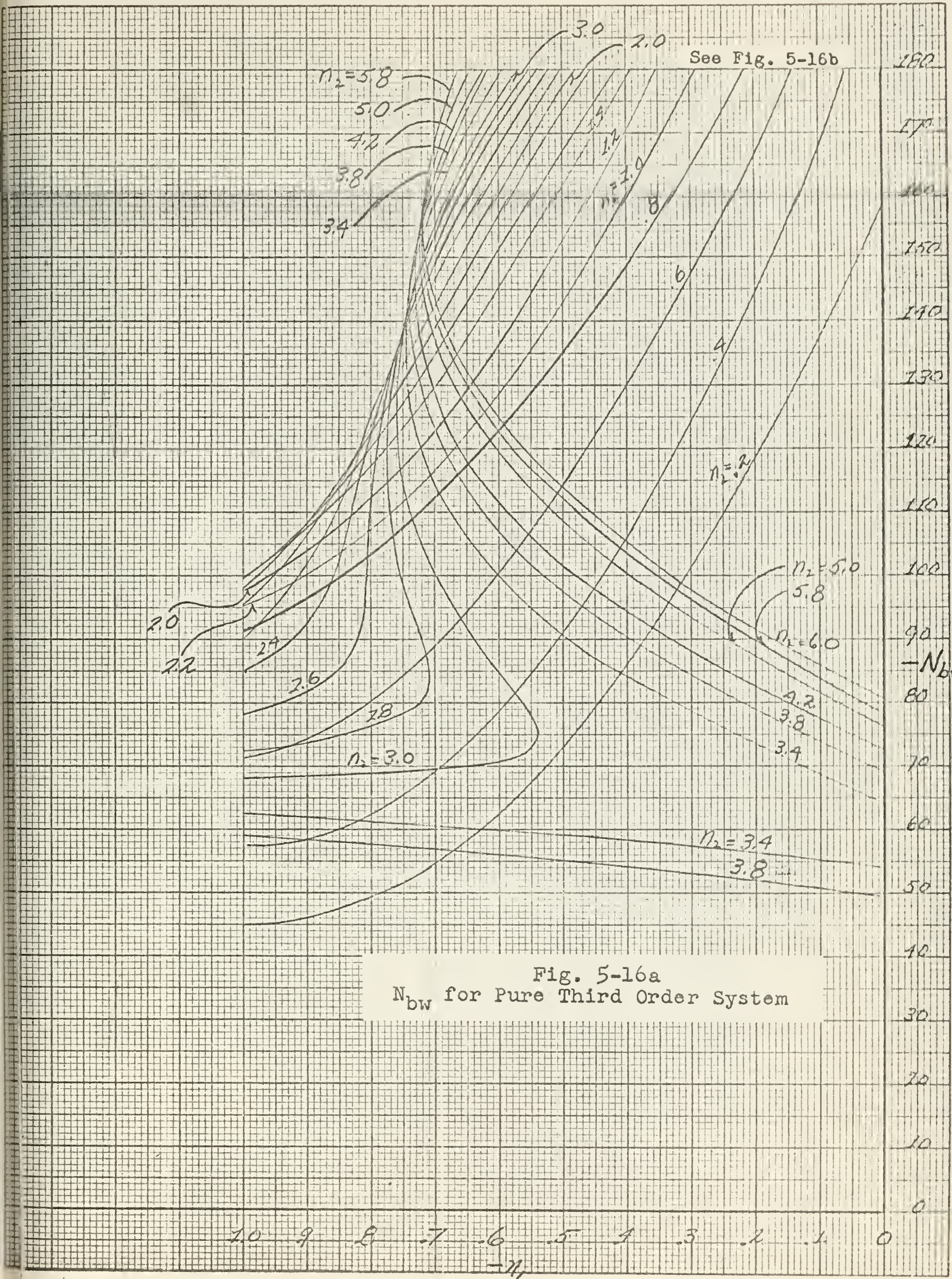

Fig. 5-16a
N_{bw} for Pure Third Order System

Fig. 5-16b
N_{bw} for Pure Third Order System

Extended

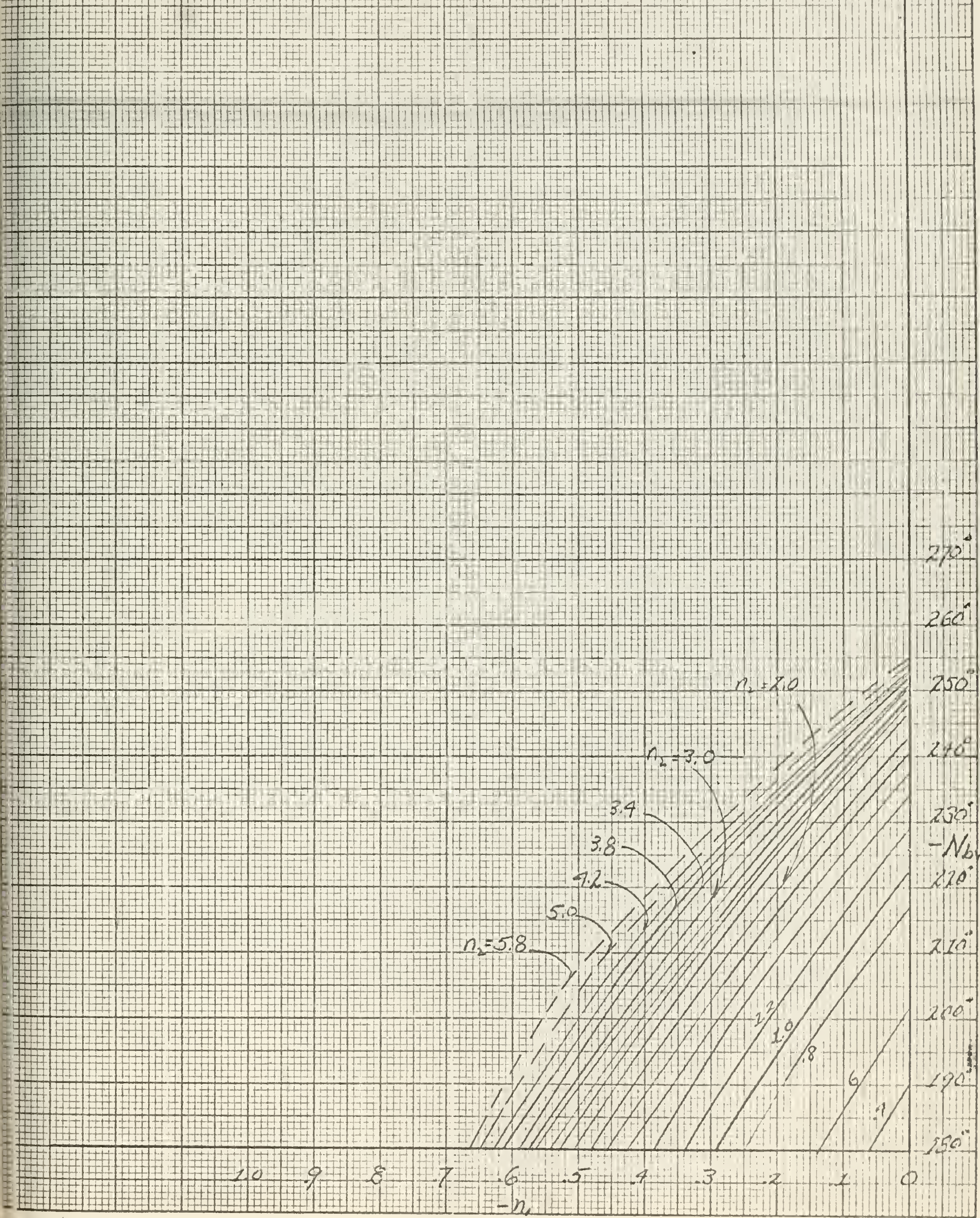

Fig. 5-17 a
N_1 for Pure Third Order System

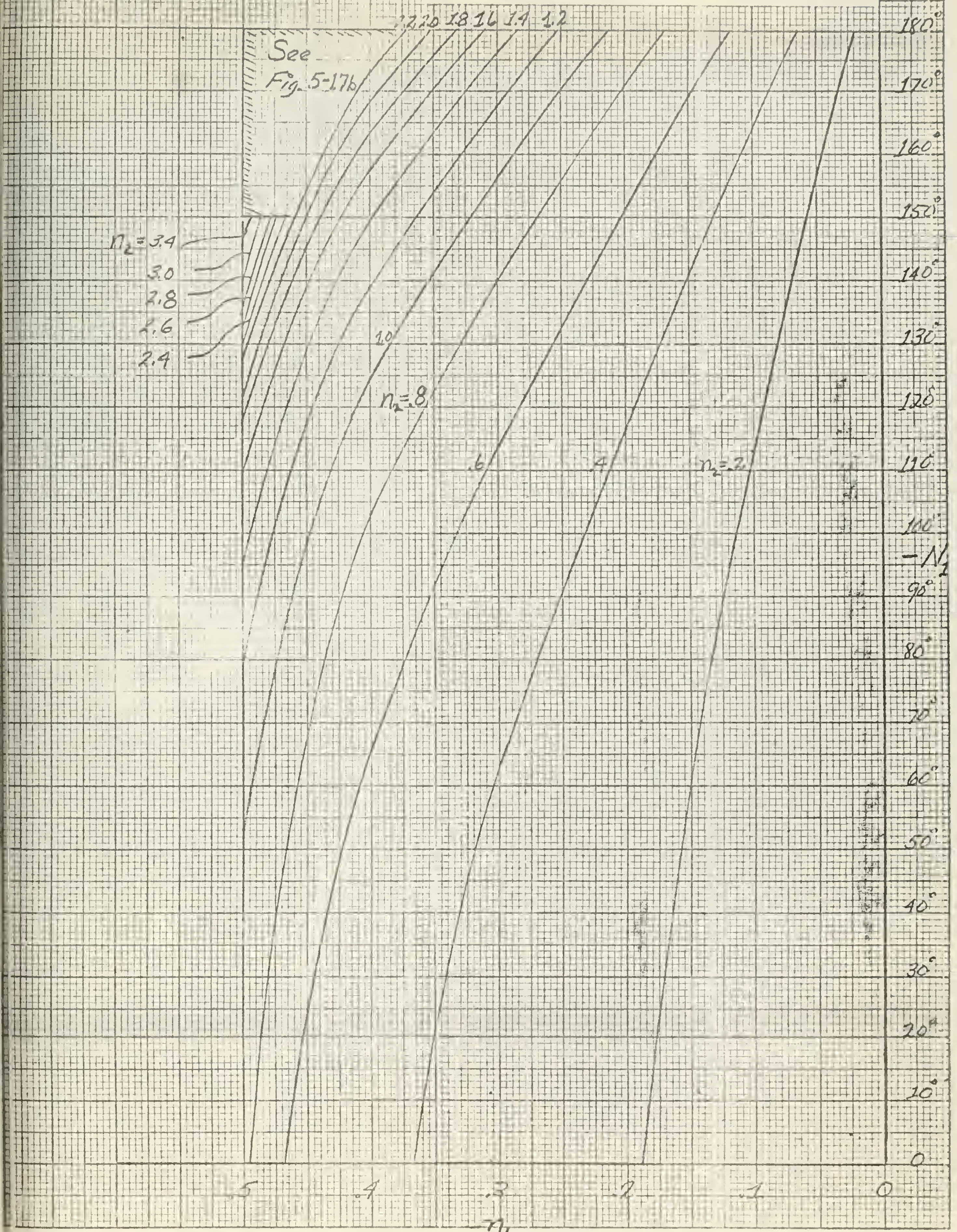

Fig. 5-17b
N_1 for Pure Third Order System

Expanded

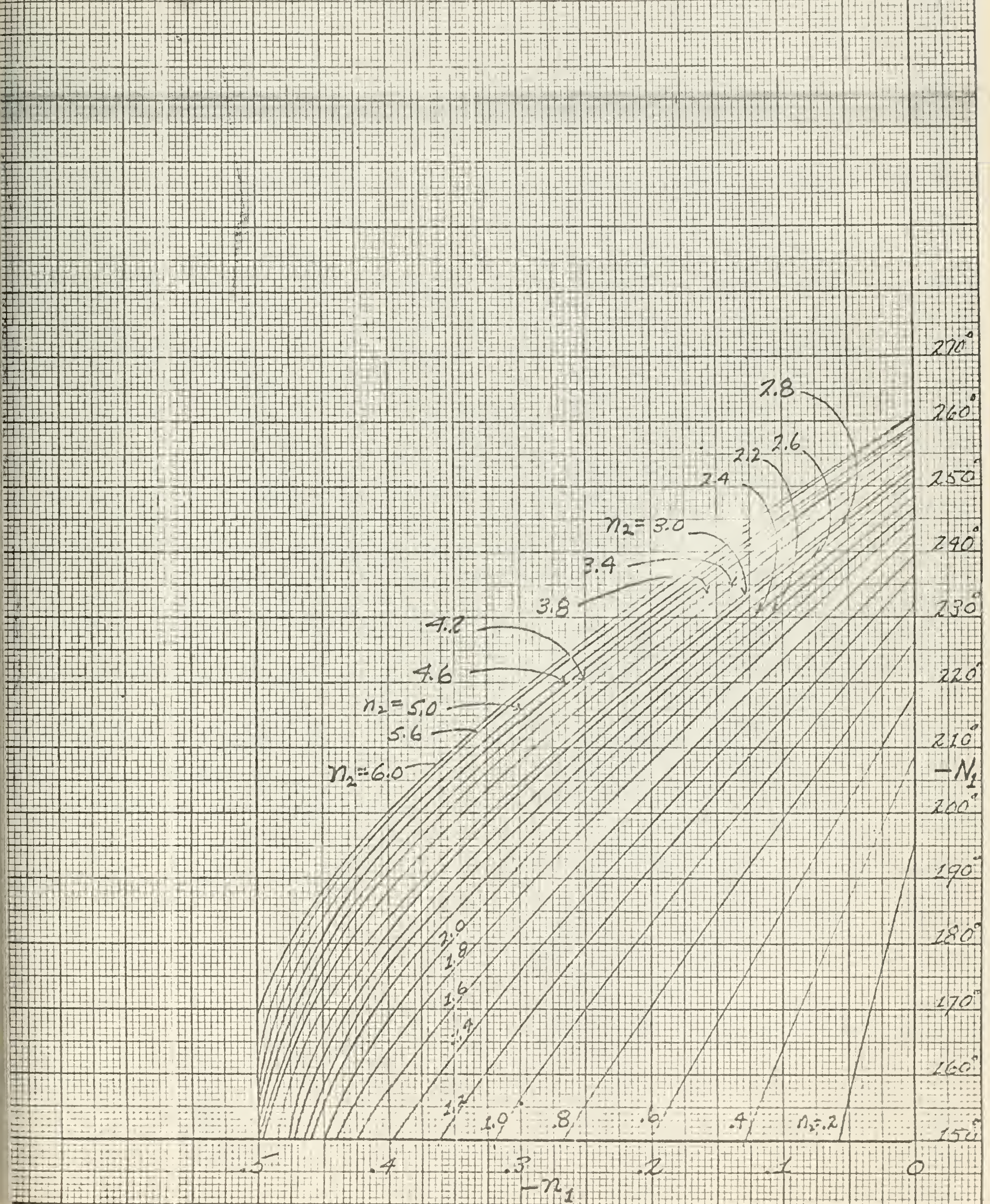

Fig. 5-17c
N_1 for Pure Third Order System

Second Value

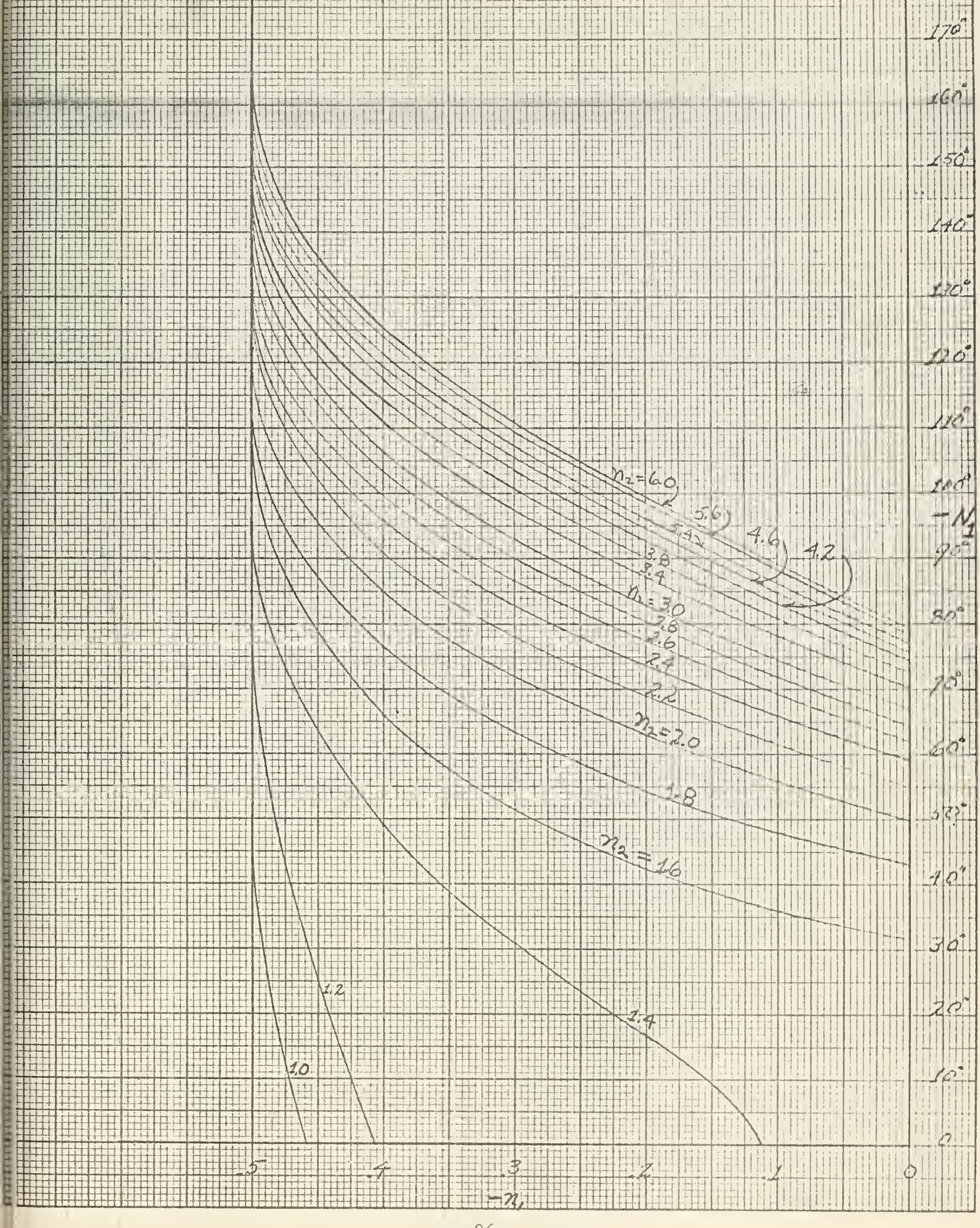

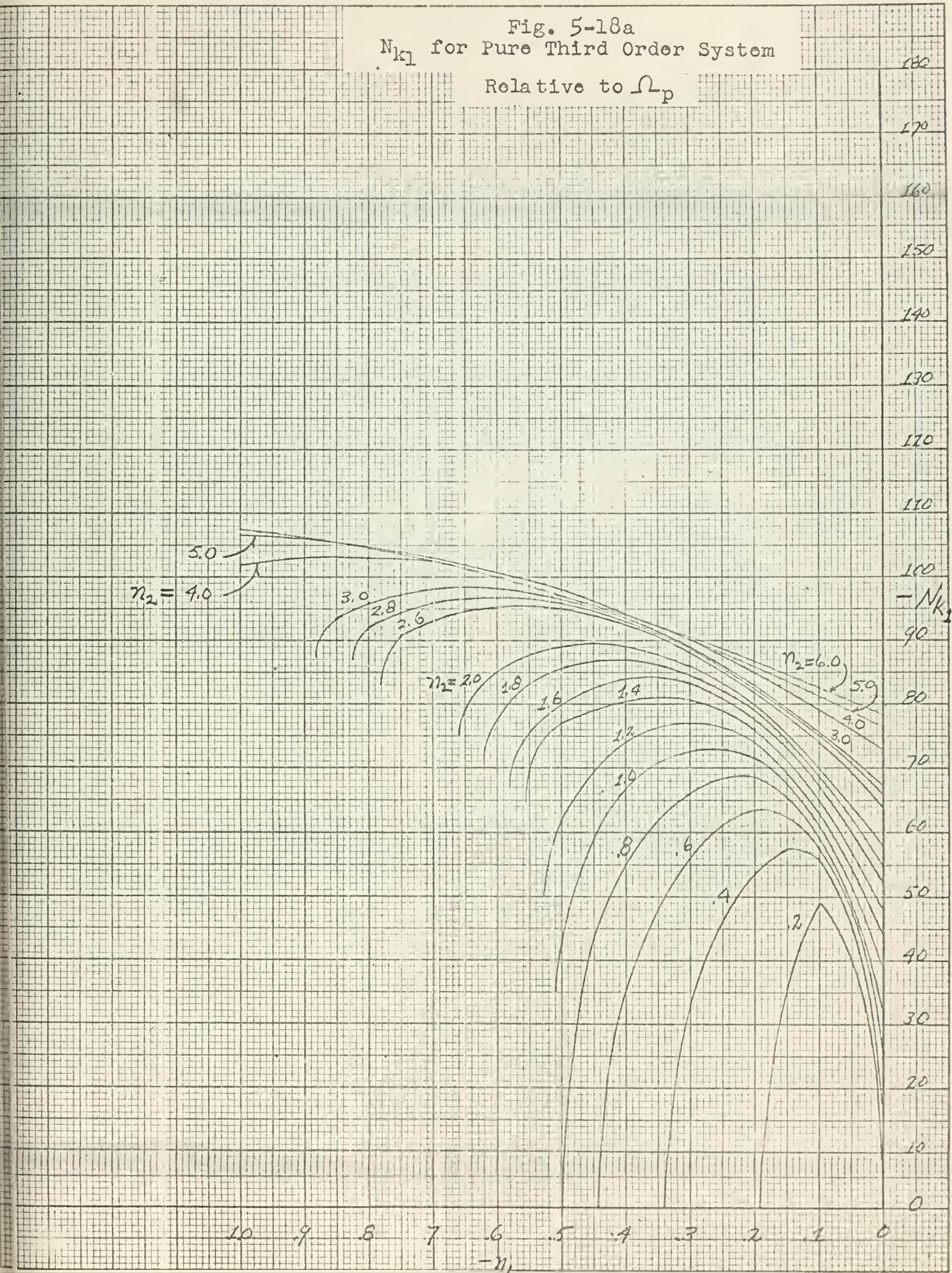

Fig. 5-18a
N_{k_1} for Pure Third Order System
Relative to Ω_p

Fig. 5-18b

N_{k1} for Pure Third Order System

Relative to Ω_m

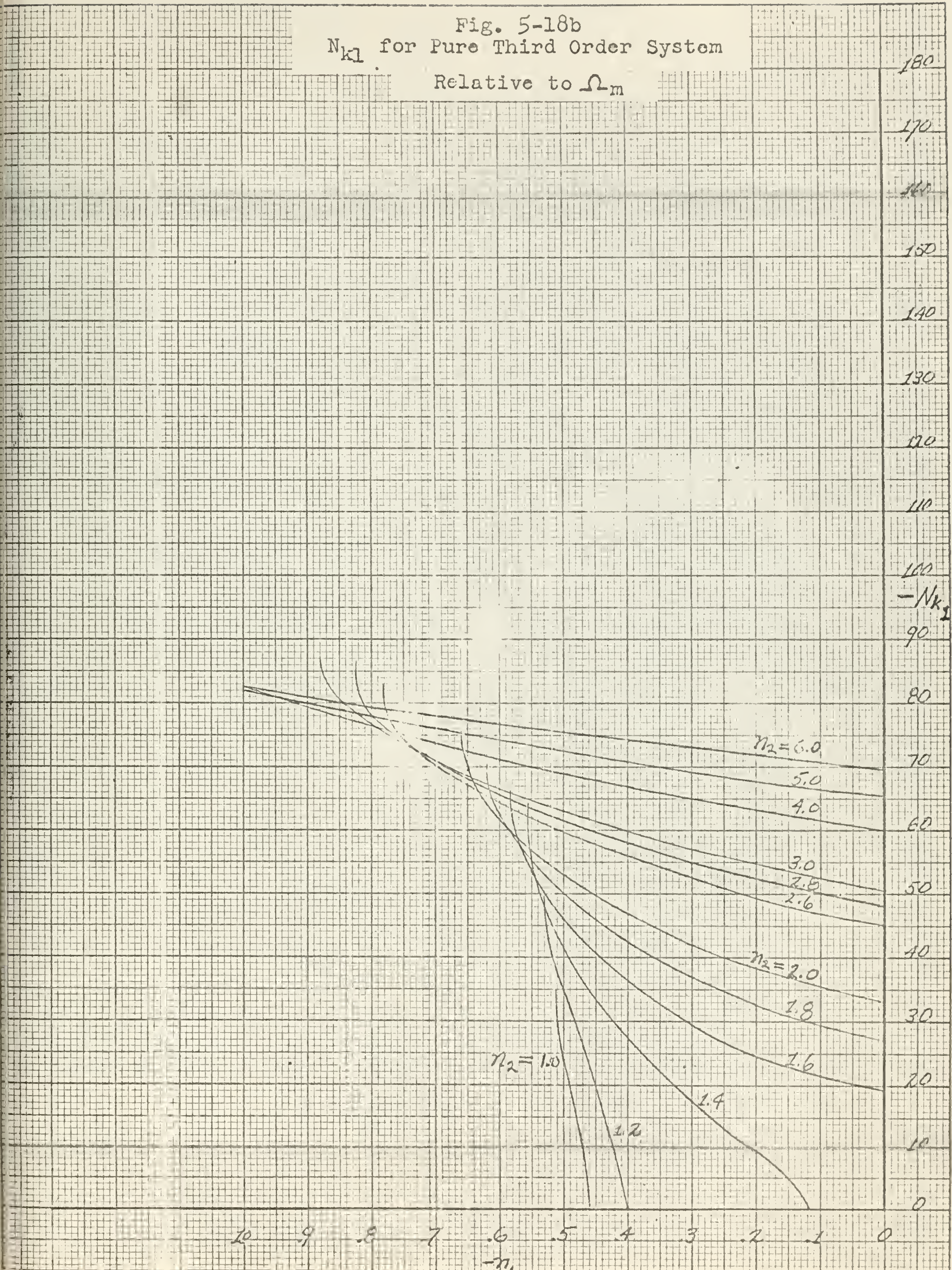

Fig. 5-19a
N_{k2} for Pure Third Order System
Relative to Ω_p

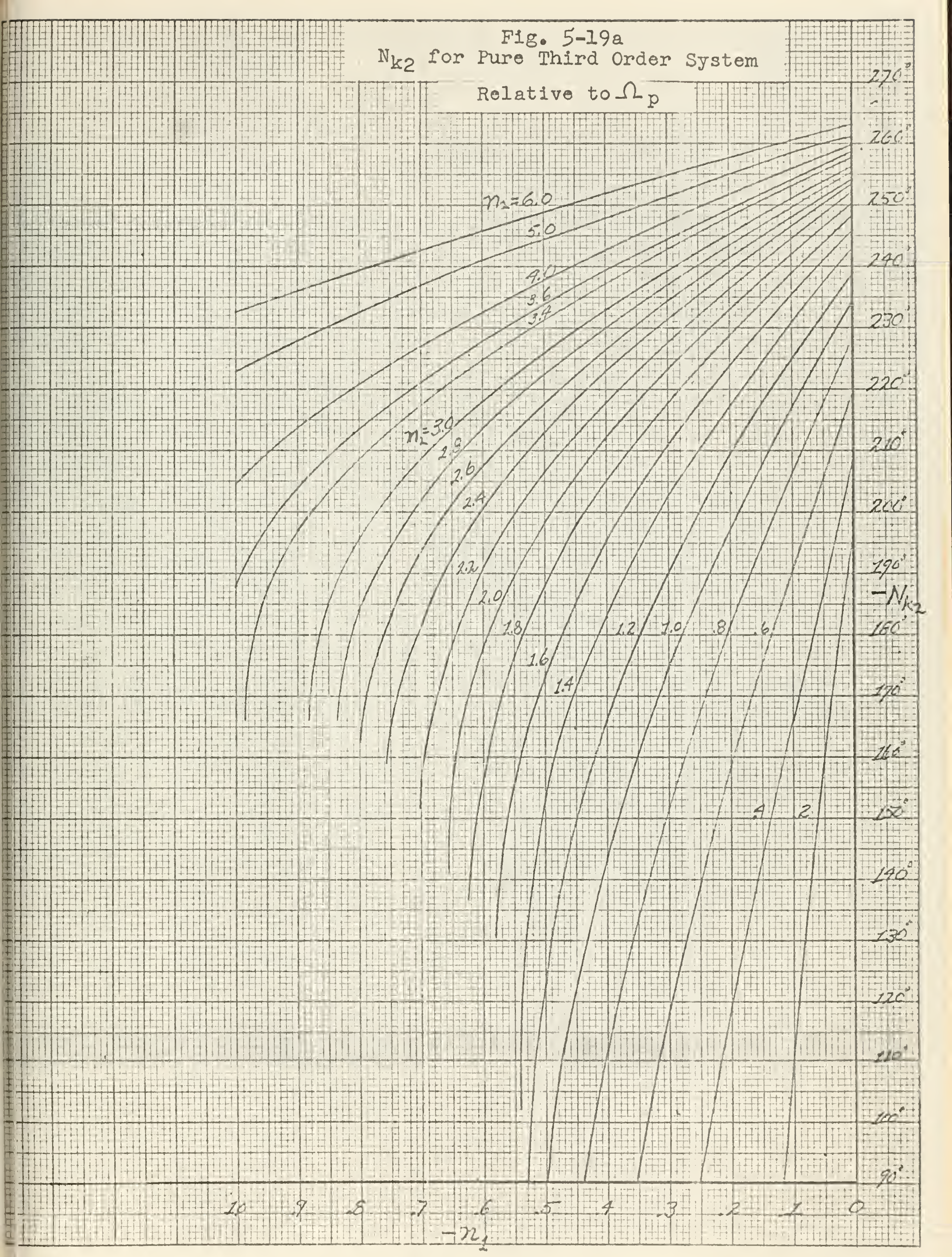

Fig. 5-19b
N_{k2} for Pure Third Order System
Relative to Ω_m

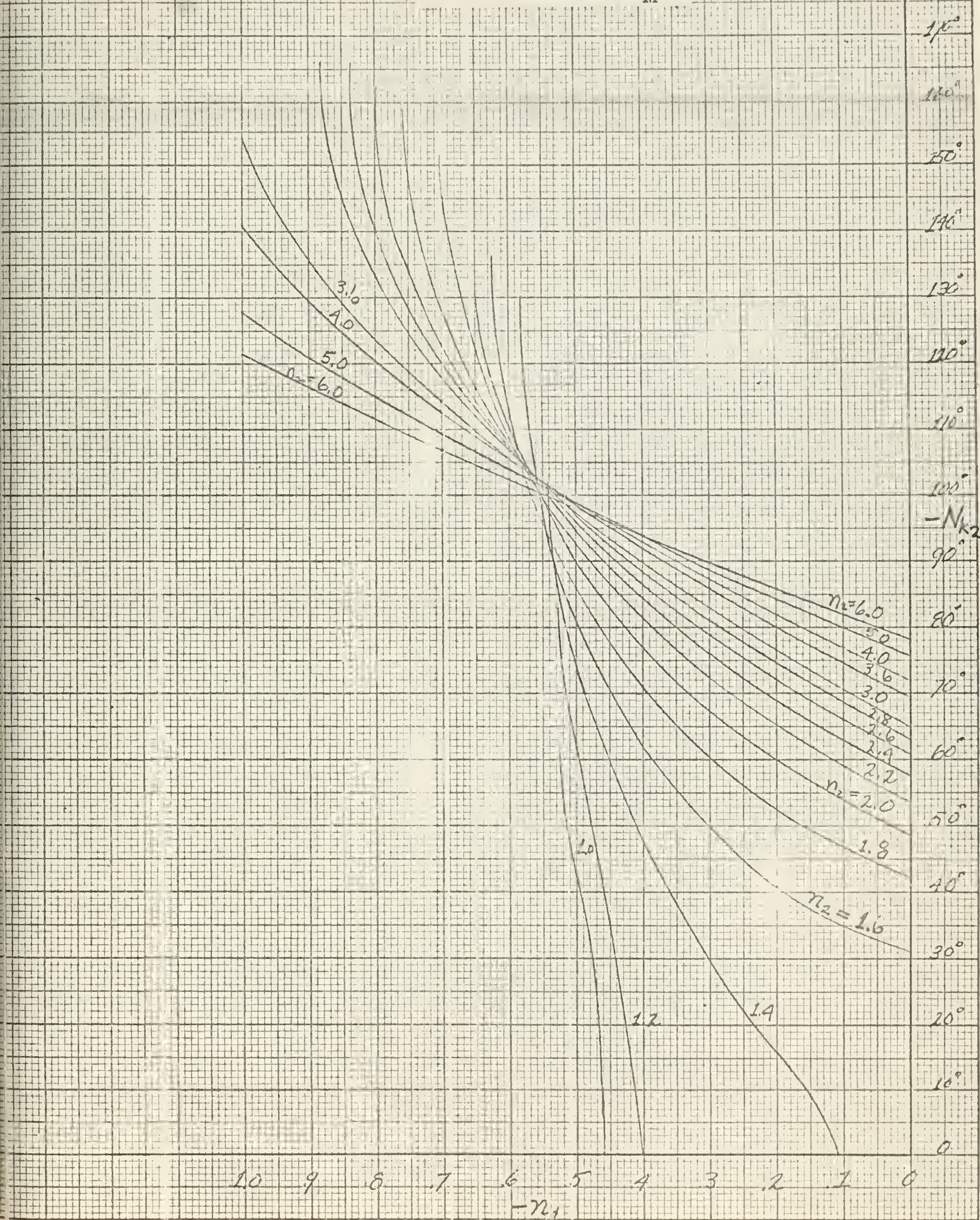

Fig. 5-20
N_{k3} for Pure Third Order System
Relative to Ω_p

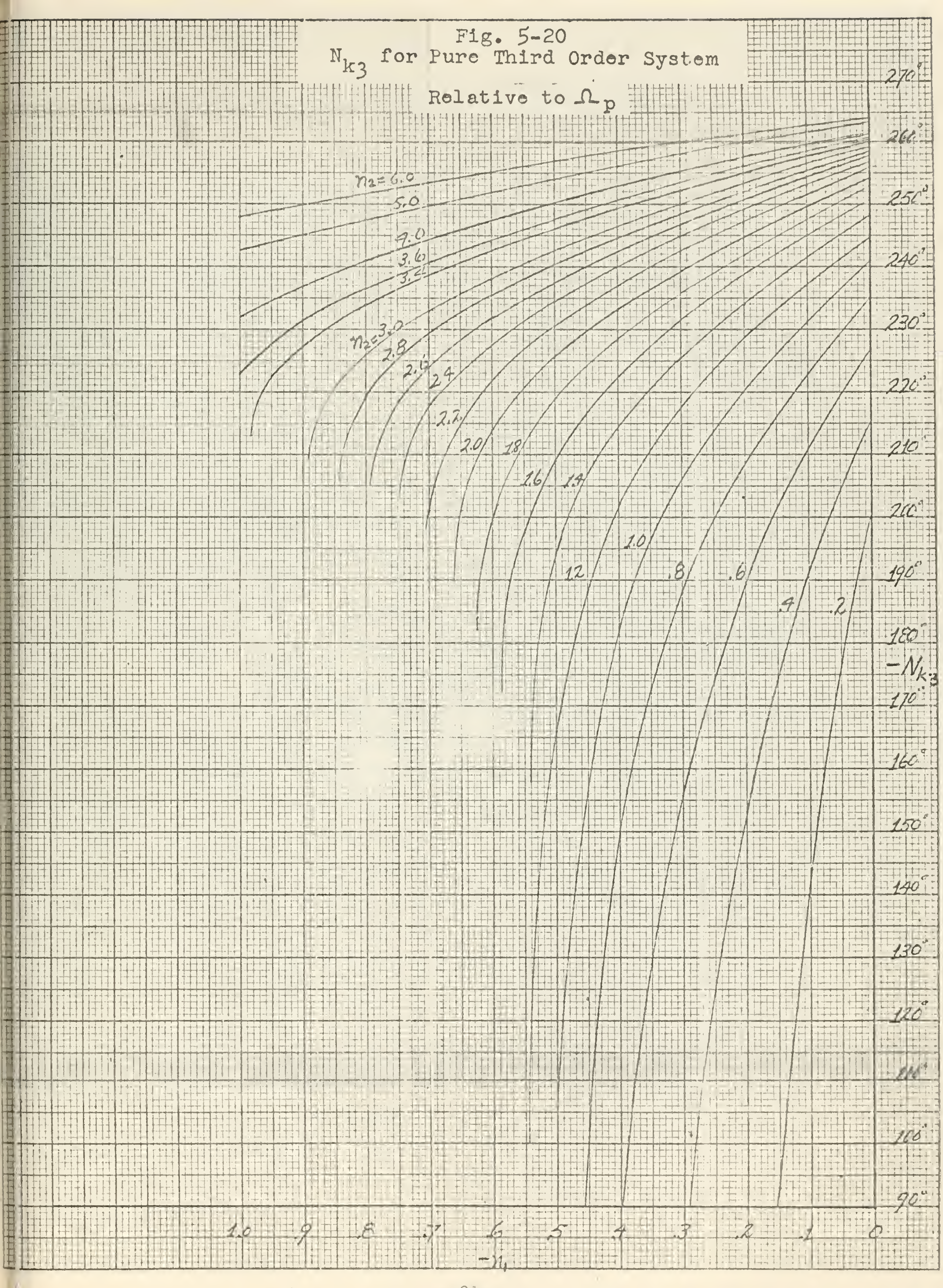

Fig. 5-21
N_{Ω_n} for Pure Third Order System

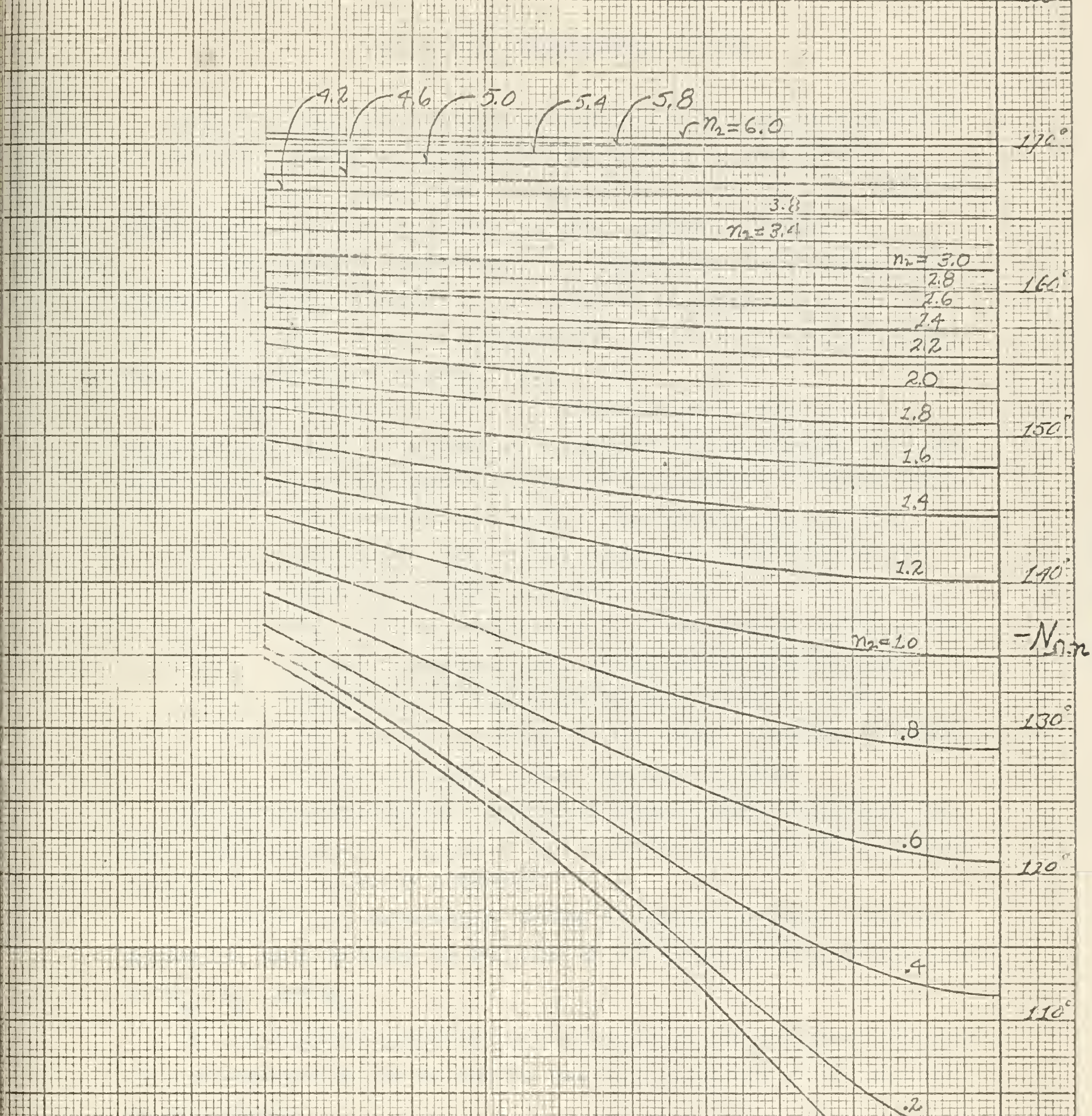

6. CONCLUSIONS AND RECOMMENDATIONS

The following conclusions were made based upon the investigation of the three classes of servomechanisms studied in this thesis:

a. All pure second order servomechanisms with the same relative complex pole location will have the same frequency response.

b. For the pure second order servomechanism, the parameter loci plotted are made applicable to any location of complex poles in the left half of the s-plane by changing the scales on the complex plane and on the parameter frequency loci.

c. The frequency response for servomechanisms with three singularities can be expressed as a function of the referred real and imaginary parts of the complex poles and the referred frequency where:

1. The referred real part of the complex poles is the actual real part of the complex poles divided by the magnitude of the real pole or zero.
2. The referred imaginary part of the complex poles is the positive imaginary part of the actual complex pole divided by the magnitude of the real pole or zero.
3. The referred frequency is the actual frequency divided by the magnitude of the real pole or zero.

d. All servomechanisms with three singularities which have the same relative pole-zero locations will have the same frequency response relative to the referred frequency.

e. Curves for determining values of several optional "fill-in" parameters were included in addition to the normally accepted parameters of $M_{p\omega}$, ω_p and ω_{bw}.

f. An accurate graphical approximation of the frequency response of a servomechanism can be rapidly obtained using the curves produced in this thesis.

It is recommended that the following areas be considered for further investigation using the technique presented in this paper;

a. Servomechanisms with more than three singularities, and

b. Systems other than servomechanisms.

7 BIBLIOGRAPHY

1. Patton, Walter Buel, Major, USMC, and LT W. B. Abbott, USN, Rapid Approximation of Servomechanism Transient Response, Thesis, Massachusetts Institute of Technology, 1961.

2. Mitrovic, Dusan, Graphical Analysis and Synthesis of Feedback Control Systems: Part I, Theory and Analysis; Part II, Synthesis, Trans. AIEE, pt II, January 1959.

3. Brown, Gordon S., and Donald P. Campbell, Principles of Servomechanisms, John Wiley and Sons, 1948.

4. Characteristics of the Model 1604 Computer, Control Data Corporation Manual, publication No. 081a, 1959.

5. Chestnut, Harold, and Robert W. Mayer, Servomechanisms and Regulating System Design, Vol. I and Vol. II, John Wiley and Sons, 1955.

6. Thaler, George J., and Robert G. Brown, Analysis and Design of Feedback Control Systems, 2nd ed., McGraw-Hill Book Co., Inc., 1960.

7. Truxal, John G., Automatic Feedback Control System Synthesis, McGraw-Hill Book Co., Inc., 1955.

8. Appendix A

The Control Data Corporation Model 1604 digital computer important characteristics are summarized as follows:

1. All transistorized
2. 48 bit word length
3. Stored program
4. Single-address logic, two instructions per 48-bit word
5. Indirect addressing feature
6. 32,768 48-bit words of magnetic core storage:
    - (a) Stored in two independent 16,384 word banks, alternate phased
    - (b) 4.8 micro-seconds effective cycle time (representative program).
    - (c) 6.4 microseconds total cycle time.